DESIGN AND SAFETY ANALYSIS OF AN IN-FLIGHT, TEST AIRFOIL

A Thesis

by

CHRISTOPHER WILLIAM MCKNIGHT

Submitted to the Office of Graduate Studies of
Texas A&M University
in partial fulfillment of the requirements for the degree of

MASTER OF SCIENCE

August 2006

Major Subject: Aerospace Engineering

DESIGN AND SAFETY ANALYSIS OF AN IN-FLIGHT, TEST AIRFOIL

A Thesis

by

CHRISTOPHER WILLIAM MCKNIGHT

Submitted to the Office of Graduate Studies of
Texas A&M University
in partial fulfillment of the requirements for the degree of

MASTER OF SCIENCE

Approved by:

Chair of Committee,	William S. Saric
Committee Members,	Helen Reed
	Rodney Bowersox
	J.N. Reddy
Department Head,	Helen Reed

August 2006

Major Subject: Aerospace Engineering

ABSTRACT

Design and Safety Analysis of an In-Flight, Test Airfoil. (August 2006)
Christopher William McKnight, B.S., The University of Dayton
Chair of Advisory Committee: Dr. William Saric

The evaluation of an in-flight airfoil model requires extensive analysis of a variety of structural systems. Determining the safety of the design is a unique task dependant on the aircraft, flight environment, and physical requirements of the airfoil. With some areas of aerodynamic research choosing to utilize flight testing over wind tunnels the need to design and certify safe and reliable designs is a necessity.

Commercially available codes have routinely demonstrated an ability to simulate complex systems. The union of three-dimensional design software with finite element programs, such as SolidWorks and COSMOSWorks, allows for a streamlined approach to the iterative task of design and simulation. The iterative process is essential to the safety analysis of the system. Results from finite-element analysis are used to determine material selection and component dimensions. These changes, in turn, produce different stress profiles, which will affect other components.

The unique case presented in this study outlines the process required to certify a large swept-wing model mounted to a Cessna O-2 aircraft. The process studies the affect of aerodynamic loading on the hard-point structure inside the wing, as well as the model mounting structure, and support strut.

The process does not end when numerical simulations indicate that each system is safe. Following numerical work, a series of static tests are used to verify that no unforeseen failures will occur. Although the process is tailored to one specific example, it outlines an approach that could be applied to any test platform. A different model may create a physically different system, but the safety analysis would remain the same.

To my parents,
Fred and Sue McKnight

ACKNOWLEDGEMENTS

This entire project would not have been possible without Dr. William Saric. He took a tremendous risk letting a guy who likes cars near aircraft, and I thank him for it. I must also thank him and Dr. Helen Reed who provided me an opportunity to live in an environment filled with horses, dogs, fish, deer, a goose named Marquette, turtles, spiders, cows, and countless other creatures.

This work could not have been completed without the financial support from the US Air Force Office of Scientific Research grant number FA9550-05-1-0044, P00001 and the Texas A&M Flight Research Laboratory.

I am grateful to Colleen Leatherman who has helped organize the most, if not all, of the paperwork associated with the project. Without her ability to keep track of deadlines, arrange travel, and handle billing procedures, the design process would have been a far more grueling task.

Without two remarkable test pilots, Roy Martin and Don Ward, the design process would have been at times frightening. Their positive outlook and willingness to fly one of the most unusual aircraft has been enjoyable and relaxing.

I have also had the opportunity to work with outstanding individuals at both Arizona State University as well as Texas A&M University. I thank; Andrew Carpenter and Celine Kluzec for helping me quickly gain a brief understanding of aircraft and piloting requirements- which at times was not easy, Tim Silverman, Heath Lorzel, and Sean Walton who provided tremendous design support, Shane Schouten who was normally responsible for the fabrication of whatever small component I forgot, Lauren Hunt who was forced to try to put into words the hundreds of images created, and Matt Hoyt and Cecil Rhodes the two mechanics who routinely had to come up with ways to make my ideas feasible.

My family has supported me throughout this endeavor. My parents have ~~never~~ or at least rarely questioned what I was doing. I consider myself extremely lucky to have always had their support in whatever I have done.

TABLE OF CONTENTS

LIST OF TABLES

LIST OF FIGURES

FIGURE Page

NOMENCLATURE

D	=	Nominal bolt diameter
F_{fail}	=	Force required for joint failure
F_i	=	Preload
F_p	=	Prying force
K	=	Nut friction factor
μ	=	Coefficient of friction
r_μ	=	Mean radius (washer) for frictional force
T	=	Pre-torque
τ_{fail}	=	Torque required to cause unwanted model

CHAPTER I

INTRODUCTION

1.1 Introduction

Designing an in-flight airfoil requires more that analyzing the airfoil. A successful design was one that could certify the safety of every system from the wing box to the model. These systems included; the hard-point brackets, the pylon and rocker arms, the airfoil mounting structure, the actual airfoil model, the support strut and the tie-down bracket. Once all of these systems were determined to be safe, flight testing of the airfoil could begin.

Design of the in-flight test airfoil began by outlining the physical requirements. The airfoil was to have a chord of 54 inches, a span of 42 inches and be swept back at 30°. It was also determined that a 4° cut at the base of the model was necessary to increase the rotational clearance at the trailing edge by an additional 3 inches. This additional clearance was necessary to prevent the corner of the model from striking the ground during landing.

Additional requirements stipulated that the airfoil needed to have a removable aluminum leading edge. This made it possible to fabricate and utilize multiple components. This would allow for one leading edge to be prepared while another is being tested. The leading-edge component also needed to extend back to the 15% chord, or 8.1 inches, to minimize the effect of the seam.

The test platform was to be designed so that it could safely be mounted under the wing of a Cessna O-2 test aircraft. The airfoil was required to interface to the aircraft

---

This thesis follows the style of the *AIAA Journal*.

using the bomb rack and pylon system originally used to carry various ordinances. Although the Air Force requires that a minimum factor of safety (FOS) of 1.5 to ultimate, the design process would require that every component demonstrate a FOS of 1.5 to yield.

Flutter concerns would require that the model achieve a high enough natural frequency to avoid damaging oscillation. The early design process focused on two likely causes of vibration, i.e. the engine RPM and the blade passing frequency. With the engine RPM limited to the range between 2200 and 2800 RPM, the two ranges to avoid were set at 38 to 47 Hz and 76 to 94 Hz.

Additionally the design of the airfoil model would be critically dependant on weight. This requirement is unique to the in-flight testing environment. While traditional wind-tunnel models can rely on massive support structures, aircraft limitations prevent such structures. Increasing the weight of the model decreases the fuel capacity of the aircraft, thereby limiting flight time. An increase in weight also creates a lateral imbalance which degrades aircraft performance, and limits takeoff requirements.

1.2 Software Selection

Before beginning the design process it was necessary to select software packages for design and evaluation. The airfoil model was designed in SolidWorks 2004 SP3.1, and evaluated using COSMOSWorks SP3.1. By using a bundled set of software the iterative process between design and evaluation is made nearly seamless. The wide scale commercial use of SolidWorks allowed for parts to be sent electronically to machine shops for evaluation throughout the process.

In order to understand the accuracy of COSMOSWorks a series of trial simulations were developed. These simulations would be compared to analytical solutions (Mischke et al. 2002, Blevins 1979), indicating the potential error in results. The first simulation used a cantilevered beam, under an end load of 250 pounds. The second used the same beam but applied a remote load 2 inches off the free end. Again

using the cantilevered beam a gravitational force of 1G was applied. The final simulation utilized a parallelogram fixed on one side to evaluate the numerical frequency analysis.

Table 1.1 shows that the results returned by COSMOSWorks are often within

Table 1.1
COSMOSWorks Verification Studies

	Deflection (in)			Stress (psi)		
Study	Theoretical	Numerical	Error (%)	Theoretical	Numerical	Error (%)
End Load	0.0863	0.0857	-0.70	9000	9325	3.61
Remote Load	0.1079	0.1071	-0.74	10500	10920	4.00
Gravity	0.0003	0.0003	0.00	43.63	41.03	-5.96
		Mode 1 (Hz)			Mode 2 (Hz)	
Frequency	65.91	64.73	-1.79	169.54	150.11	-11.46

5% of the true values. Many of the cases develop stress concentrations near the fixed surface and, the results can be improved by looking at the values within one node of the maximum value. It was also observed through other frequency trials that COSMOSWorks appeared to return conservative values. While the first mode was close to the true value the second numerical result was always lower than the true value.

1.3 Maximum Design Loads

Evaluation of structural systems was based on reactions to a worst case scenario. This condition was determined to be a collision avoidance maneuver, where the aircraft would be in a 30° bank and a 2G pull up. This type of maneuver would place the airfoil model at an angle of attack of 7°. Computational simulations of the aircraft and airfoil determined that this could produce 550 lbs of lift, and 40 pounds of drag. These two forces in combination with twice the weight of the airfoil would be used to create a maximum load set.

The drag of the model was not a main concern during most of the design process. When firing, the rocket launcher applied a 1000 pound thrusting force to the aircraft

system. By comparison the minute drag force was not expected to cause conflicts with any aircraft systems.

The weight of the model was not a concern when evaluating aircraft systems due to the previous certification of the aircraft. Without an airfoil model the aircraft was certified 3.8G with 350 pounds on each pylon. With the flight envelope for the airfoil model restricted to 2.0G, and the objective to minimize the airfoil weight it was anticipated that all the aircraft systems would be able to survive the 2G loading.

The lifting force was the most severe load in the set. The large force directed towards the fuselage created a large bending moment. This moment was not typical of the munitions certified for the O-2.

CHAPTER II

HARD POINT BRACKETS

2.1 Individual Bracket Comparison

The first aircraft system investigated was the hard point system. The Cessna O-2 was designed to carry a variety of munitions under its wings (Figure A.1). These munitions were held in bomb racks inside of pylons bolted to the aircraft wing box through four brackets (Figure A.2). These brackets were replaced as one of the initial steps to prepare the aircraft for testing.

The original hard-points in wings were fabricated from sheet metal, probably 2024-T3 aluminum. Three small rivets and two larger rivets secured each bracket to the spar. The pylon was attached to the bracket by means of a ¼" bolt. These bolts would enter into the brackets and thread through a nut plate riveted to the sheet-metal base. Each pylon relied on four such connections, securing a payload to both the leading edge and trailing edge spars.

The replacement brackets were designed based on the knowledge that the airfoil model would generate a lifting load not seen with any of the approved wing stores. The brackets would be machined from solid 7075-T6 aluminum. The change in material increased the yield strength of the aluminum by 46%, 50,000 psi to 73,000 psi. In addition to increasing material strength the new brackets were thicker than their predecessors. The side wall thickness increased to 0.075 inches, and the base increased to 0.160 in. Additionally the base of each bracket was now smooth and seamless (Figure A.3), unlike the previous brackets which had a step due to the layered sheet metal. Without such a step the bracket could not experience a stress concentration due to the sharp corner.

Individual comparisons between the old and new brackets revealed the vast improvement. Comparison of the brackets was done by applying a 332.5 pound force vertically down. Figure A.4 shows the vertical force and the restraints applied to each bracket. The results from each simulation can be seen in Table 2.1. The old brackets

Table 2.1
Individual Bracket Comparison

Component	Material	Yield Strength (psi)	Max Stress (psi)	FOS
Orig. Outboard LE	2024-T3	50000	37710	1.3
Orig. Outboard Aft	2024-T3	50000	43394	1.2
Orig. Inboard LE	2024-T3	50000	36458	1.4
Orig. Inboard Aft	2024-T3	50000	46234	1.1
New Outboard LE	7075-T6	73000	14625	5.0
New Outboard Aft	7075-T6	73000	14343	5.1
New Inboard LE	7075-T6	73000	14010	5.2
New Inboard Aft	7075-T6	73000	15241	4.8

had an average FOS of only 1.2 while the new brackets averaged 5.0. The individual comparison illustrated the increase in strength of the new brackets.

2.2 Evaluation of Outboard Bracket Assembly

To evaluate the effects of proposed airfoil loading on the brackets a larger assembly was created (Figure A.5). The assembly contained four brackets, two spars, four spar caps, and a section of the aircraft skin. The model loads were applied to the system remotely, eliminating the need to create a model, or simulate the pylon components. The first remote loads were the lift and drag forces. They were applied to the radial surfaces of the bolt holes. The weight was applied to remotely to the offset surface around the bolt hole, simulating the nut plate (Figure A.6). The forces were assumed to be located approximately 30 inches below the brackets, and were based on the location of the center of pressure and CG of early airfoil models.

The sides of the assembly were held fixed, and each rivet hole was given two restraints. The first restraint prevented radial motion, and the second prevented

translation normal to the surface. Figure A.7 shows that the restraints are identical to those used in the individual bracket evaluation.

A standard mesh was used on the assembly with an element size of 0.25 inches. The simulations were run using 84,574 elements and 161,420 nodes. The simulation assumed that all components were bonded.

Analysis of the system revealed the system is capable of surviving the airfoil loading. The lower trailing edge spar cap demonstrated the lowest FOS, 3.9. The stress in the component is concentrated around the bolt hole in the base of the bracket (Figure A.8). This can bee seen in each of the four brackets, and is responsible for the maximum stress of nearly 18,000 psi in the outboard leading edge bracket (Figure A.9).

The remaining components saw significantly lower stress values compared to the bracket, and had higher FOS. As Table 2.2 shows both the brackets and the aircraft

Table 2.2
Outboard Bracket System Stress Results

Component	Material	Yield Strength (psi)	Max Stress (psi)	FOS
Outboard LE	7075-T6	73000	17889	4.1
Inboard LE	7075-T6	73000	15503	4.7
Outboard TE	7075-T6	73000	16329	4.5
Inboard TE	7075-T6	73000	14106	5.2
LE Spar	2024-T3	50000	6966	7.2
LE Spar Cap (Upper)	2024-T3	50000	2488	20.1
LE Spar Cap (Lower)	2024-T3	50000	10077	5.0
TE Spar	2024-T3	50000	6977	7.2
TE Spar Cap (Upper)	2024-T3	50000	2131	23.5
TE Spar Cap (Lower)	2024-T3	50000	12673	3.9
Skin	2024-T3	50000	10371	4.8

structure have fairly large factors of safety. Had the original brackets been left in place it was quite unlikely that they would have been able to endure the airfoil loading.

CHAPTER III

MOUNTING STRUCTURE

3.1 Explanation of Mounting Structure

Allowing for the model to interface with the bomb rack, the mounting structure serves a unique role. Most of the mounting structure (Figure A.10) was designed by Timothy Silverman (2005) and the final structure (Johnson) changed very little from his design. The mount which is composed of two pieces, a channel and alignment component, must be rigidly attached to the model, yet allow for the angle of attack of the model to vary between -5° and 5°.

The alignment component is simple. Its only tasks are to interface with the rocker arms and the bomb rack. Interfacing with the rocker arms is done via the two angled faces on the inboard and outboard side. The rocker arms can easily press against these surfaces locking the airfoil in place. The interface with the bomb rack is accomplished through two eyebolts (Figure A.11). These eyebolts, each with a 5000 pound load limit, are recessed into the component and bolted through the top of the mount.

The channel is not as simple as the alignment component. A series of holes and arcs (Figure A.12) have been cut through the part allowing for fasteners and wires. The component was also designed to allow for instrumentation to be mounted aft of the main bolt if necessary.

There are eight arcs that are all concentric with the main bolt hole. These arcs lie above 10-32 tapped holes in the model and allow for fasteners to pass through the mount, steel plate, and into the model (Figure A.13). The arcs allow for the required 10° range of motion. These fasteners helped to ensure that the mount is rigidly attached to the model.

The slot cut in the front of the model facilitates the ability to change angles of attack (Figure A.14). The slot lies above a second slot cut in the model, but is perpendicular. A pin can be placed through the two intersecting slots and mated to a block on a section of ¼-28 threaded rod. With thread locking nuts and thrust bearings on each end of the rod, it is possible to turn the rod and allow the block to travel along the length of the rod. As it travels the two slots must rotate to allow for the movement. This movement causes the angle of the model with respect to the mount to vary from -5° to 5°.

Behind the slot is a ½ inch arc. This arc allows for a ½-20, grade-8 bolt to pass through the model and mount. This bolt, referred to as the support bolt is used to relieve some of the force exerted on the main bolt. The head of the bolt is inside the model and Figure A.15 illustrates the flat surfaces on the threaded end that are required to preload the connection.

Aft of the support bolt a 2 inch diameter hole was cut (Figure A.16). This hole has no structural purpose and was designed to allow for wiring to exit the model. By selecting such a large diameter it is possible to allow for a variety of plugs to be passed through the opening without needing to disassemble the model.

The final hole is the clearance hole for the main bolt. Designed to be in line the CG of the model the main bolt is a ¾-10, grade-5 bolt. Designed to withstand severe loading the main bolt represents the strongest connection in the system. The bolt is aligned with the axis of rotation of the model and is secured in place using a jack bolt (Figure A.17) to ensure accurate preloading. Further discussion concerning the safety of the bolted connections can be found later.

CHAPTER IV

AIRFOIL MODEL DESIGN

4.1 Preliminary Design

Design of the airfoil model began by creating as many concepts as possible. From these early concepts four models began to emerge. Two of these models, the pocketed model and the shelled model, were based on a three-component design. These two were to be fabricated from aluminum and included a leading edge, test surface and non-test surface (Figure A.18). The composite model was a two-piece design that included an aluminum leading edge and a composite body. The fourth design featured a substantial number of components, each fabricated from aluminum. This design, the airframe model, was based on traditional wing design.

The pocketed model features a 4 by 4 array of hollow cavities (Figure A.19) cut into each half of the body. These pockets were separated by 0.1875 inch thick ribs and spars. The skin thickness was also held constant at 0.1875 inches. At the intersection of the ribs and spars a 1 in^2 block was used to allow for fasteners to join the components. An arc was cut into each rib and spar allowing for wiring to be run between any combination of pockets.

The shelled model was an extension of the pocketed model. If there was no structural need for these ribs, then their elimination would further lighten the model. Figure A.20 shows the interior cavity of a shelled model with 15 support blocks. The support blocks were used to secure the two halves of the body together and were 1 inch by 1 inch extrusions. These extrusions matched those seen in the pocketed model.

Concerns over weight prompted the investigation into the use of lightweight materials. The result was a composite model, whose body was made of fiberglass or

carbon fiber. The design featured a foam (Figure A.21) core although if it was hoped that the fiber body could support all of the loading, allowing for the removal of the foam. Like the other designs a removable leading edge would still be utilized.

The fourth design was based on a more traditional airframe design. The model would be composed of rips and spars that matched the outer mold line, OML, of the airfoil. A series of skin panels could then be secured to the rib and spar structure (Figure 22) forming the completed airfoil. Again the leading edge would be a stand alone component. Unlike traditional airframe design each component would be significantly thicker. The thicker components would eliminate much of the flexibility associated with airframes as well as allowing the structure to handle the aerodynamic loads.

4.2 Preliminary Decision Analysis

In order to simplify the numerical modeling of the models a simple decision analysis was used to reduce the four designs down to two. The analysis focused on five criteria: the ability to meet test requirements, weight, design complexity, cost, and maintenance. Each criterion was assigned a weight-factor that indicated its importance to the design process. The weight and ability to match test requirements were the most important while the maintenance of the model was the least important.

The ability to meet requirements included the ability to integrate pressure taps into the surface of the airfoil. Previous models indicated that there was little problem integrating the taps into an aluminum structure, but there was concern over the ability to create a smooth interface between a composite surface and the pressure taps. For this reason the composite model received the lowest value of the four designs. The airframe model also received a low mark due to the complexity associated with running all the necessary pressure lines around all of the various components. The pocketed and shelled models were given identical values in that they are both essentially the same three-component model, in terms of test requirements.

The weight reflects the designed weight of each model. The composite model received the highest ranking from the lightweight materials used to create the body of

the model. Although not as light as the composite model the shelled model represented the lowest weight of any completely metal design. The airframe and pocketed models had nearly the same weight and were given equal ratings.

Complexity was responsible for the termination of the airframe design. With so many components hundreds of fasteners would be needed to join all of the components together. The variety of pieces also required that the tolerances on each piece be quite small to eliminate gaps after assembly. The composite model also received a low rating primarily due to the fact that the entire body was a single component. Although this would simplify assembly it would make fabrication difficult.

The cost of each model was based on any foreseeable manufacturing difficulties. The low rating on the composite model was driven by the need for a large composite airfoil with tight tolerances. Creating a composite structure nearly 4 ft by 3.5 ft was not likely to be an economical process. The airframe model received high marks since the majority of the components are small enough for an average machine shop to handle. The pocketed and shelled models by comparison require that two large aluminum components be fabricated.

Maintenance of a design is an indication of the ability to replace components should they become damaged. With the pocketed, shelled, and composite model being fabricated from only a few components, replacing any part would be a costly process. The airframe model was an exception. While some components would still be expensive to replace leading edge or test side skin, many other components could be fabricated quickly and at a lower cost.

Putting this information into the decision analysis reveals that the shelled and pocketed models were significantly better designs. Table 4.1 reveals that their

Table 4.1
Preliminary Decision Analysis

		Pocketed		Shelled		Composite		Airframe	
Criteria	Weight	R	V	R	V	R	V	R	V
Test Req.	9	9	81	9	81	1	9	5	45
Weight	8	3	24	7	56	10	80	3	24
Complexity	6	6	36	6	36	3	18	1	6
Cost	4	3	12	3	12	1	4	8	32
Maintenance	2	3	6	3	6	1	2	8	16
		Sum	153	Sum	185	Sum	111	Sum	107

dominance in terms of test requirements and complexity far outweighed their poor ratings in categories such as maintenance. The next step in the design process required a numerical analysis of both the pocketed and shelled models to determine which design would ultimately be fabricate.

4.3 Numerical Modeling of Early Designs

With the mounting structure conceived the two dominant designs could be numerically evaluated. With the mounting structure incorporated into each airfoil design an identical set of restraints and loads were applied to each assembly. Following the analysis of each design a second decision analysis would be used to determine which design would be finalized and fabricated.

Applying the restraints (Figure A.23) to the assemblies began with two restraints placed on split surfaces on the inboard side of the mounting structure. These two surfaces were prevented from moving in the radial direction, simulating the effect of the rocker arm assemblies of the pylon. There were no restraints placed on the two outboard split surfaces as the lifting load would pull the model away from those rocker arms preventing any reaction. The other restraints were applied on the top of the alignment component. These restraints prevented normal motion as well as radial motion, replicating the effects of the eyebolts.

During frequency analysis all four rocker-arm locations were restrained. With the model oscillating, all four rocker arms would resist motion, not just the inboard or outboard side. The eyebolt restraints would remain the same during frequency analysis.

The loading was applied to the model with three forces (Figure A.24). The lifting force was applied along a split line at 30% chord, which had been determined to be the center of pressure of the airfoil. The drag was applied along the trailing edge of the model. The weight of the assembly was applied by using the gravity feature of COSMOSWorks. The acceleration was set at 772.2 inches/sec^2, to simulate a 2G maneuver.

The models would be compared based on worst case loading. When the comparison was done this loading was much more severe than was discussed in section 1.3. Early CFD modeling indicated that the 7° maneuver would create 1600 pounds of lift and 120 pounds of drag. Coupled with twice the weight, many of the early models were evaluated with this load set.

4.3.1 Evaluation of Pocketed Model

The first of the designs to be evaluated was the pocketed airfoil. The mesh used during the simulations was based on an element size of 0.67 inches with a control of 2 inches on the outer surface. The result was a mesh of 296,725 nodes and 169,911 elements. Table 4.2 illustrates the results of the simulation. With a minimum factor of safety of

Table 4.2
Pocketed Model Stress (Maximum Loading)

Component	Material	Yield Strength (psi)	Max Stress (psi)	FOS
Leading Edge	6061-T6	40000	622	64.3
Test Surface	6061-T6	40000	8396	4.8
Non-Test Surface	6061-T6	40000	4762	8.4
Channel	7075-T6	73000	16091	4.5
Alignment Comp.	7075-T6	73000	38795	1.9

1.9 the model demonstrated an adequate ability to handle the worst case scenario. Aside from the alignment component all of the other parts had factors of safety above 4.0 indicating that the majority of the components could easily endure the worst case loading. The maximum stress, 38,795 psi, appeared in the region around the leading edge eye bolt location.

Examining the deflection of the model revealed a very uniform deformation (Figure A.26). The base of the model had shifted little more than 0.15 inches during the loading. More importantly the middle of the airfoil had an even deformation of approximately 0.08 inches. With most of the testing focusing on this region a consistent uniform deformation was ideal.

A second simulation determined that the natural frequencies of the pocked model were outside of the engine RPM and blade passing frequencies. With a frequency of 51.7 Hz it appeared as though the model's lowest frequency would occur between the two ranges to avoid. Aside from the first two frequencies, Table 4.3 shows that the higher modes are significantly higher than any expected oscillation.

Table 4.3
Natural Frequencies: Pocketed Model with Mounting Structure

Mode	Period (sec)	Frequency (Hz)
1	0.0193	51.7
2	0.0085	117.6
3	0.0075	132.7
4	0.0036	276.9
5	0.0029	350.3

4.3.2 Evaluation of Shelled Model

Analysis of the shelled airfoil began in the same fashion as the previous assembly. A mesh was created based on an element size of 0.67 inches with a 0.5 inch control on the leading edge and a 2 inch control on the outer surface. This created an assembly using 188,264 nodes and 100,347 elements.

The results of the maximum loading, seen in Table 4.4, again revealed that the lowest FOS of the shelled airfoil was 2.0. The value is again the result of a stress

Table 4.4
Shelled Model Stress (Maximum Loading)

Component	Material	Yield Strength (psi)	Max Stress (psi)	FOS
Leading Edge	6061-T6	40000	2924	13.7
Test Surface	6061-T6	40000	13328	3.0
Non-Test Surface	6061-T6	40000	11995	3.3
Channel	7075-T6	73000	10253	7.1
Alignment Comp.	7075-T6	73000	35075	2.1

concentration around the leading edge eye bolt location. Figure A.27 also shows a region of stress developing between the leading edge of the mounting structure and the airfoil. Unlike the pocketed model the three model components exhibited much lower factors of safety. Although these values were not close to the limit of 1.5 each of these components were subjected to a great deal more stress in this design.

The deflection of the shelled model also exhibits an undesirable characteristic of the shelled design. The skin of the airfoil appears to bulge (Figure A.28) near the application of the lifting load. The magnitude of this deflection was approximately 0.21 inches, and was nearly located in the middle half of the airfoil test surface. The simulation revealed that the deflection of the shelled airfoil would not be as uniform as the pocketed model.

The lack of interior structure was responsible for the significantly lower natural frequencies of the model. The lowest frequency, 44.2 Hz, fell inside of the engine RPM range, and the second frequency, 89.7 Hz, was located in the range of the blade passing frequency. Both values were nearly above the ranges to avoid, and noting that COSMOSWorks tends to return conservative values may have indicated that the true values were safely outside of this range. Again it is seen in Table 4.5 that modes higher than 2 are well above expected values.

Table 4.5
Natural Frequencies: Shelled Model with Mounting Structure

Mode	Period (sec)	Frequency (Hz)
1	0.0226	44.2
2	0.0111	89.7
3	0.0082	122.5
4	0.0073	136.4
5	0.0069	145.1

4.4 Control of Airfoil Center of Gravity

During the evaluation of both the designs there were growing concerns over the CG location of the airfoil model. Flight tests with the aircraft revealed that an aft aircraft CG degraded the stability of the aircraft. It was also believed that flutter could be avoided if the CG of the airfoil model was located in front of the elastic axis of the aircraft. The elastic axis of the aircraft was assumed to be 40% chord. In order to minimize the effect of the large lifting force it was also hoped that the airfoil center of pressure could be located inline with the aircraft CG.

Aligning the model center of pressure with the aircraft CG was accomplished by setting the mounting distance to 12 inches. This distance is the distance from the leading edge corner of the airfoil model to the leading edge of the aircraft wing. By setting the value to 12 inches it also served to move the airfoil model's CG in front of the elastic axis.

Unfortunately, pushing the mounting location forward only resulted in a couple of inches of clearance between the model CG and the elastic axis. In order to increase the clearance a counter weight was added to the upper corner of the leading edge in the shelled design. By adding 20 pounds of weight the CG moved an additional 4.5 inches further in front of the elastic axis (Figure A.29). Adding 20 pounds had a significantly lower effect on the pocketed model (Figure A.30) as its prior weight was nearly 40 pounds greater. A more detailed examination into flutter concerns is discussed following the airfoil design.

4.5 Intermediate Decision Analysis

The numerical results from the simulations along with the plan to use an insert to control the CG were used to again compare the two models. This time the criteria used to differentiate between designs would include safety, weight, stiffness, deflection and adaptability. Safety was always the highest weighted category and the deflection was the lowest.

Ratings for safety were based on the numerical results of the two models under the maximum loading scenario. The rating takes into account the minimum FOS as well as the FOS for each component. The similar numerical results for both designs resulted in identical ratings. While the shelled model exhibited a higher FOS, the pocketed design had much lower stress values in the three model components.

The only changes in the weight that occurred since the previous decision analysis were the addition of the mounting structure, and insert. Since identical components were added to both assemblies the difference in weight remained the same. With a difference of nearly 50 pounds, 126.15 to 179.34 pounds, the shelled model received a significantly higher rating.

The pocketed model exhibited a much better frequency response, with no natural frequencies inside the two ranges to avoid. Consequently it received a high rating, while the shelled model struggled. Having two frequencies inside of the avoided ranges signaled that further design may be necessary dropping its rating.

Although the deflections of both models is quite small, below 0.25 inches, the uniform deformation of the pocketed model was seen as being much more advantageous than the bulging surface of the shelled model.

The final criterion, adaptability, was in response to the need to control the model CG. With a lower starting weight it would take smaller counterweights to shift the shelled CG to a desired location. This would allow for a variety of smaller counterweights to be fabricated allowing for a great many different CG possibilities.

The results of the analysis, seen in Table 4.6, revealed that the shelled model was the superior design. Its low weight and ability to adapt to a variety of situations

Table 4.6
Intermediate Decision Analysis

		Pocketed		Shelled	
Criteria	Weight	R	V	R	V
Safety	10	5	50	5	50
Weight	8	4	32	9	72
Stiffness (Freq)	5	7	35	4	20
Deflection	2	8	16	2	4
Adaptability	4	3	12	7	28
		Sum	145	Sum	174

propelled the design ahead of the pocketed model. Confirming the safety of the design after adding an insert was done by rerunning the two simulations to obtain a new set of stresses and natural frequencies. The results in Table 4.7 confirmed that an insert has little effect on the overall characteristics of a design.

Table 4.7
Insert Effects on Stress Analysis

Shelled Model with Insert (Maximum Loading)				
Comp	Material	Yield	Max.	FOS
Leading Edge	6061-T6	40000	2875	13.9
Test Surface	6061-T6	40000	13696	2.9
Non-Test Surface	6061-T6	40000	12160	3.3
Insert	Alloy Steel	90000	4930	18.3
Channel	7075-T6	73000	10092	7.2
Alignment	7075-T6	73000	35437	2.1
Pocketed Model with Insert (Maximum Loading)				
Comp	Material	Yield	Max.	FOS
Leading Edge	6061-T6	40000	581	68.8
Test Surface	6061-T6	40000	8506	4.7
Non-Test Surface	6061-T6	40000	4799	8.3
Insert	Alloy Steel	90000	120	748.1
Channel	7075-T6	73000	16491	4.4
Alignment	7075-T6	73000	39168	1.9

4.6 Finalization of Airfoil Design

4.6.1 Structural Changes to Airfoil

Discussions with the manufacturer (Gideon) revealed a major fabrication concern. The shelled model would take far longer, and cost much more to fabricate than originally hoped. With a smooth inner cavity, and a wall thickness of only 0.1875 inches machining would have to be done slowly with precision tooling. This process was expected to at a minimum double the cost and manufacturing time for the model. In order to reduce the machining time and cost it was suggested that the design be revised to include flat surfaces that could be machined with large face mills. It was also advised that the thickness of the model should not drop below the 0.1875 inch thickness.

In order to minimize the weight of the airfoil while complying with the machining requirements the once smooth inner cavity was replaced by a series of 2 inch steps. Each step would have a minimum thickness of 0.1875 inches and have a surface parallel to the seam between the two halves of the body. In addition to the steps, several supports were added to the structure. These supports, similar to ribs, would not create a solid region, but were added to retain some level of resistance to deflection. A cut away view of the proposed design (Figure A.31) clearly shows the newly devised design. All of these changes to the model dramatically reduced the machining time and cost, but also added a great deal of weight to the model.

Other fabrication changes made to the model included the leading edge. For similar reasons the component could not be smoothly shelled, but rather a series of steps would be created inside the component (Figure A.32). The sweep angle made it difficult to machine the inside of the upper corner, and it was therefore left solid. The solid corner does not take away from the design as it leave metal in the region where a counterweight was to be added.

The final changes to the design included the addition of steel plates (Figure A.33) to the top and bottom of the airfoil. These plates allowed for additional fasteners to joint the two halves together. The upper plate also prevented the sharp edges of the mounting

structure from digging into the softer aluminum airfoil. One of the lower plates would also be used to create an attachment point for a strut to be added to the back of the model. While tremendously useful the plates did add 17 pounds to the overall weight of the structure.

4.6.2 Numerical Evaluation of Stepped Model

Obtaining numerical results on the stepped model followed the same procedure as the previous designs. A mesh was created based on an element size of 0.5 inches, creating an assembly with 451,553 nodes and 249,489 elements. All forces and restraints were applied in a similar fashion to the previous simulations. The results (Figure A.34) showed that the stepped model was also capable of withstanding the maximum loading with a FOS of 1.9. Again the minimum FOS occurs around the leading edge eye bolt. Table 4.8 shows that all of the other components easily passed with individual factors

Table 4.8
Stepped Model Stress (Maximum Loading)

Component	Material	Yield Strength (psi)	Max Stress (psi)	FOS
Leading Edge	6061-T6	40000	3148	12.7
Insert	Alloy Steel	90000	2808	32.0
Non-Test Surface	6061-T6	40000	8781	4.6
Test Surface	6061-T6	40000	11329	3.5
Trailing Edge Strip	6061-T6	40000	1039	38.5
Strut Plate	17-4 H-1025	170000	1306	130.2
Lower Plate	17-4 H-1025	170000	2528	67.3
Upper Plate	17-4 H-1025	170000	13228	12.9
Channel	7075-T6	73000	11037	6.6
Alignment Comp.	7075-T6	73000	37901	1.9

of safety above 3. The structure of the stepped model was also sufficient to prevent the bulging effect (Figure A.35) seen in the shelled model.

The greatest surprise of the evaluation was the frequency response of the model. The natural frequencies of the stepped model, Table 4.9, were far below the

Table 4.9
Natural Frequencies: Stepped Model with Mounting Structure

Mode	Period (sec)	Frequency (Hz)
1	0.0257	38.9
2	0.0102	97.7
3	0.0091	110.0
4	0.0059	169.2
5	0.0050	201.7

values of the other designs. Further investigation into flutter had revealed that a 40 Hz natural frequency would be sufficient to alleviate concerns.

4.6.3 Final Decision Analysis

Comparing the most recent design to the previous two models revealed the superiority of the design. Table 4.10 illustrates the narrow margin separating each design. The cost

Table 4.10
Final Decision Analysis

		Pocketed		Shelled		Stepped	
Criteria	Weight	R	V	R	V	R	V
Safety	10	5	50	5	50	5	50
Weight	8	6	48	9	72	3	24
Cost	9	3	27	1	9	9	81
Stiffness (Freq.)	5	8	40	5	25	6	30
Deflection	2	6	12	4	8	7	14
Adaptability	2	2	4	4	8	6	12
		Sum	181	Sum	172	Sum	211

of each design was added as an additional criterion, and the definition of adaptability was changed. Since the concerns over flutter had been eased there was not a strong desire to have a large range of CG locations. Instead it was more advantageous to have a model that could allow for a variety of instrumentation to be mounted internally. This equipment included accelerometers and pressure scanners.

The results of the analysis revealed that the latest, or stepped, design was a better-quality design. Although heavier, its inexpensive fabrication pushed the design

ahead of both the pocketed and shelled designs. The stepped model also benefited from the flat surfaces and partial ribs throughout its structure. These features allowed for instrumentation to be easily mounted and secured inside the cavity.

4.7 Re-evaluation of Maximum Loading

As was previously mentioned the worst case loading was re-evaluated resulting in a reduction of nearly 33%. Reevaluating the stepped design with the new loads demonstrated the dramatically lower stress values expected. Since the airfoil was already being fabricated it was not possible to change the structure. The new loading did however allow for a key change in the mounting structure. By reducing the loads by a factor of three it was no longer necessary to fabricate the mount from aluminum 7075-T6. Instead more economical aluminum 6061-T6 could be used. Table 4.11

Table 4.11
Stepped Model Stress (Revised Maximum Loading)

Component	Material	Yield Strength (psi)	Max Stress (psi)	FOS
Leading Edge	6061-T6	40000	1081	37.0
Insert	Alloy Steel	90000	963	93.4
Non-Test Surface	6061-T6	40000	3027	13.2
Test Surface	6061-T6	40000	3888	10.3
Trailing Edge Strip	6061-T6	40000	356	112.4
Strut Plate	17-4 H-1025	170000	461	368.8
Lower Plate	17-4 H-1025	170000	871	195.2
Upper Plate	17-4 H-1025	170000	4382	38.8
Channel	6061-T6	40000	3831	10.4
Alignment Comp.	6061-T6	40000	13902	2.9

illustrates that by using a weaker material the reduced loading resulted in an increased FOS of the system to 2.9. The values for the individual components also soared. Outside of the alignment component no part was returning a FOS below 10. Recalling that these values are calculated to the yield strength and not the Air Force required ultimate strength clearly shows the safety of the design.

CHAPTER V

EXPLANATION OF FLUTTER CONCERNS

5.1 Development and Resolution of Flutter Concerns

One of the large concerns facing the design of a large test platform designed to hang from an aircraft wing is flutter. Flutter can be defined as a potentially destructive result of increase oscillation due to aerodynamic loading.

In order to decrease the risk of flutter the design needed to place the CG of the airfoil model in front of the elastic axis of the wing. At the time the elastic axis was believed to be at the 40% chord location of the wing. To accommodate this request the CG of the model need to be shifted forward. As previous sections have shown, counterweights could easily shift the airfoil CG to a suitable location.

All of these concerns would be eliminated after learning that the actual elastic axis of the aircraft is close to 25% chord. This was likely due to the fact that the support strut is tied into the front spar of the wing. With the elastic axis so far forward there was no way that the CG of the airfoil could be moved in front of this value. The forward location also meant that all munitions designed to be carried had CG's located beyond the elastic axis as well.

Even though the location of the airfoil CG with respect to the elastic axis was no longer a concern there were still concerns over the airfoils natural frequencies. The models appeared to have at least one frequency that was near the limit of either the engine RPM or the blade passing frequency. Reviews of the flutter report completed by the Cessna Corporation revealed that the primary flutter mode was observed at nearly 6 Hz. This mode involved the tail and boom structure of the aircraft. The report also noted

that the flutter characteristics of the aircraft were nearly independent of both fuel load and wing stores.

In order to verify the safety of the aircraft a conservative flutter flight test was planned (Saric, et al. 2006). In addition to this flight test the model would undergo an engine run up test prior to its first flight. This test would allow for the model to be visually inspected as the engine is swept through a variety of RPMs. Along with the visual inspection the model was flown with accelerometers during its early flights to ensure that there was no growing oscillation within the structure.

CHAPTER VI

ROCKER ARM AND PYLON ASSEMBLIES

6.1 Recognition of Potential Problem in Rocker Arm Assembly

Examining the simulations of the model and mounting structure exposed a dangerous situation at the restraints (Saric, et al. 2006). Those surfaces restrained to simulate the presence of a rocker arm, returned incredibly high reaction forces. In some simulations the resultant reaction force approached 2000 lbf. The final simulations on the stepped model with reduced loads returned reaction forces on the leading edge and trailing edge rocker arms of 1232 and 949 lbf respectively. With such a large force it was not possible to assume that the original rocker arms would be capable of withstanding the load.

Verifying the safety of the rocker arms began in a similar fashion to other aircraft systems. A model of the assembly was created (Figure A.36) as carefully as possible. This process revealed the first potential problem of the assembly, the weld on the C-channel. Only a few of the C-channels contained a reliable weld (Figure A.37). Most were quite poor, and there was no way to determine the effectiveness of the weld. The simulated assembly would use a variable radius fillet, but there was no way to model the actual part. It was also difficult to determine what materials were used to fabricate the original parts. Without knowing the true material any results would be based on a level of speculation.

6.2 Numerical Evaluation of Original Assembly

Applying the largest reaction forces to the pad at the base of the rocker arms revealed just how dangerous the system was. These forces were considerably greater than the final values as the simulations were conducted prior to the knowledge of the reduced

loading. Even without knowing the actual material, the maximum stress, 613,730 psi, was far beyond any likely material. Having made the assumption that the components were fabricated from steel with yield strength of 90000 psi, Figure A.38 shows large portions of the assembly that failed to achieve a FOS of 1.0. Among the most critical regions were the arm between the C-channel and the pylon. With four holes for adjustment the part was simply too weak to be able to survive the loading. It was also observed that the C-Channel had significant regions of failure.

6.3 Improvement of Rocker Arm Assembly

The results indicated that the original rocker arm assemblies could not be safely used with the airfoil model. In order to correct the failures of the original system a new system was designed (Figure A.39). This new system would rely on newly fabricated C-channels and arms to increase the FOS of the system above the mandatory value. These new components were fabricated from 17-4 PH condition H-1025 stainless steel. Using this material the yield strength of the new components was known to be 170000 psi.

The C-channel was fabricated from a solid block eliminating the need for a weld. Leaving a rectangular block that blended into the channel using a constant radius fillet produced the threaded section. The walls of the channel were thicker than its predecessor in an attempt to eliminate the large stress values seen in the previous design.

The redesigned arm focused on eliminating the need for multiple holes. Modeling the mounting structure revealed that the third hole on the original arm was the best option for mounting. Using this knowledge a new arm was created. The arm had the same profile, but only two holes, one to attach to the pylon and one to attach to the channel. Similar to the channel the arm was also fabricated to be thicker than the original component.

Simulating the new components revealed that the rocker arm system was significantly improved. The new components increased the FOS to 3.1. While the simulation cleared the rocker arm for use there was still a degree of uncertainty in the system. The material of the elevator bolt was still unclear, as well as the interaction

between the rocker arm assembly and the pylon. These doubts were eliminated after performing a series of static load tests to verify the system prior to flight.

6.4 Potential Pylon Concerns

Between the rocker arms and the hard points in the wing is a pylon structure designed to hold a bomb rack, and serve as the mating structure between any ordinance and the aircraft. Composed almost entirely of sheet metal, concern over survivability began to increase after learning about the intense forces acting on the rocker arms. These rocker arms are incorporated into the design of pylon, and are bolted into thin internal ribs.

Modeling the pylon (Figure A.40) proved to be quite difficult. The sheet metal components have dozens of holes of rivets, in addition to other openings. Due to the age of the components many had become damaged, making it difficult to obtain dimensions. There was also little knowledge as to what types of loading the pylon was designed to withstand.

In order to plan ahead for any potential problems the pylon to be used for the model, was reinforced (Saric, et al. 2006). First, the rivets that hold the C-channel to the pylon body was replaced (Figure A.41) with steel rivets. Second, a small piece of sheet metal was attached the side of the pylon skin (Figure A.42) to strengthen likely the location of buckling.

The third step was developed, although it would not be needed. This step included the replacement of the thin sheet metal ribs with solid blocks (Figure A.43). These blocks would greatly increase the stiffness of the pylon, while allowing for a much more rigid connection between the pylon and the rocker arm.

The concerns over the pylon would continue until the system successfully completed both static load tests. Following their successful completion the changes to the pylon assembly stopped. Prior to every flight the pylon is carefully inspected for any damage.

CHAPTER VII

SUPPORT STRUT

7.1 Design of Airfoil Support Strut

In order to eliminate some of the force being placed on the rocker arm assembly, as well as to stiffen the airfoil a strut was added to the back side. From the beginning the design of the strut was focused around the idea that the system should be fabricated in house with a minimum amount of outside fabrication required. By eliminating custom fabrication the strut profile began to fall to two separate profiles (Figure A.44). One was a Cessna 172 strut and the other a fairing available through an aircraft supply company.

The Cessna strut was considerably larger than the fairing profile, but the newly determined maximum loads reduced the required size of the profile. In addition to the reduced loads, there was no clear source for the Cessna strut. Although Cessna struts could be purchased used, the lack of knowledge concerning the struts history did not make this an attractive option. As a result the decision was made to move forward with the fairing profile, until it could be proven unsafe.

Complicating the strut design was the need to accommodate the potential change in model angle of attack. By turning the model the attachment point on the model shifts considerably, causing the angle and length of the strut to change. The change in angle was overcome by placing a ball joint at each connection point (Figure A.45). The ball joint would offer more than enough range of motion, and be strong enough to serve as the link between the strut and the mounting points.

By allowing for one part to be replaceable after changing angle of attack it was possible to overcome the changing length. All of the fastener locations at the tie down point would be fixed. This included the insert and the bolt pattern joining the insert to

the strut. At the model mounting point the strut would have a similar bolt pattern, but the insert (Figure A.46) would not be drilled until the system was assembled on the aircraft. In this way any dimensioning error would be allowed to stack up at this single point and be taken into account before the final fabrication steps. The process required that unique insert be made for each angle of attack. Since the profile of the insert does not change, only the location of the bolt holes several blanks were made prior to flight so that fabrication time would be minimized should the angle of attack be changed.

The fabrication of the strut revealed a unique problem. With a ball joint at either end of the strut, the component was free to rotate about the axis between the ball joints. The solution of the problem was solved by Shane Schouten, who observed that the ball joints have a nut incorporated into their design. By placing a small plate around the nut and attached to the mounting block the rotation was restrained.

7.2 Numerical Evaluation of Strut Design

Evaluating the strut design would prove to be a difficult process. Integrating the assembly into the model assembly created a situation that quickly surpassed the memory of the computer. Attempting to create a mesh over such a large part that also featured thin components became futile. In an effort to work around this problem the strut assembly was evaluated without integration into a larger system.

Without the model in the assembly it was necessary to obtain two pieces of information to evaluate the strut. First it was necessary to know what forces were acting on the strut at the model attachment point, and the second piece of information was the displacement of the strut. With these aspects known they could be applied to the strut assembly, simulating the effect of the model. The strut displacements were determined by taking the average deflection of the rectangular extrusion during simulations of the airfoil and mount with out the strut. The forces were determined by rerunning the airfoil simulations with a fixed restraint placed on the rectangular extrusion. The deflections and forces would then be applied to the same location in the strut assemblies.

While neither the deflections or forces represent the true values they can both be seen as approximations. The deflections being used are well below an inch, often times below 0.10. It was unlikely that the addition of the strut would radically change these values.

The force is a conservative value in that there was no chance the strut could see larger values than the ones applied. Since the strut cannot hold the base of the model fixed the actual forces at the attachment point would be less than those returned with the fixed restraint.

After applying the deflections and forces to the rectangular extrusion at the base of the assembly, restraints were applied to the top (Figure A.47). Two restraints were applied to the tie down block, the first prevents the top surface from moving in the normal direction and the second prevents the bolt hole from moving radially. These two restraints simulate the effect of the bolted connection between the strut and the tie down bracket attached to the spar.

7.2.1 Stress Analysis of Strut Assembly

Evaluating the strut assembly began by applying the reactions from the airfoil simulation with maximum loading. The results in Table 7.1 show that the majority of stress in the model is located around the ball jointed connections. While the maximum

Table 7.1
Strut Stress (Revised Maximum Loading)

Component	Material	Yield Strength (psi)	Max Stress (psi)	FOS
Mounting Plate	6061-T6	40000	1261	31.7
Model Block	6061-T6	40000	12567	3.2
Lower Shank	Bearing Steel	295000	17492	16.9
Lower Ball	Bearing Steel	295000	23804	12.4
Lower Insert	6061-T6	40000	9139	4.4
Strut	6061-T6	40000	3506	11.4
Upper Insert	6061-T6	40000	14725	2.7
Upper Ball	Bearing Steel	295000	33104	8.9
Upper Shank	Bearing Steel	295000	17493	16.9
Tie-Down Block	6061-T6	40000	12897	3.1

stress occurs in the ball joints (Figure A.48) the lowest factor of safety is found in the upper insert. The value of 2.7 is still well above the limit of 1.5 to yield and substantially above the air force required 1.5 to maximum.

7.2.2 Buckling Analysis of Strut Assembly

The strut is a long slender component and was therefore subject to buckling. In order to verify that no loading condition could cause such a situation a buckling analysis was done on he assembly. The analysis used results from a reverse loading scenario. Positive angles of attack would cause the strut to be placed in tension and would therefore prevent buckling. If the model were subject to negative angles of attack then loading would be oriented correctly for buckling to occur.

Knowledge of the airfoil indicated that at negative angles of attack the airfoil is only about 50% as efficient. With this knowledge a reverse set of loading was created using values for lift and drag of 275 pounds and 40 pounds respectively. The final load would again be the weight of the model and a comparison of values revealed that the 2G scenario was actually worse than 0.5G.

These loads were first applied to the airfoil models to obtain an approximate set of displacements and loads to employ on the strut assembly. With these values in place a buckling analysis can be run, and a buckling load factor (BLF) can be determined. The buckling load factor is the ration between the critical load, and the actual load. This ratio needed to be above 1.5 to agree with the required FOS. Completing the analysis revealed that the BLF for the strut was 3.7. The value was above the 1.5 required and fabrication of the strut began.

CHAPTER VIII

TIE-DOWN LOCATION

8.1 Evaluation of Tie-Down Bracket

With a strut in the design an additional aircraft component was thrust into the design process. One end of the strut interfaced with the tie down located further outboard of the model. Unlike the brackets examined previously the tie down location had no replacement components.

Examining the tie-down bracket revealed that it was not identical to the brackets used in the hard points. The tie-down bracket was made of thicker sheet metal, and also had a section of L-channel (Figure A.49) attached to its inboard side. It is likely that these differences result from the fact that the tie down bracket must be able to keep the aircraft stationary in severe weather.

The modeling of the bracket was similar to that of the four-bracket system, in that a section of skin and spar was used in the simulation. Assuming the rivets used to secure all of the components in the assembly were critical, the decision to use a node-to-node analysis (SolidWorks 2004) was used. This decision would require that the rivets be included in the simulation. Due to the fact that running a node-to-node analysis is extremely time consuming, it was decided to only include the rivets attaching the bracket to the L-channel and any component attached to the spar. Any other connection was assumed to be bonded.

The only restraints applied to the system were fixed restraints on the cut surfaces of the spar, skin, and spar caps. These restraints assume that the assembly is a small section of a larger system, and that the overall system is not affected by the strut loading. The loads applied to the system came directly from simulations of the strut assembly.

The reaction forces at the tie down bolt location were applied to corresponding surfaces in the tie down assembly.

Results of the simulation revealed that the tie down assembly was capable, FOS 4.8, of withstanding the loading caused by the strut. The results in Table 8.1 revealed

Table 8.1
Tie-Down Assembly Stress Analysis

Component	Material	Yield Strength (psi)	Max Stress (psi)	FOS
Tie-Down Bracket	2024-T3	50000	10405	4.8
L-Channel	6061-T6	40000	6340	6.3
Spar	2024-T3	50000	9915	5.0
Upper Spar Cap	2024-T3	50000	5521	9.1
Lower Spar Cap	2024-T3	50000	5902	8.5
Upper skin	2024-T3	50000	2275	22.0
Lower Skin	2024-T3	50000	7292	6.9

that the tie down bracket was by far the weakest component. With the factor of safety knowledge it was determined that there was no need to replace the bracket at the tie down location.

CHAPTER IX

EVALUATION OF BOLTED CONNECTIONS IN THE MOUNTING STRUCTURE

9.1 Preloading of Model Fasteners

There are a variety of fasteners that join the airfoil components together. Each of these bolts was given an assigned torque to ensure the safety of the system. An analysis for determining the safety of the bolted connections in the mounting structure was outlined by Timothy Silverman (2005) in his report. An identical analysis will be used to demonstrate the safety of the mounting structure in its final form.

The bolts joining the two main halves of the airfoil are ¼-28 socket head cap screws. Each of these eleven bolts is torqued to 180 lb*in. The individual weights of either half is not sufficient to shear even one bolt, indicating that there is little chance of all eleven failing in shear. The bolted connections could separate under the lifting force if it is greater than the preload. Using

(9.1) $T = KF_iD$

and the assumption that K≈0.3 for fasteners with a black oxide finish (Mischke, et al. 2002), it is possible to determine the approximate preload of each bolt to be 2400 lb. With the lifting force distributed over each fastener this indicates only 50 pounds per fastener, well below the preload value.

The leading edge is held in place by a series of seven ¼-28 socket head cap screws which enter through the non-test side of the leading edge, pass through both of the main half components and thread into the test side of the leading edge. These bolts are torqued to only 70 lb*in. The dramatic decrease in torque is a result of the hollow airfoil structure. During inspection of the airfoil it was observed that by increasing the torque on the leading edge fasteners one could compress the components, and create a

significant deflection. To avoid deforming the airfoil shape and also allowing for allowing for repeatable torquing the value was set significantly lower. Using (9.1) it is observed that even with the lower value each bolt is still applying over 900 pounds of clamping force.

The 10-32 screws and bolts fastening the plates to the model are all torqued to 25 lb·in. Failure in these regions would likely be a result of loosening due to vibration. The fasteners are not needed to overcome any of the torques or loads produced by the lift or weight of the model.

The two components of the mount are fastened together by 5/16-24 bolts torqued to 110 lb·in. The most probable cause of failure in the joint is the separation of components due to a 2G maneuver. With each bolt applying over 1900 lbs of clamping force there is almost no chance that the 440 pounds of weight experienced would result in failure.

9.2 Bolt Analysis of Mounting Structure

The original design of the mount was based around a maximum lifting condition of 120 lb. From this, Silverman (2005) designed a system which relied on a main bolt to overcome joint failure. Any additional hardware was auxiliary. His analysis showed the ability of the main bolt to survive the three most likely failures of joint prying, joint sliding, and model rotation. A similar approach will be used to demonstrate the safety of the final design.

The preload on the main bolt must be greater than the forces acting upon it (Bickford 1981). If this condition is not met the joint will separate and likely fail. Determining the forces acting on the main bolt is done by multiplying the aerodynamic forces by an appropriate lever arm and then dividing by the distance the main bolt is from rotation. The lift force is centered approximately 21 inches below the bolt and the model half span is 3 inches. Using a maximum lift of 550 lb creates 3850 lb acting on the bolt. The drag is also located 21 inches below the bolt, and the trailing edge of the mount is 11.18 inches behind the bolt. With 40 lb of drag the force on the bolt is 75 lb.

The weight of the model is in line with the bolt and therefore during a 2G maneuver the force on the bolt is nearly 440 lb. Summing the forces produces 4465 lb attempting to separate the joint. The bolt is preloaded to 18400 lb resulting in a FOS of 4.1 against joint separation.

Joint sliding is a measure of the shear force acting on the bolt. By determining the resultant of the lift and drag, 551.5 lb, it is possible to determine the likelihood that the forces will cause misalignment of the model. Assuming that the coefficient of friction between aluminum and steel is approximately 0.3 the force required to break the joint free can be found by (Bickford 1981),

$$F_{fail} = \left(F_i - F_p\right)\mu \tag{9.2}$$

Using (9.2) the force required to cause sliding is 3970 lb. The aerodynamic loading is more than 7 times smaller than the required loading.

The final failure mode investigated was the ability of the bolted connection to resist the model torque. With the ability to alter the angle of attack of the airfoil it is necessary to ensure that the aerodynamic loading will not cause a sudden change.

The airfoils center of lift occurs at approximately 30% chord. At the mid span this point is 5.82 inches in front of the main bolt location. This creates 266.75 lb·ft of torque.

Determining the torque required for failure is done by determining the value of the torque generated by the frictional force of the bolt (Bickford 1981).

$$\tau_{fail} = \left(F_i - F_p\right)\mu r_\mu \tag{9.3}$$

The coefficient of friction is again assumed to be 0.3 and the radius of the washer, r_μ, is assumed to be 0.7 inches. Placing these values into (9.3) reveals that the jointed connection will rotate at 243.9 lb ·ft. This would indicate that the FOS against rotation is only 0.91.

In order to achieve the necessary FOS the support bolt which is neglected in Silverman's analysis must be included. The support bolt force acts 8 inches from the axis of rotation and is assumed to have an identical coefficient of friction. With the prying

force already subtracted from the main bolt F_p is set to zero. By applying 40 lb·ft to the bolt the preload is determined to be 4800 pounds through (9.1). Taking this result and inserting it into (9.3) produces 960 lb·ft of torque. The two bolts produce a total of over 1200 lb·ft of resistive torque. This value is significantly above the torque created by the lifting force creating a FOS of 4.5.

The analysis of the fasteners reveals that the connection between the mounting structure and airfoil is adequately safe. It is important to note that the eight 10-32 bolts are never taken into account during the analysis, and that they provide even more safety. Like many of the other calculations and results a series of static load tests would verify the confidence in the joint.

CHAPTER X

STATIC LOAD TESTS

10.1 Preliminary Static-Load Test

Designed to verify the numerical results gathered over several months, static testing of the airfoil system would be done in two tests. The first test would evaluate the mounting structure and strut, without risking the airfoil model or aircraft. The second test would be done on the entire system. The loading for the static load tests was based on 1.5 times the maximum values. This required that a system be able to survive 800 pounds of lift and 600 pounds of weight. Drag was ignored during the testing, as it was an order of magnitude smaller.

The initial static-load test required that a substitute airfoil model and aircraft be created. The mounting structure and strut could then be attached and tested. The replacement aircraft was provided by Dr. Keating and the civil engineering department. Rather than use an aircraft, the system was evaluated in the civil engineering lab. The aircraft was simulated by bolting the system to the floor of the facility (Figure A.50). In doing so the system was inverted. In addition to the facility Dr. Keating provided the load cells and technicians to perform the testing.

The replacement model (Figure A.51) was created from an S6X17.25 I-beam. A plate was attached to either end of the beam to allow for it to be connected to the mount and the strut. Smaller gusset plates were added to ensure that the beam would not fail during testing.

With the system bolted into the floor of the facility two load cells were attached to the assembly (Figure A.52). One would pull on the beam at a location that matched lifting location of the model. The second would pull up on the model simulating a multi-

G maneuver. The loads were slowly stepped up to their final values, and at each step the system was inspected. Once the loads on the system were approximately 1.5 times the maximum scenario, they were left applied for several minutes. This was done to ensure that the system could support the loading for more than a few brief moments.

During the test it was observed that the lifting force does pull the model, causing separation between two of the rocker arms and the alignment component. With no observed failures the test was considered a success and plans were made to prepare for the second static test.

10.2 Final Static Load Test with Model and Aircraft

The second static load test was conducted with the model, mounting structure, strut assembly, and aircraft. With all model systems installed the aircraft was moved to a secure location. The loads were again applied to the system via two load cells. One was placed below the model in line with the CG. The other was placed in a jig (Figure A.53), created by Cecil Rhodes, which held it in line with the lifting force.

Once everything was in place the load cells were again slowly steeped up until the desired loads were reached. Approximately halfway through the test it was observed that the tie down location was not performing as expected. A close inspection of the bracket system revealed that the skin was separating from the spar cap (Figure A.54). Testing was halted while the problem was studied and ultimately the loads were removed while the problem was corrected.

The separation in the tie down was unexpected because the simulation of the assembly assumed that the spar cap was bonded to the skin. With most of the attention focused on the survivability of the bracket, no rivets were added to hold the spar cap to the skin. This assumption was used to save computational time, and proved the necessity of static testing.

The solution to the problem was a small steel clip that would fit around the tie down bracket inside the wing and be secured by several screws (Figure A.55) passing through the clip, spar cap, skin, and into the tie down block. With the clip in place the

testing was resumed. The clip prevented the earlier observed separation and allowed the loading to progress to the test values.

The static load testing confirmed that the model would not damage the wing box structure of the aircraft. The testing verified that the airfoil model and all supporting structures would be able to endure the expected conditions. Verification that the pylon could support the lifting loads with the new rocker arms officially confirmed that no additional modifications were necessary. The bolted connections between the airfoil and the mount were also successful supporting the results outlined by Timothy Silverman in his mount design.

CHAPTER XI

CONCLUSIONS

11.1 Recommendations

Following several assemblies of the model, it became clear that it would have been beneficial to have etched lines into the top of the upper plate (Figure A.56). It is not a simple process to verify that the mount is attached in a manner such that the model will be at 0° angle of attack. As a result it is even more difficult to verify any other angles of attack. While the adjustment mechanism was designed to simplify the process it is not perfect. It would have been simple to etch lines at each angle of attack adjustment from -5° to 5° while the component was already on a CNC mill.

Another aspect of the model that could have been improved during the design process was the interior, stepped structure. The structure was developed in a compressed time frame and not all possibilities were considered. Among those designs not focused on, one of the more interesting was the use of uneven steps. In the final design each step was 2 inches wide. In regions of high curvature, this created a step that went from the minimum 0.1875 inches thick to almost 0.75 inches thick. In order to reduce weight it would have been possible to design a stepped structure that defined the minimum and maximum thickness of each step, and allow the width to be uncontrolled. The process would have created more steps in regions of high curvature and few steps where the model flattens out.

Another interior feature that has caused some undesired effects during testing is the use of the partial ribs and spars to stiffen the model. Thermal analysis of the model showed that these regions cool down far slower than the rest of the model. As Figure A.57 shows the regions associated with internal support are still several degrees warmer

than the rest of the model even 20 minutes after the model has been exposed to colder air. This causes the cold soak prior to testing to take nearly 30 minutes. If the structure was moved to be outside of the test section then it may be possible to lower the cold soak time and speed up the testing process.

With the cost of aluminum increasing it may be beneficial to investigate the use of alternative materials. Although composite materials were rejected early in the process due to their potential inability to hold tolerances and interface with pressure ports, they may be able to be used for other components. These components could include the mounting structure as well as the plates that bookend the model.

During meetings with engineers at Tri-Models it was proposed that the non-test side be rapid prototyped. The concept was never developed due to the time frame, and no research had been done into this area. Since the non-test side does not have many of the requirements of the test side, it may be possible to utilize this technology. Rapid prototyping of the component would save machine time, but it is unknown what type of surface finish could be achieved, as well as the materials performance in the flight environment.

11.2 Conclusions

Even though there are a number of potential ways that the model design could be improved, the fabricated model achieved its goals. None of the aircraft systems have been compromised by flying with the airfoil model. The test platform has flown on many occasions without incident. When testing completes the airfoil model and all support structure can be removed leaving the aircraft ready for whatever future testing is needed. This demonstrates the true success of the design; a safe test platform that can be attached, flown and safely removed without permanently affecting the aircraft.

The removable leading edge has been utilized with great success. With testing requiring both pressure ports, and a clean, smooth surface, the ability to have a leading edge for each requirement has demonstrated the advantage of the unique system. In addition to the leading edge the flat surfaces of the model proved to be advantageous.

Mounting both the pressure scanner and the accelerometer benefited from the flat surfaces throughout the inner cavity.

REFERENCES

Bickford, John H. *Introduction to the Design & Behavior of Bolted Joints*. Marcel Dekker, Inc., New York. 1981.

Blevins, Robert D. *Formulas for Natural Frequency and Mode Shape.* Van Nostrand Reinhold Co., New York. 1979.

Gideon, Mike. Personal Communication. Tri-Models, Inc, Huntington Beach, CA. August 2005.

Johnson, Bill. Personal Communication. Athena Manufacturing, Austin, TX. October 2005.

Mischke, Charles R., and Shigley, Joseph Edward. *Mechanical Engineering Design*. 5th Ed. McGraw Hill., New York 2002.

Saric WS, Carpenter AL, Hunt LE, McKnight CW, Schouten SM. 2006b "SWIFT – Safety Analysis for Swept-Wing Experiments." *TAMUS-AE-TR-06-002*, Technical Report, January 2006.

Silverman, Timothy. *Design and Safety Analysis of a Model-Mounting Structure for the Cessna O-2 Aircraft.* Honor's Thesis, Department of Mechanical and Aerospace Engineering, Arizona State University, Tempe, AZ. 2005.

SolidWorks, Software Package, Ver. SP03.1, SolidWorks Corporation, Concord, MA, 2004.

APPENDIX A
FIGURES

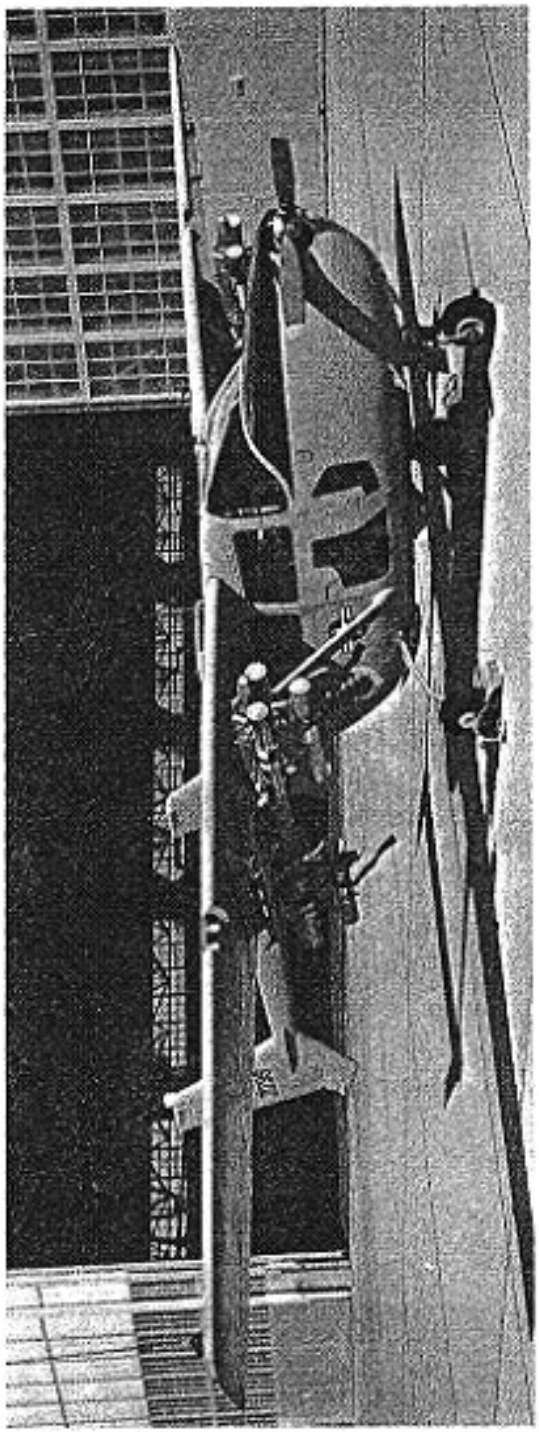

Figure A.1 Cessna O-2 with Multiple Wing Stores

Figure A.2 Pylon Bracket System Removed From Aircraft

Figure A.3 Visual Comparison: Original Bracket (Left) and Replacement Bracket (Right)

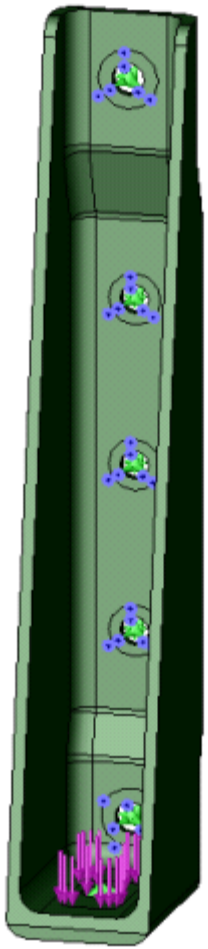

Figure A.4 Load Application (Magenta) and Restraints (Blue and Green) for Individual Bracket Analysis

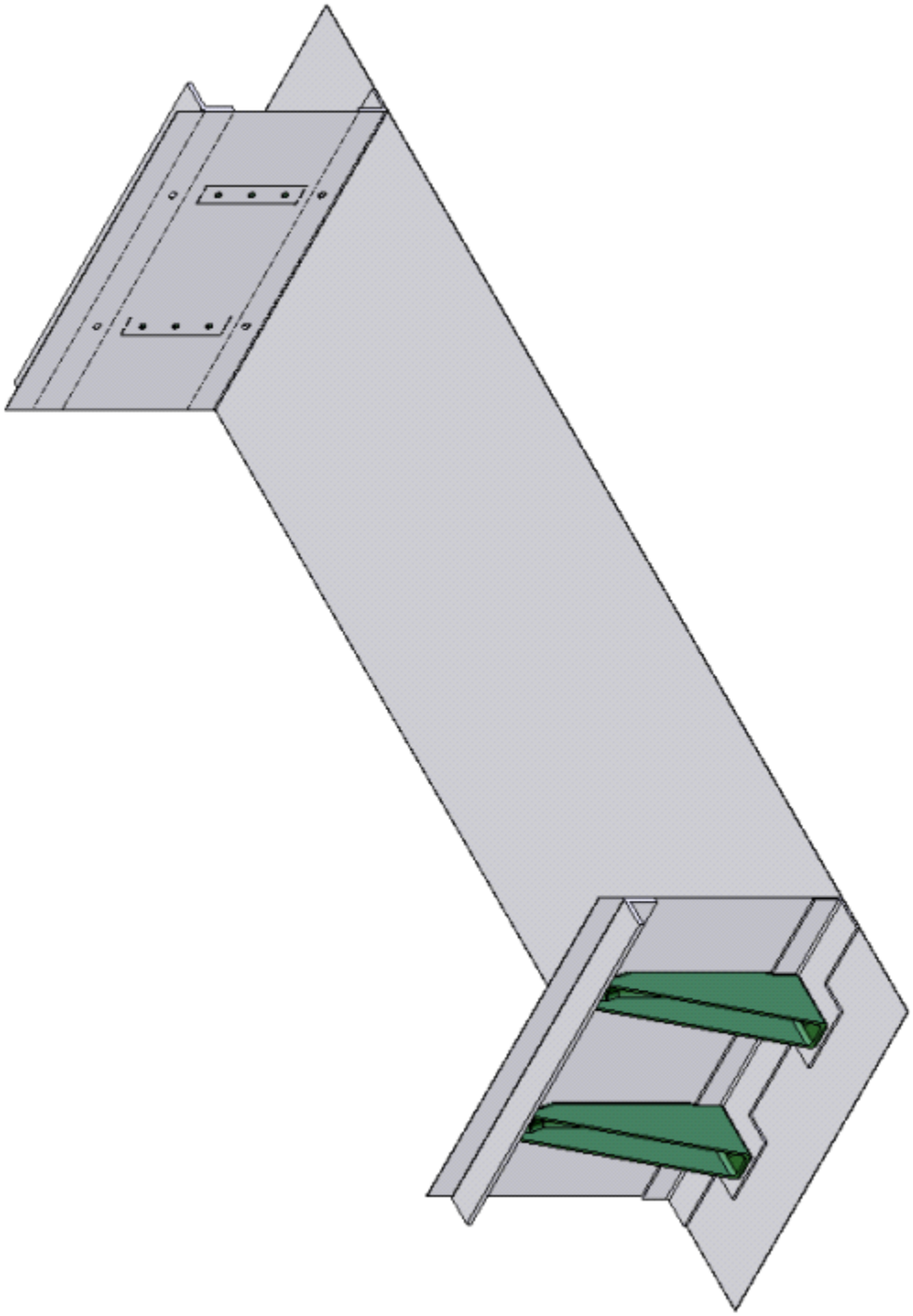

Figure A.5 Outboard Pylon Bracket System

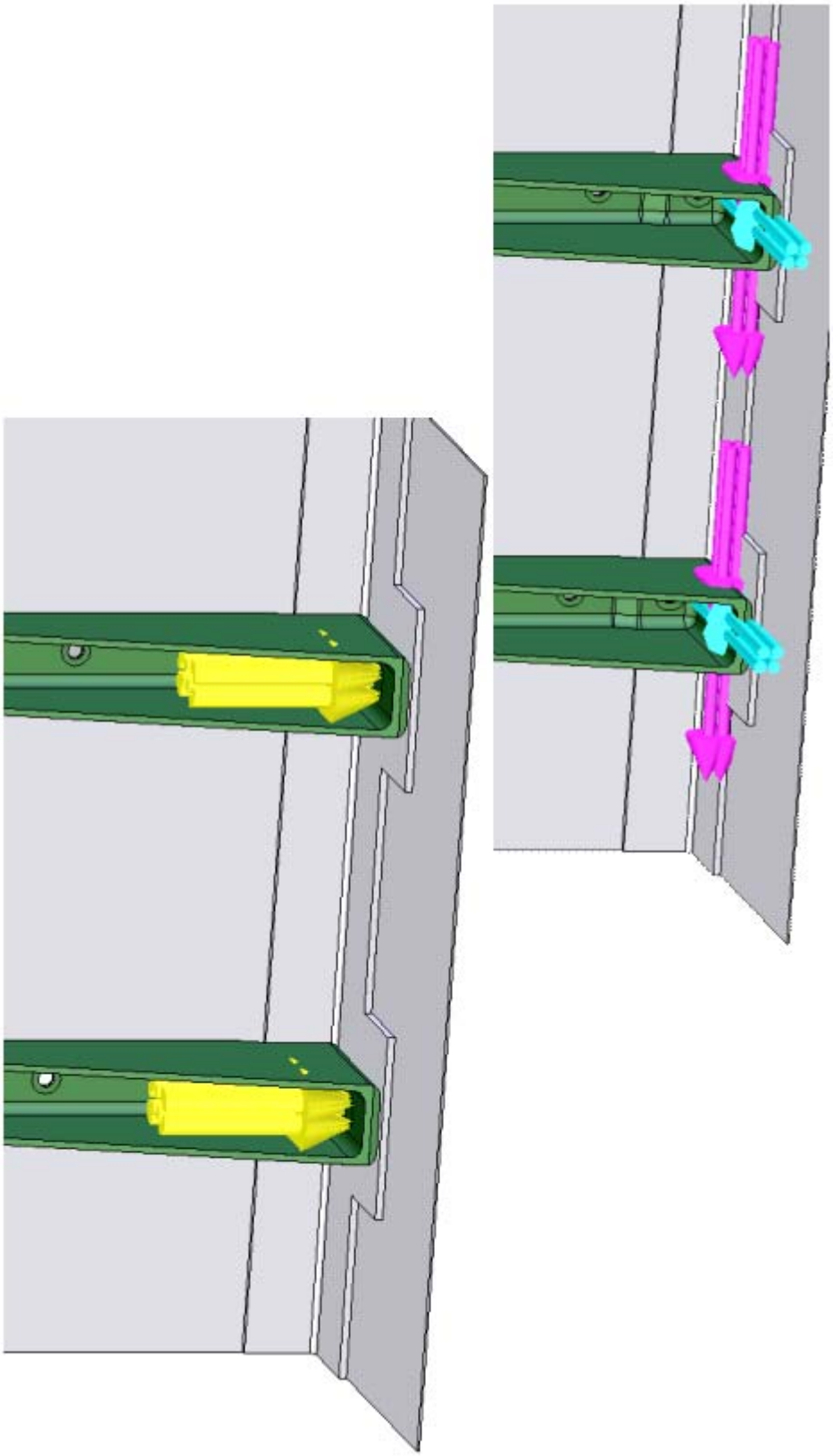

Figure A.6 Application of Lifting (Magenta), Drag (Cyan), and Gravitational (Yellow) Forces to the Four Bracket System

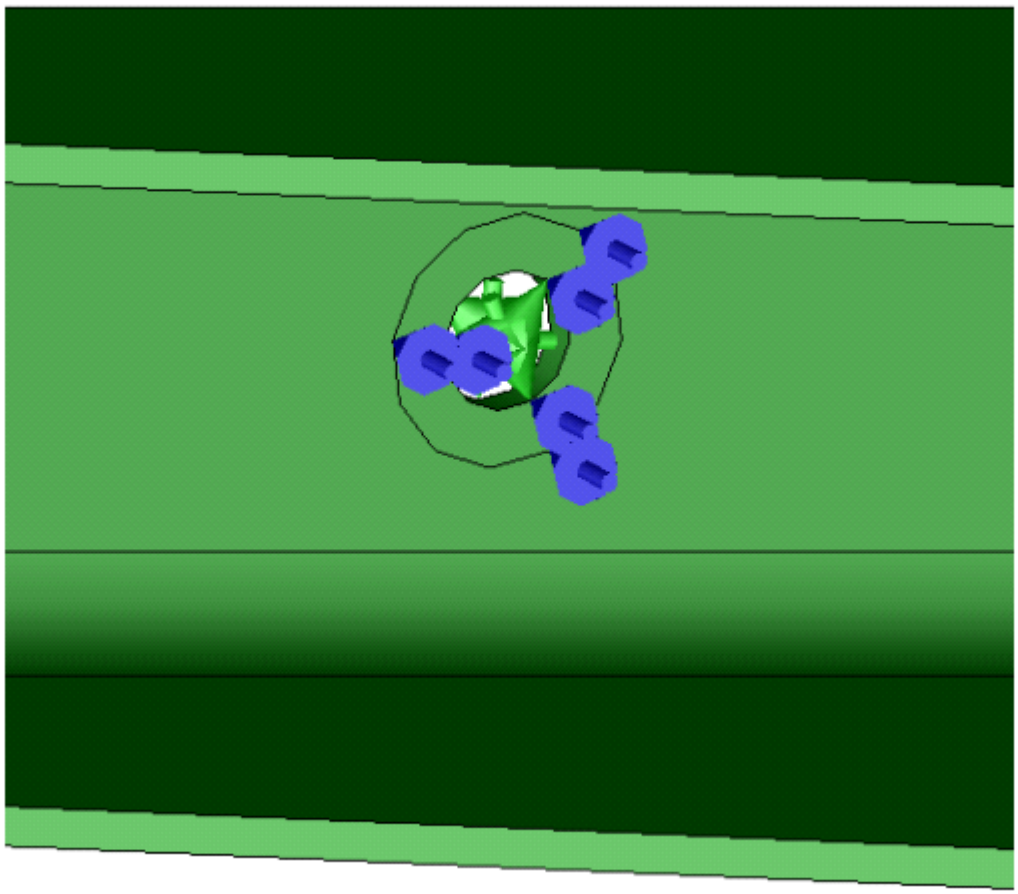

Figure A.7 Restraints Applied to Each Bracket Hole in the Four Bracket System

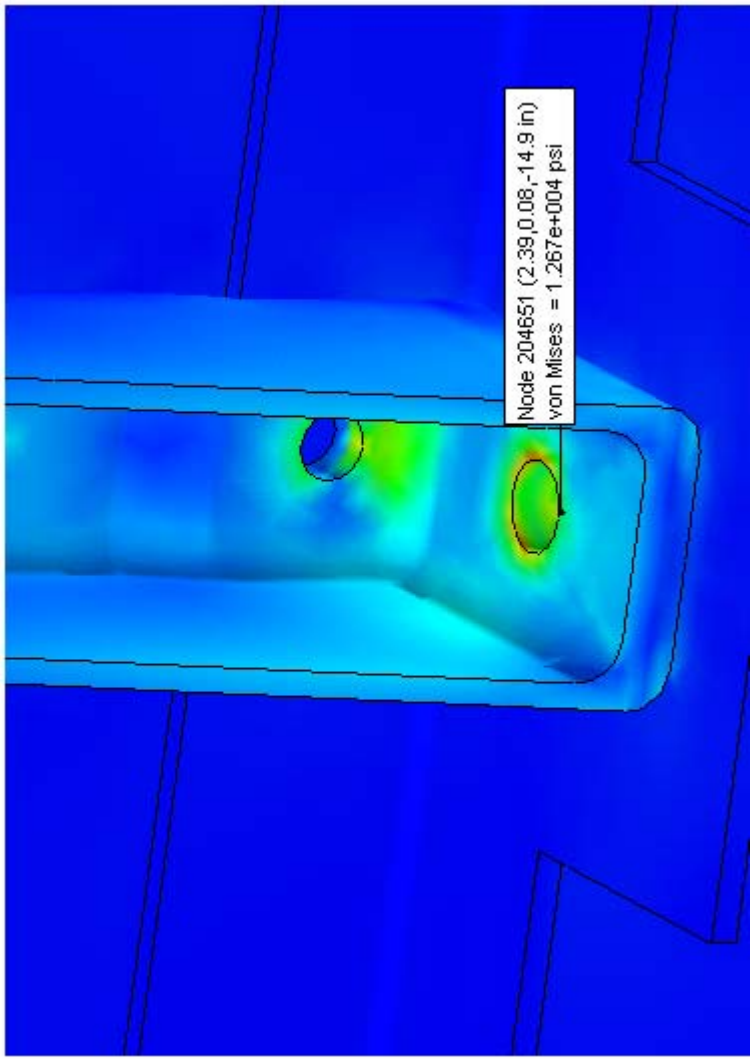

Figure A.8 Stress Concentrations Leading to Minimum Factors of Safety

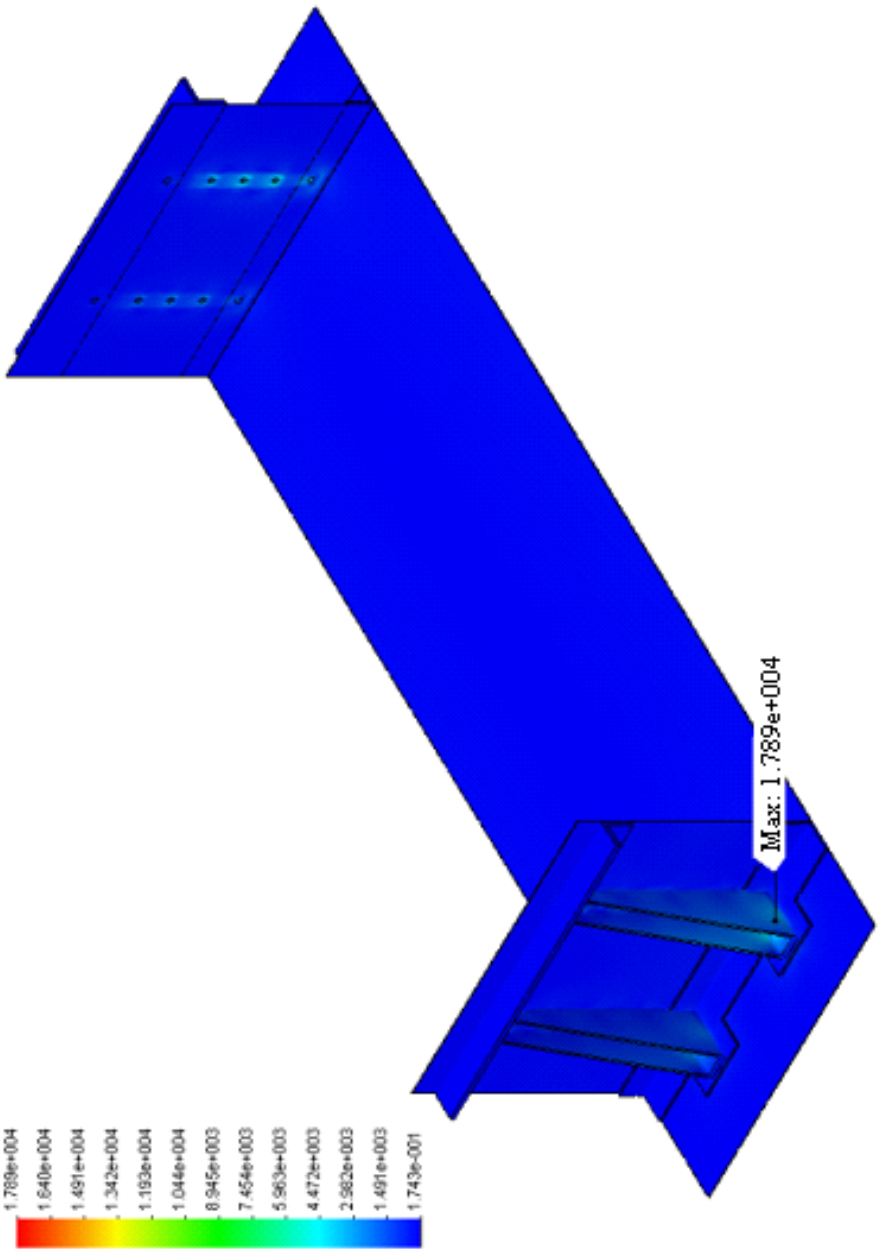

Figure A.9 Maximum Stress in the Four Bracket System

Figure A.10 Airfoil Mounting Structure

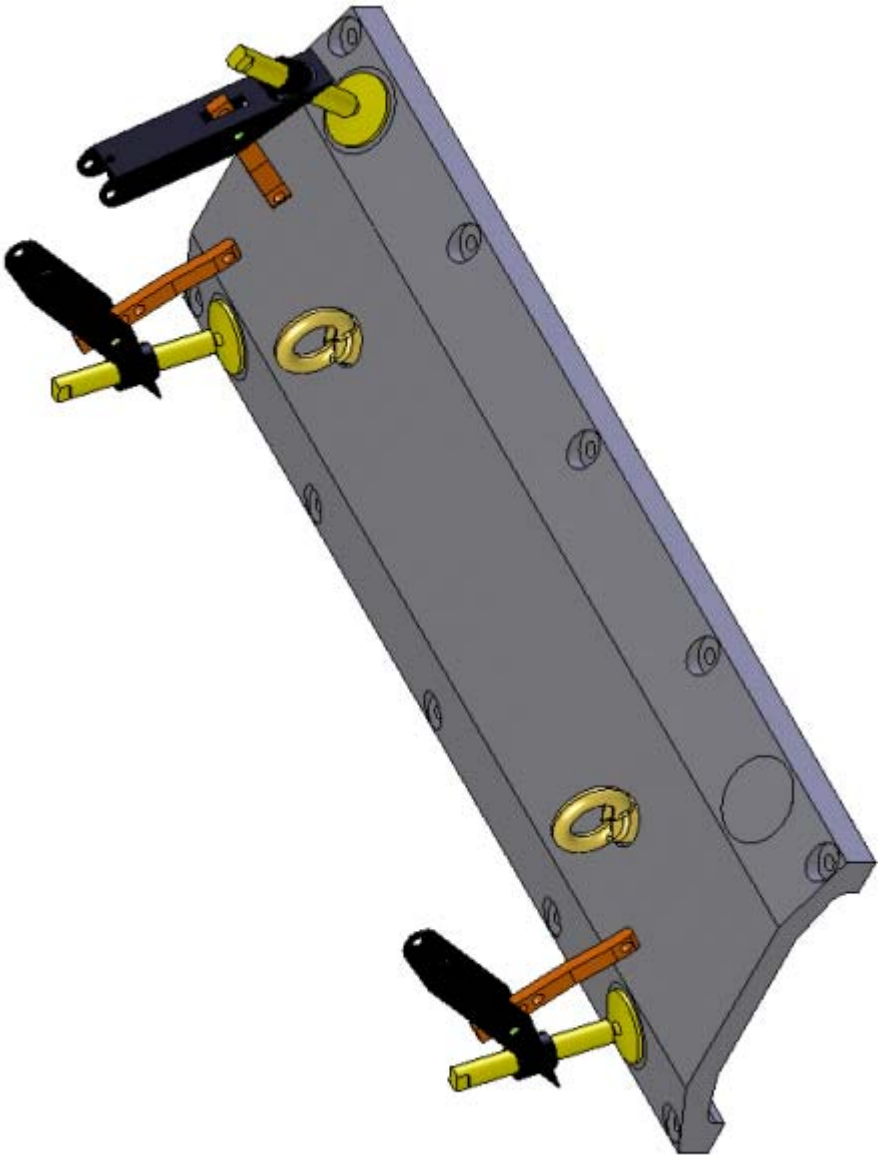

Figure A.11 Alignment Component with Three Rocker Arm Assemblies and Eye Bolts

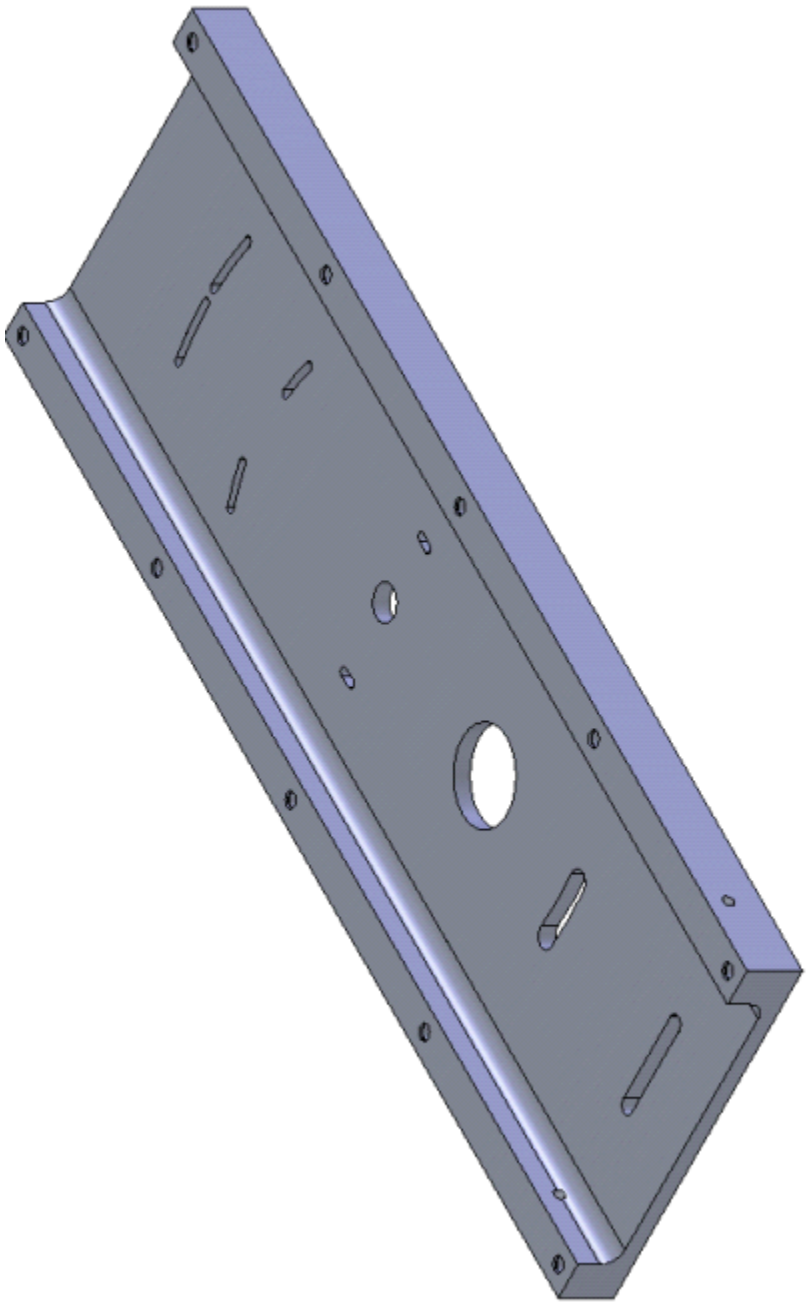

Figure A.12 Mounting Channel

Figure A.13 Arcs Allowing for Mounting into Top Surface of Airfoil

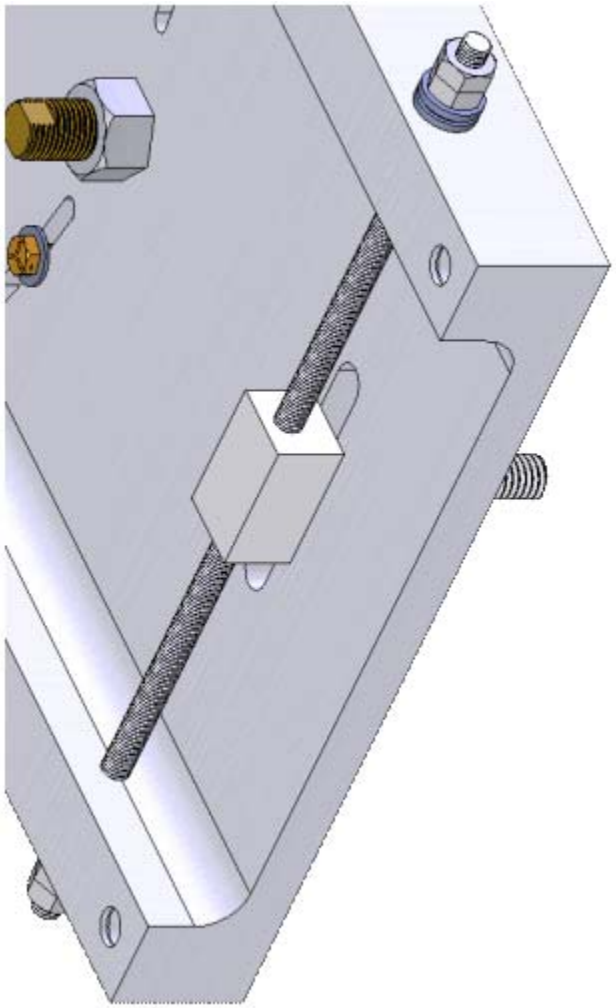

Figure A.14 Angle of Attack Adjustment Mechanism

Figure A.15 Support Bolt

Figure A.16 Two-Inch Diameter Wiring Hole

Figure A.17 Main Bolt Before and After Preloading with Jack Bolt

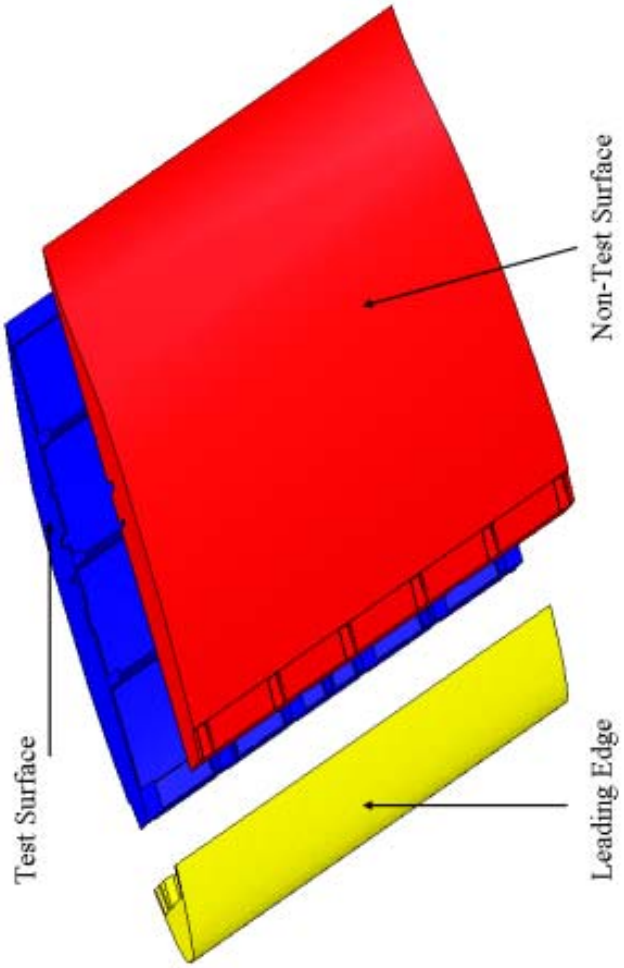

Figure A.18 Components in Three Piece Design

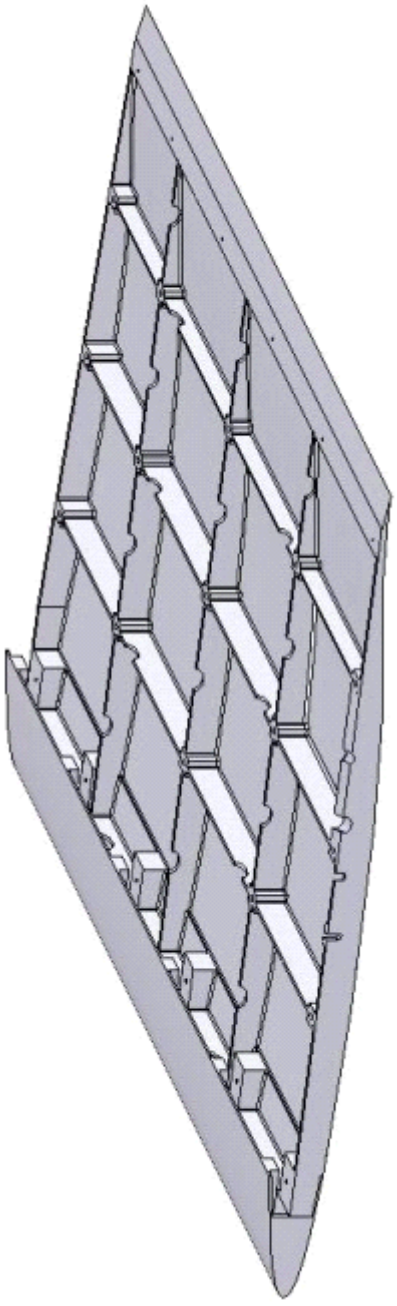

Figure A.19 Pocketed Model Showing 4X4 System of Weight Removal

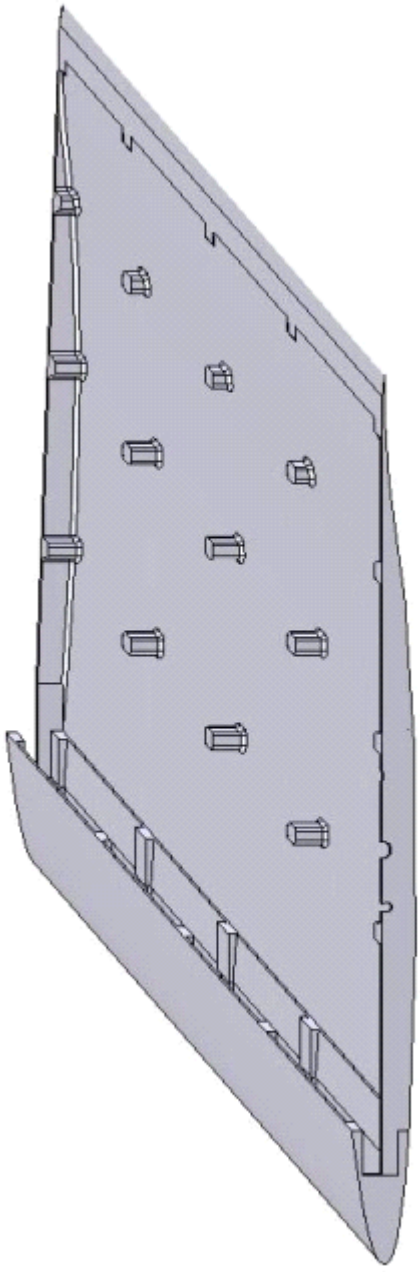

Figure A.20 Shelled Model Without Test Surface

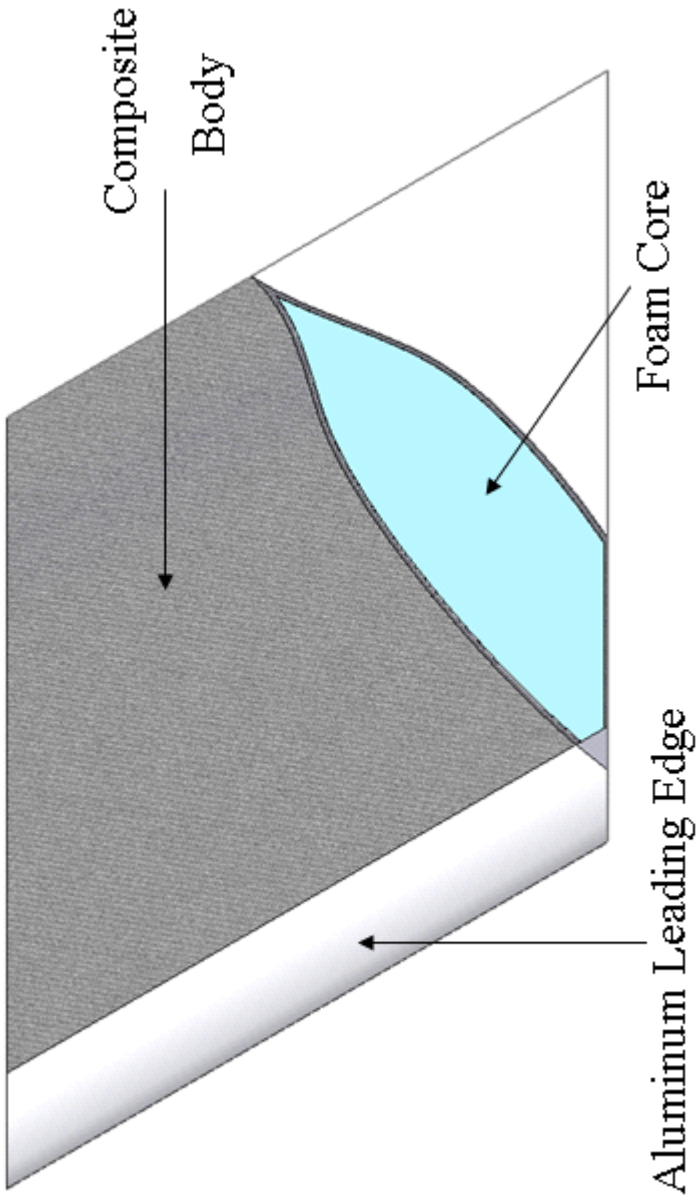

Figure A.21 Composite Airfoil Model

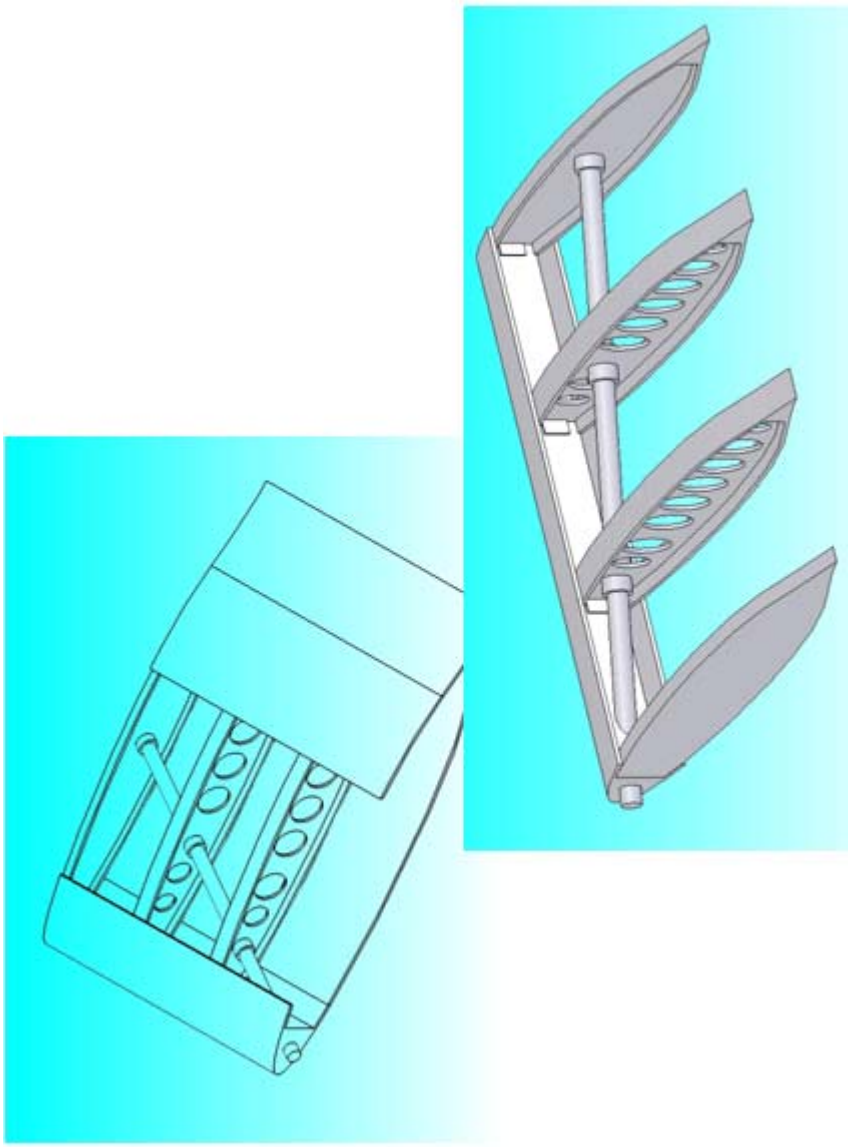

Figure A.22 Airframe Design Illustrating Rib and Skin Panel Design

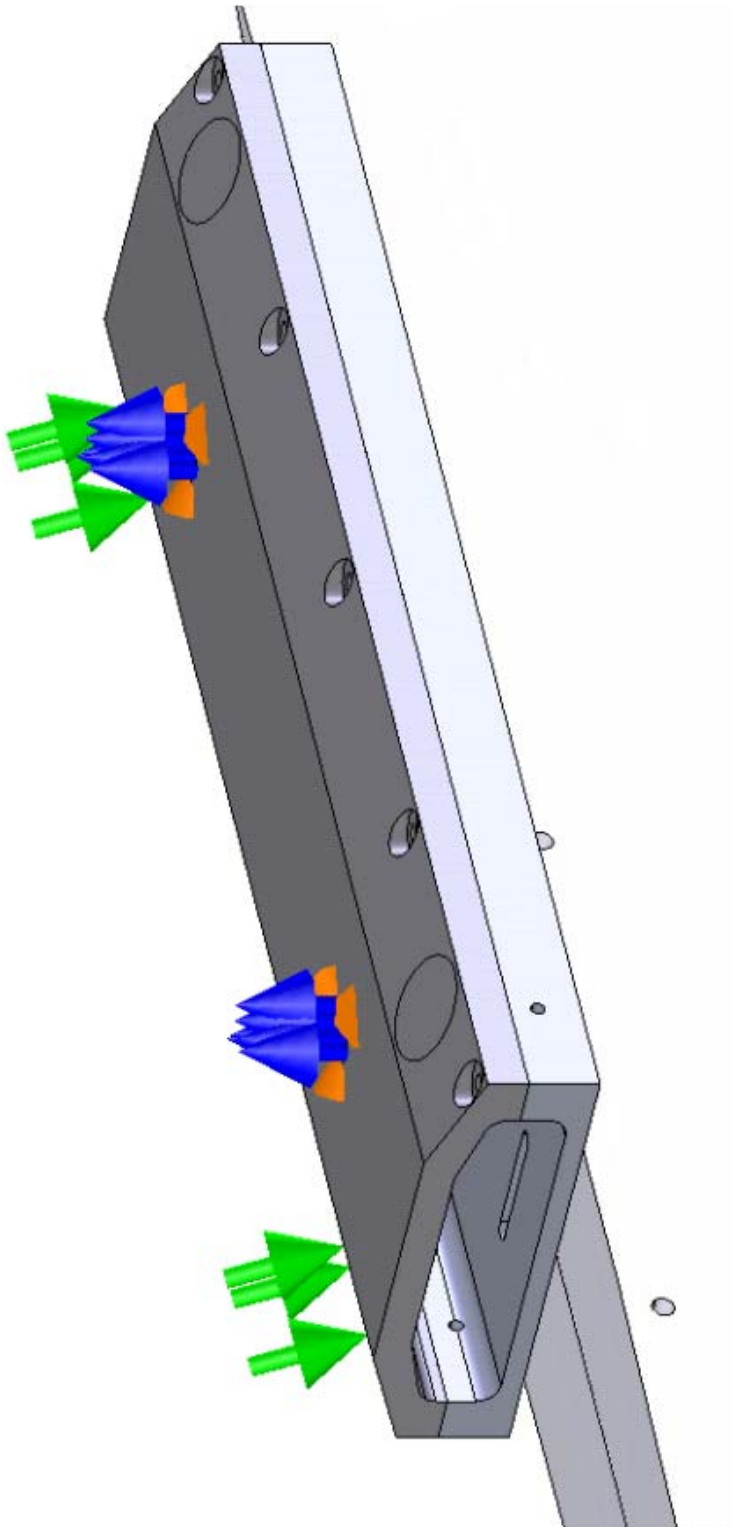

Figure A.23 Restraints Applied to Airfoils After Integration of Mounting Structure

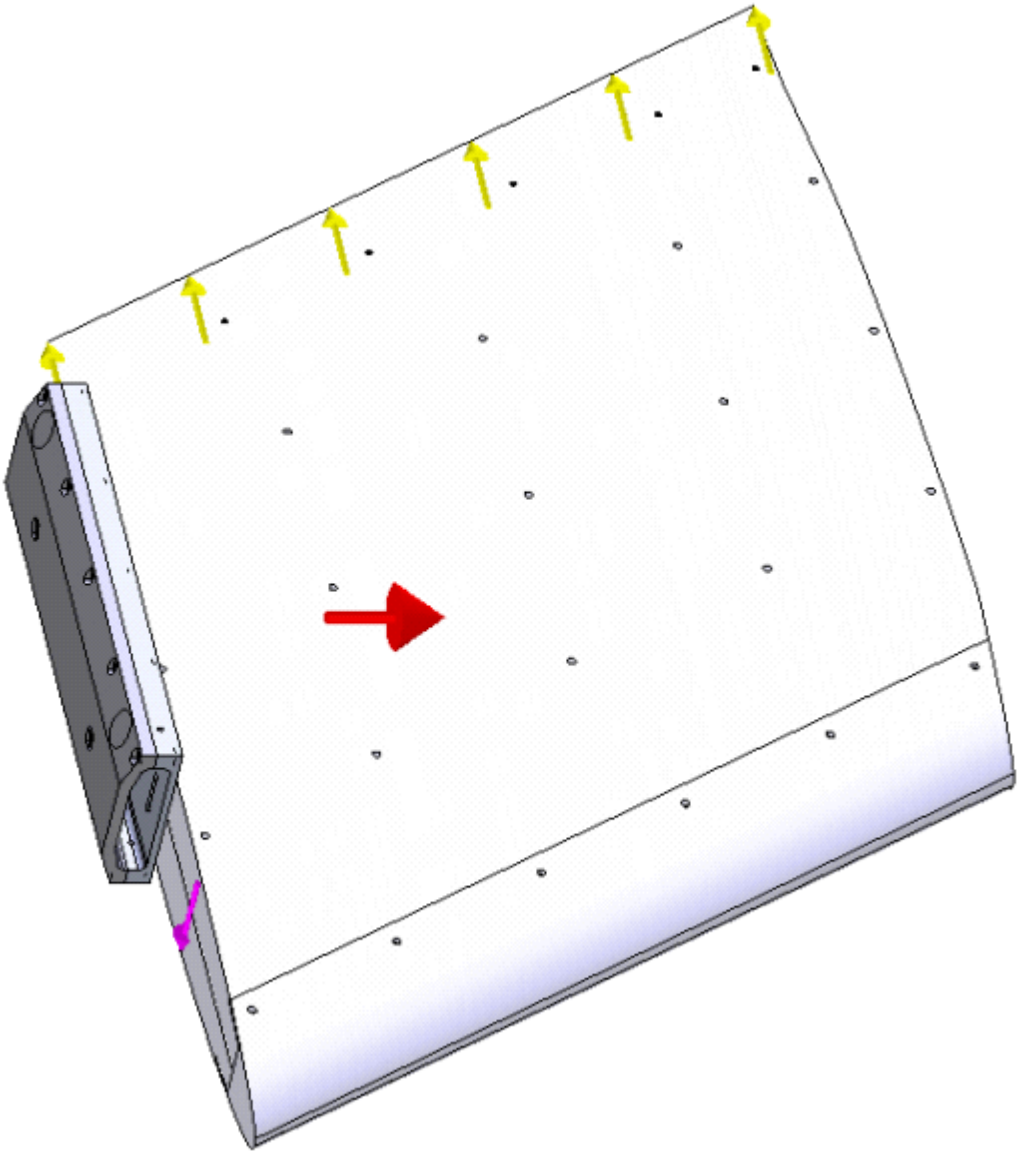

Figure A.24 Force Application for Airfoil Model Evaluation

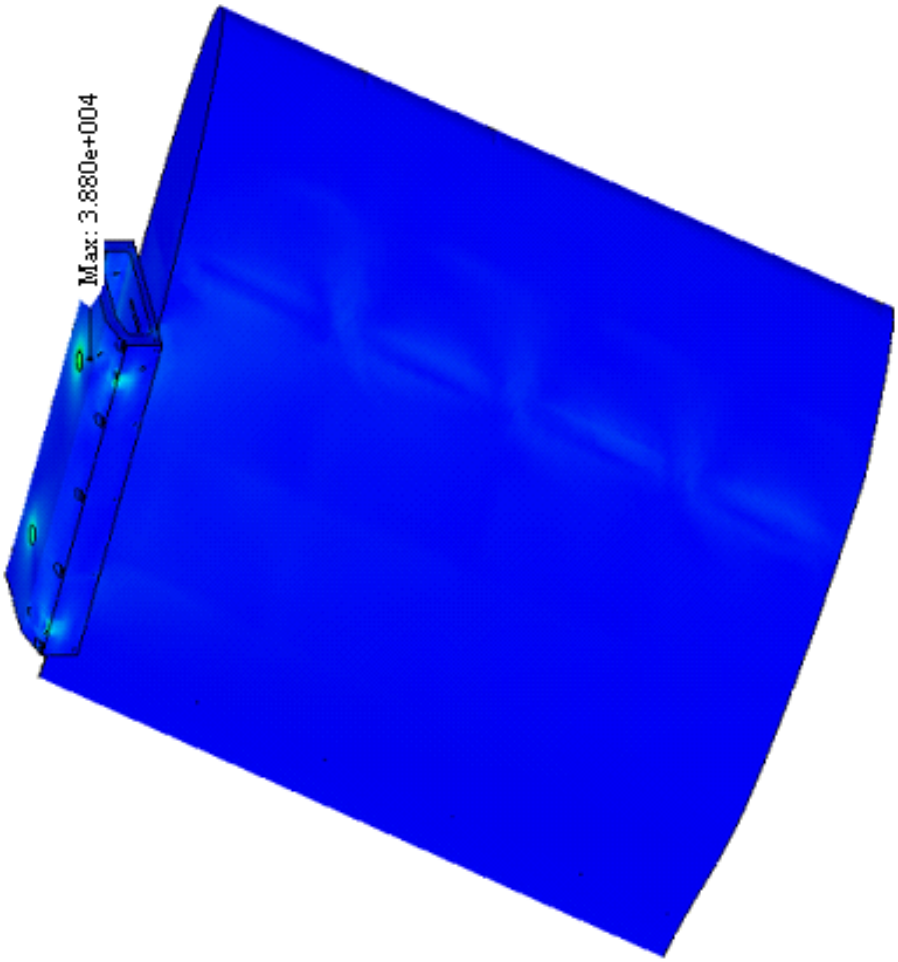

Figure A.25 Stress Analysis Results of Pocketed Model under Maximum Loading

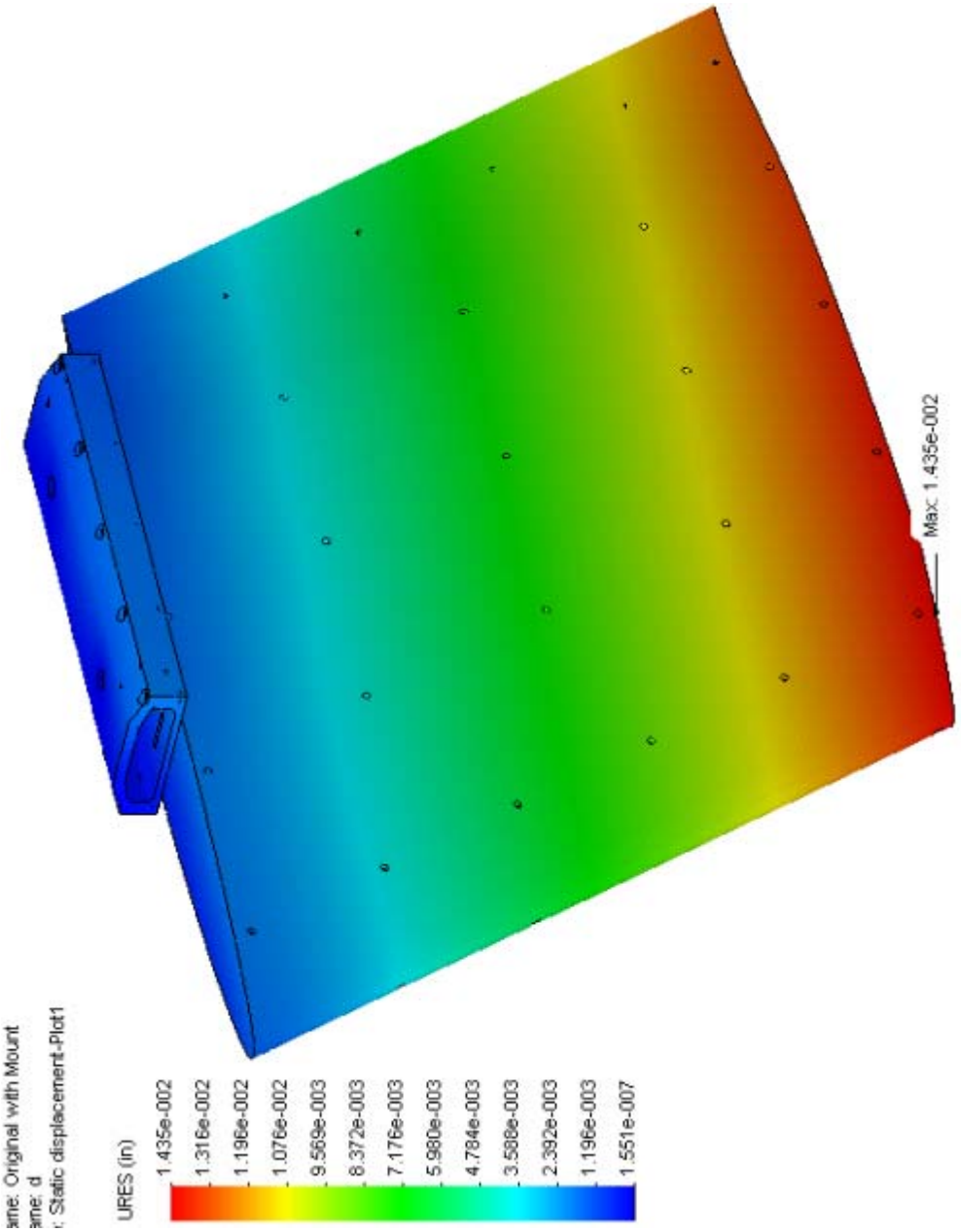

Figure A.26 Uniform Deflection of Pocketed Model under Maximum Loading

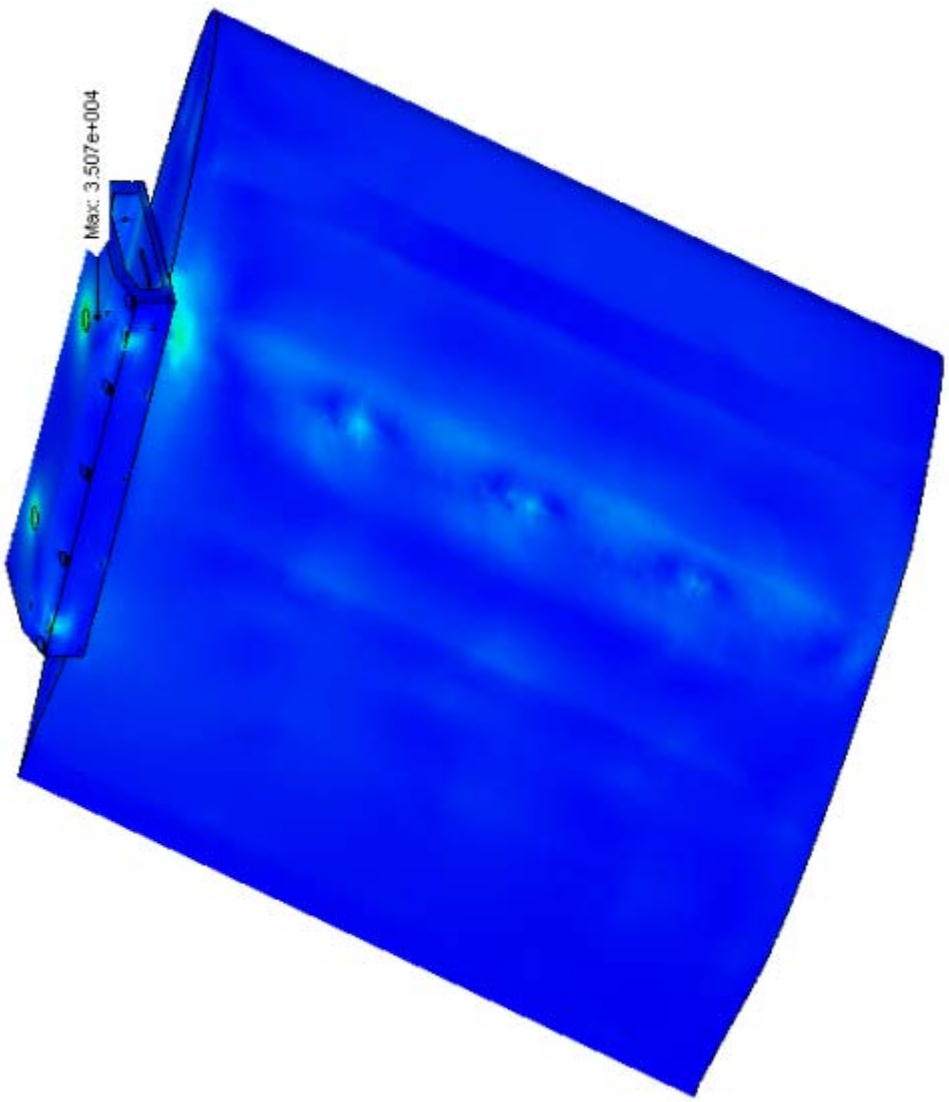

Figure A.27 Stress Analysis Results of Shelled Model under Maximum Loading

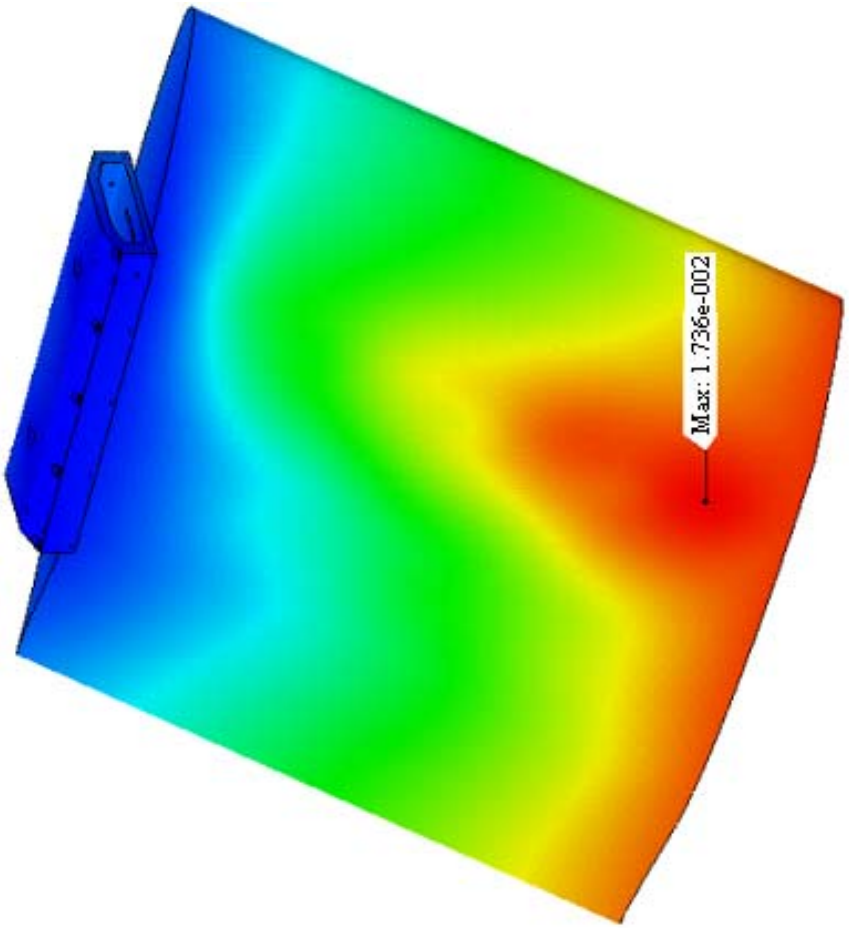

Figure A.28 Deflection of Shelled Model due to Maximum Loading

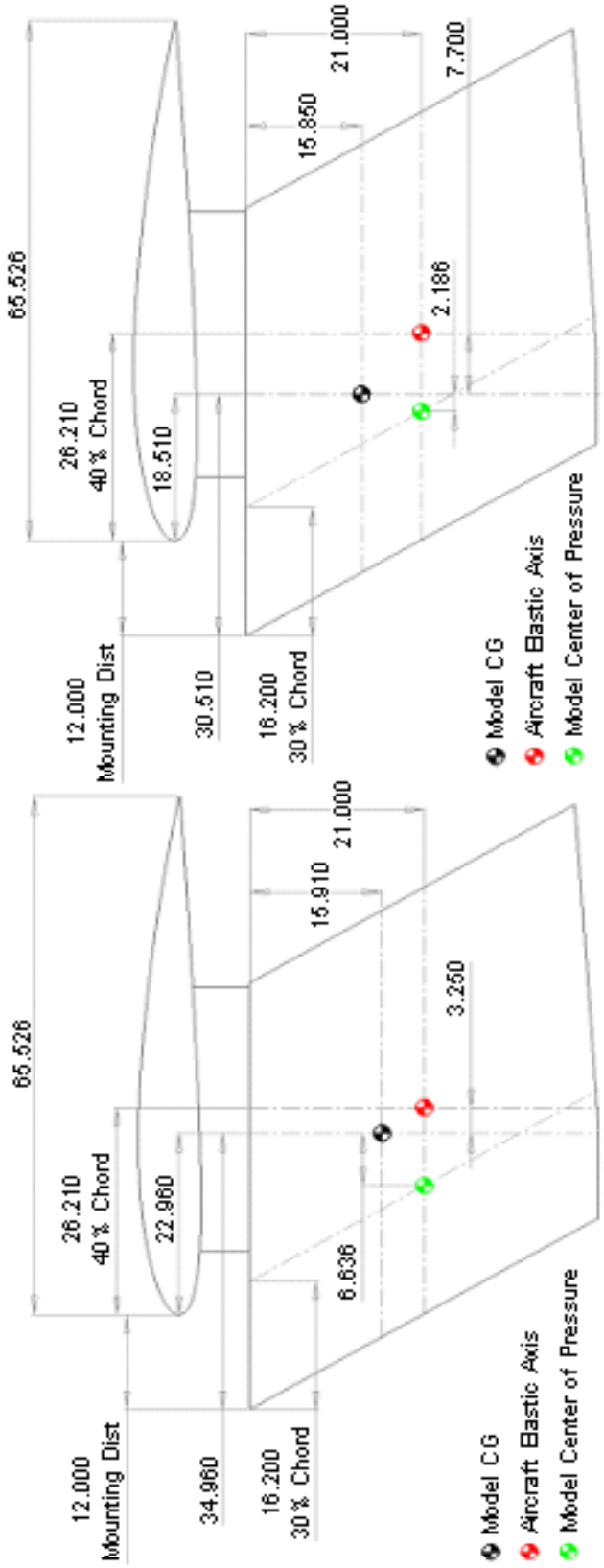

Figure A.29 Shift in Shelled Model CG with Addition of 20 lb Counterweight

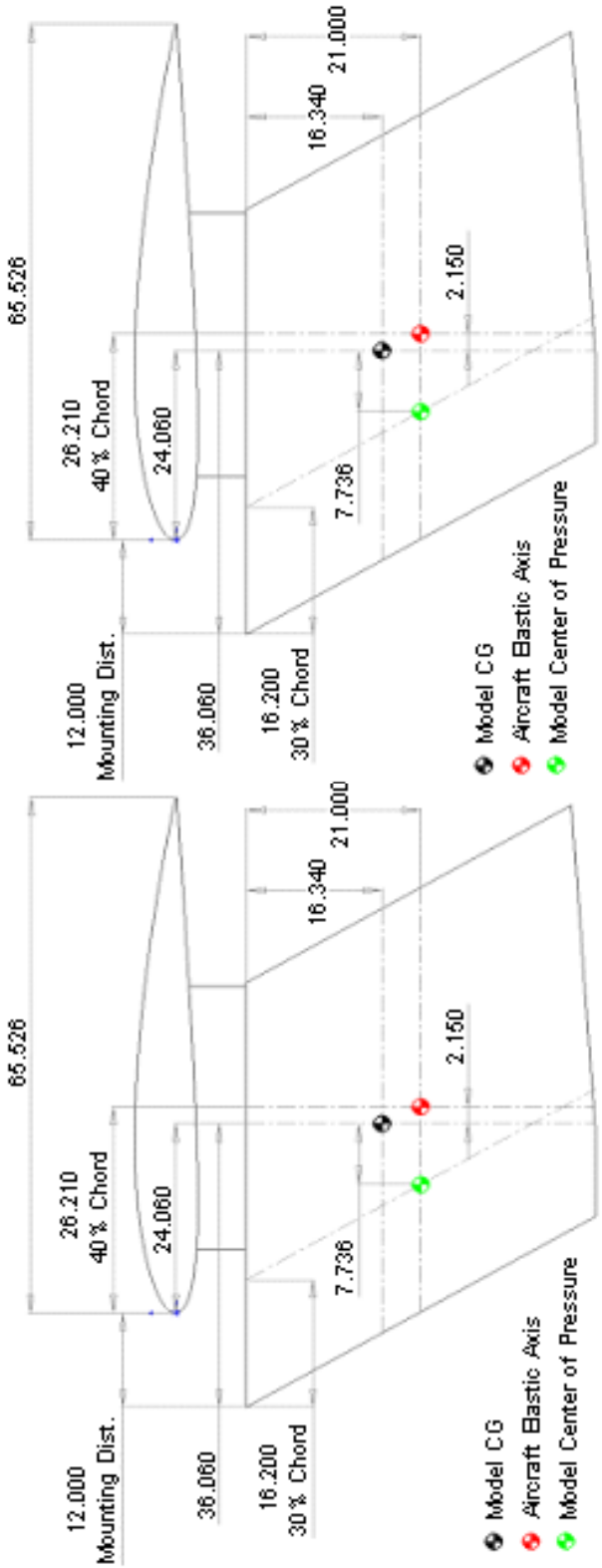

Figure A.30 Shift in Pocketed Model CG Location with Addition of 20 lb Counterweight

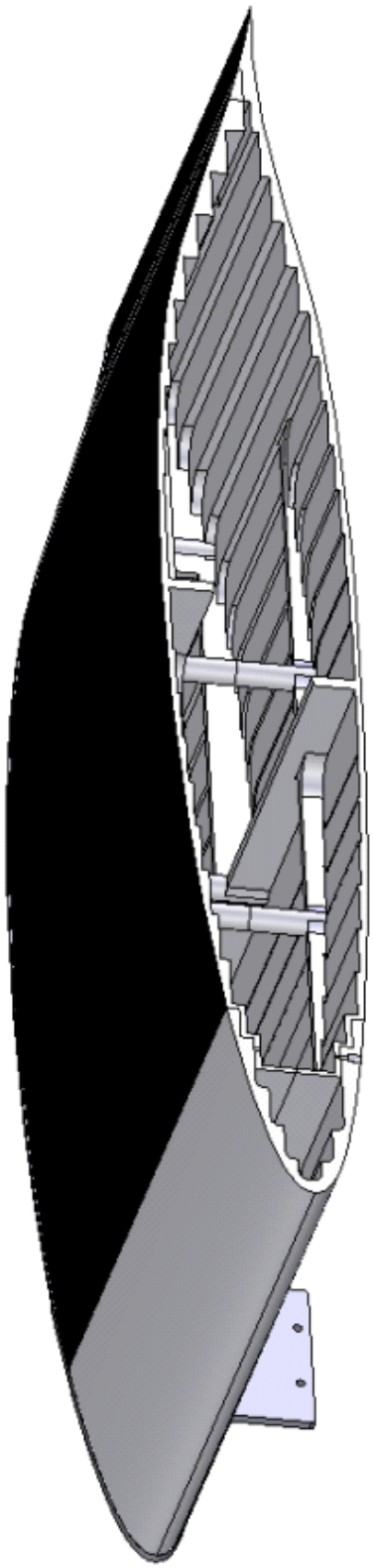

Figure A.31 Cross Section Revealing Stepped Structure of Final Model

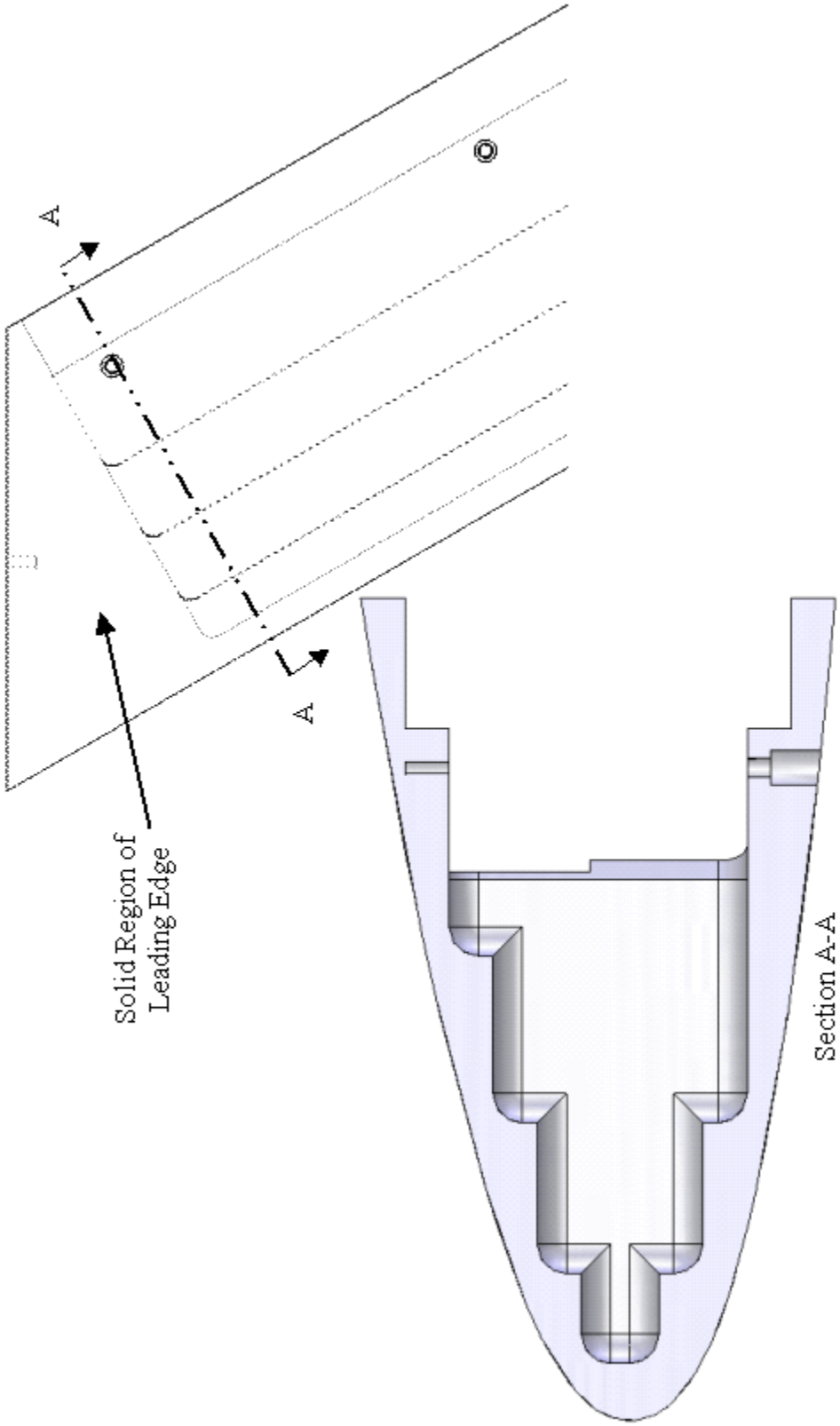

Figure A.32 Stepped Structure Applied to Leading Edge

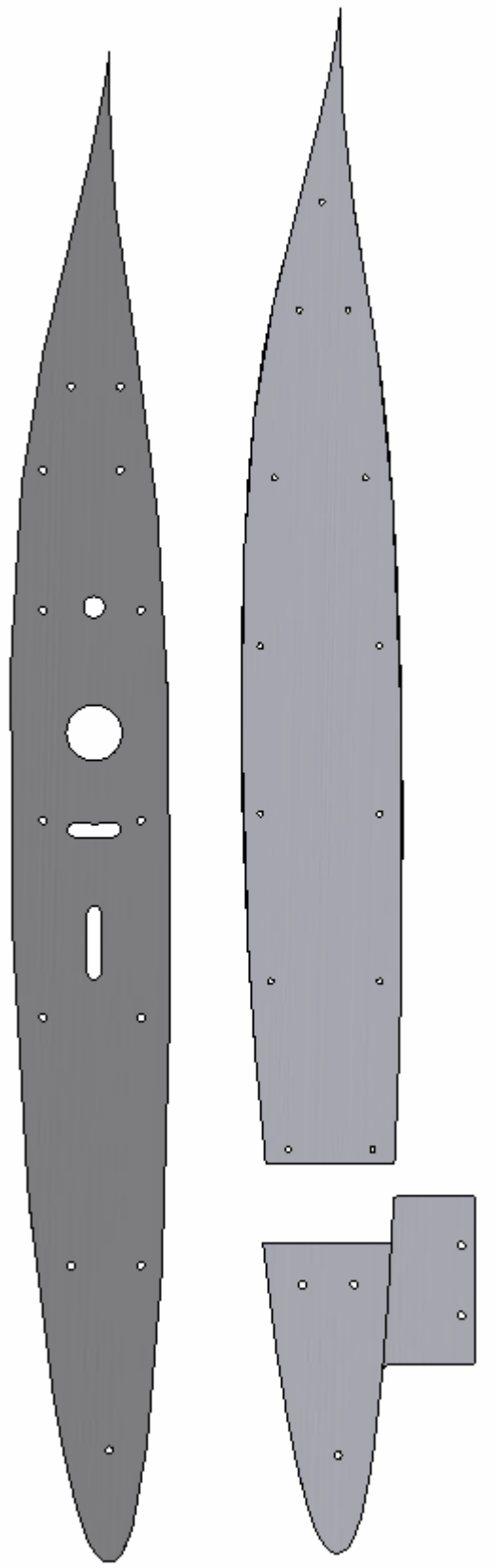

Figure A.33 Plates Added to the Top and Bottom of Airfoil Model

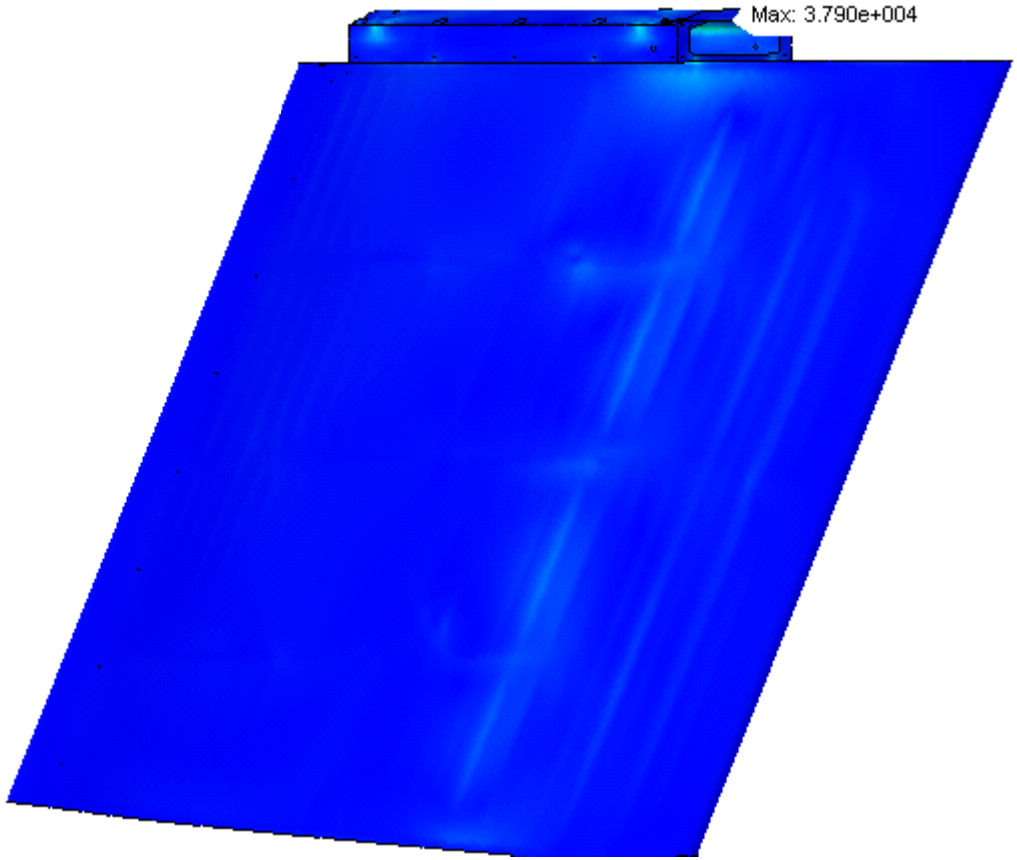

Figure A.34 Stress Analysis of Stepped Model Under Maximum Loading

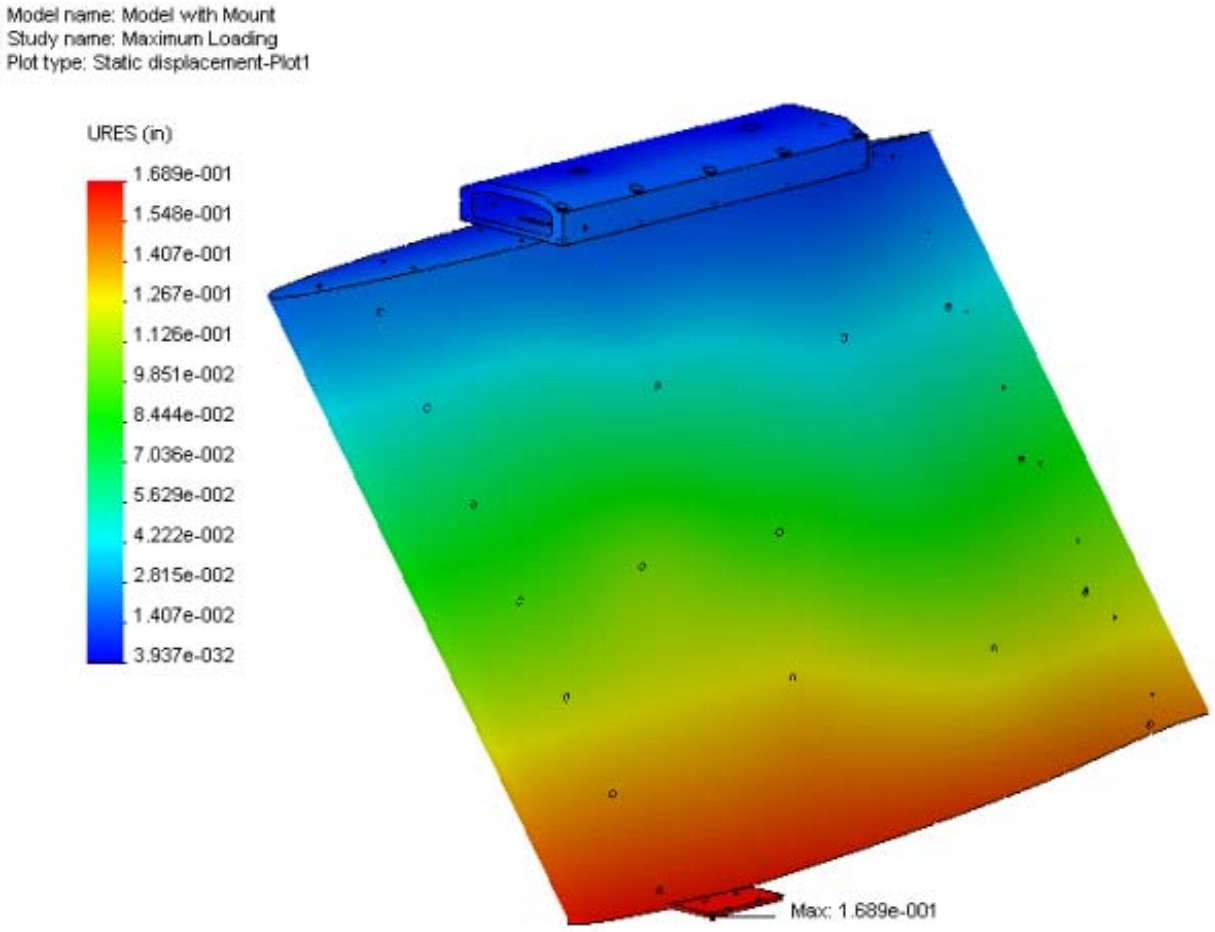

Figure A.35 Deflection of Stepped Model Illustrating Pattern Similar to Pocketed Model

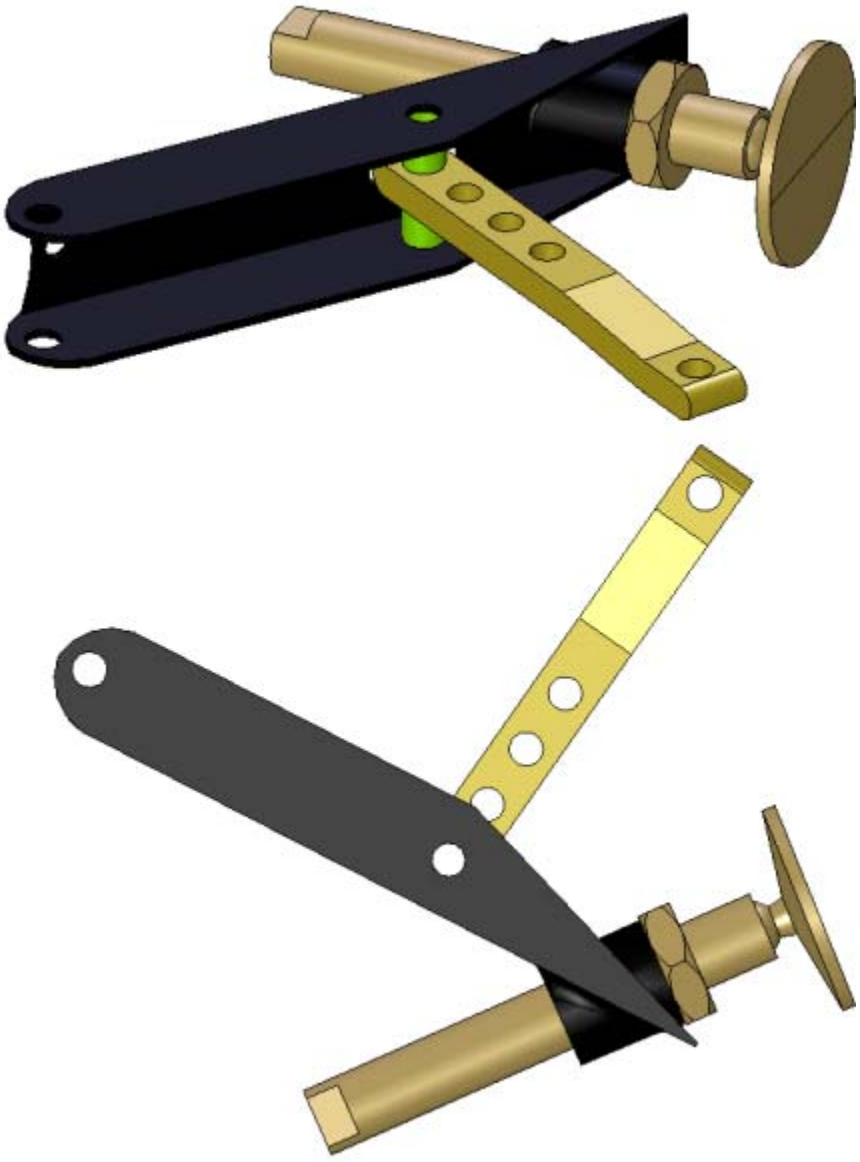

Figure A.36 Original Rocker Arm Assembly

Figure A.37 Weld on Original Rocker Arm Assembly

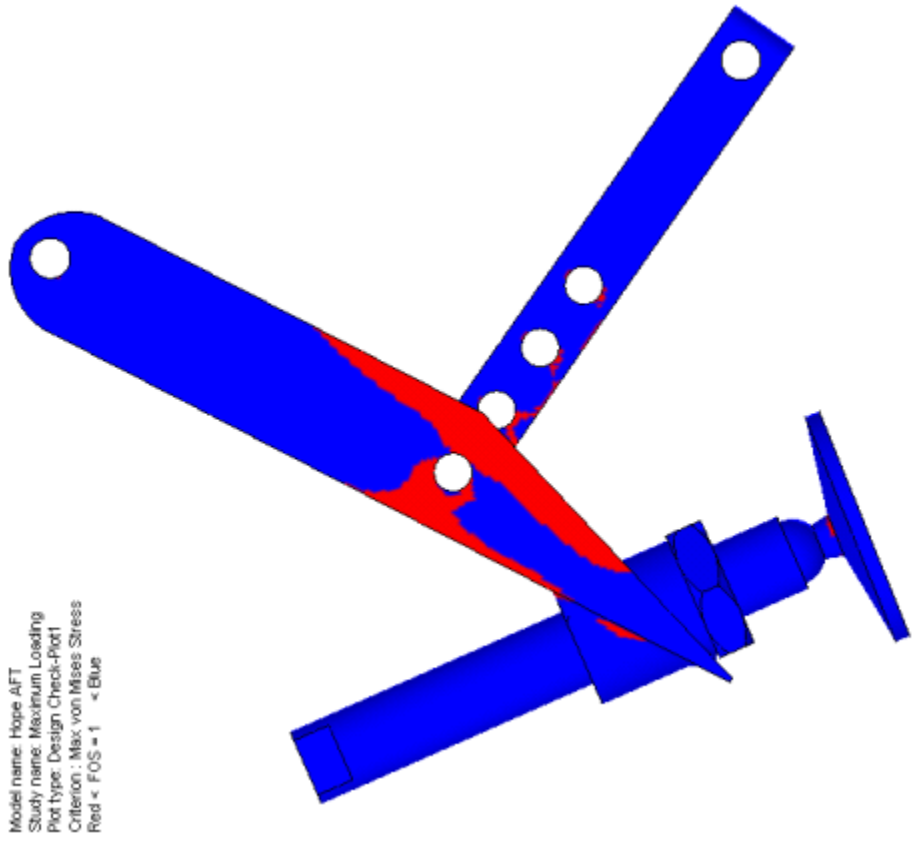

Figure A.38 Factor of Safety Diagram, Yield Strength 90,000 psi

Figure A.39 Redesigned Rocker Arm Assembly

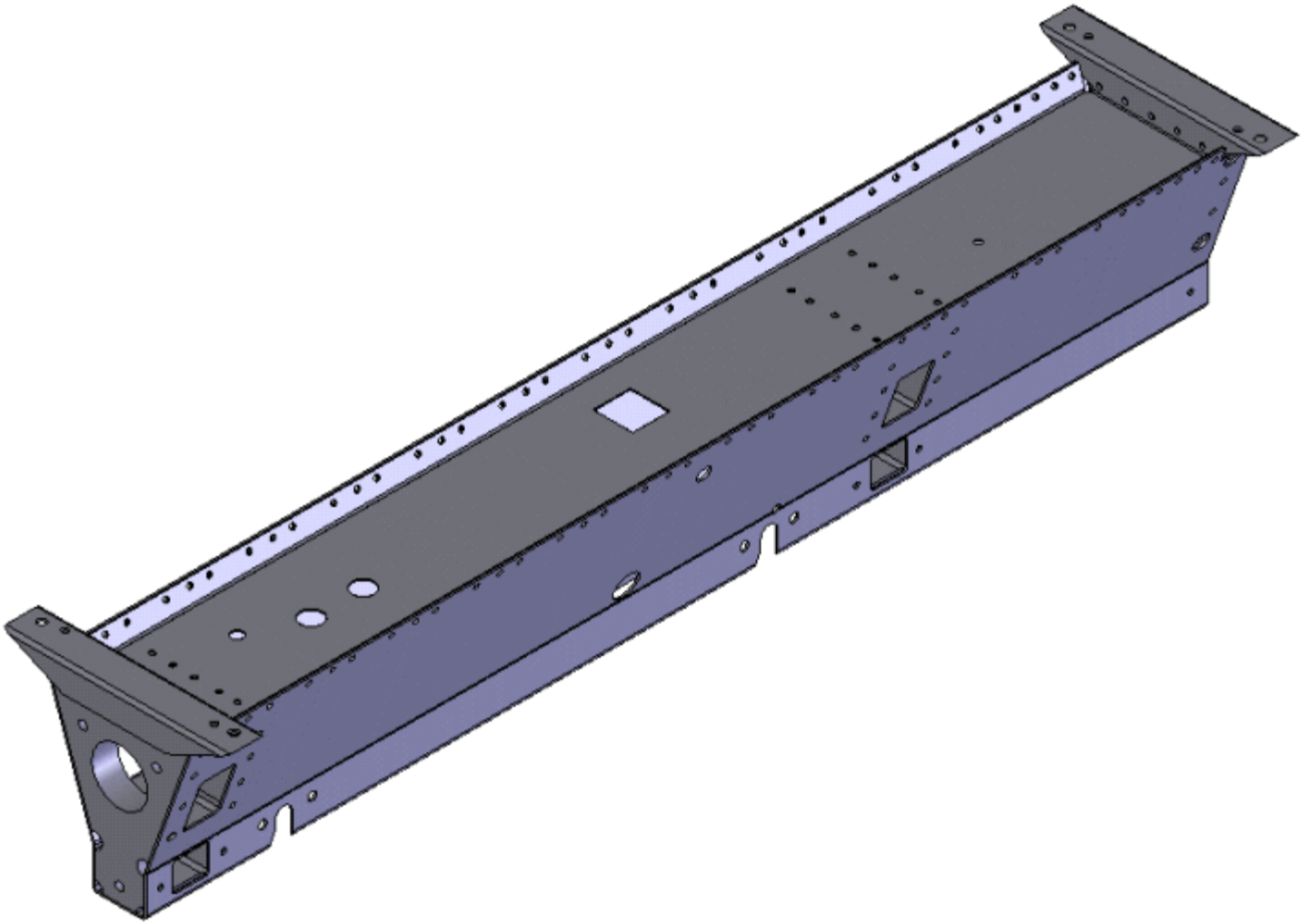

Figure A.40 Modeled Pylon

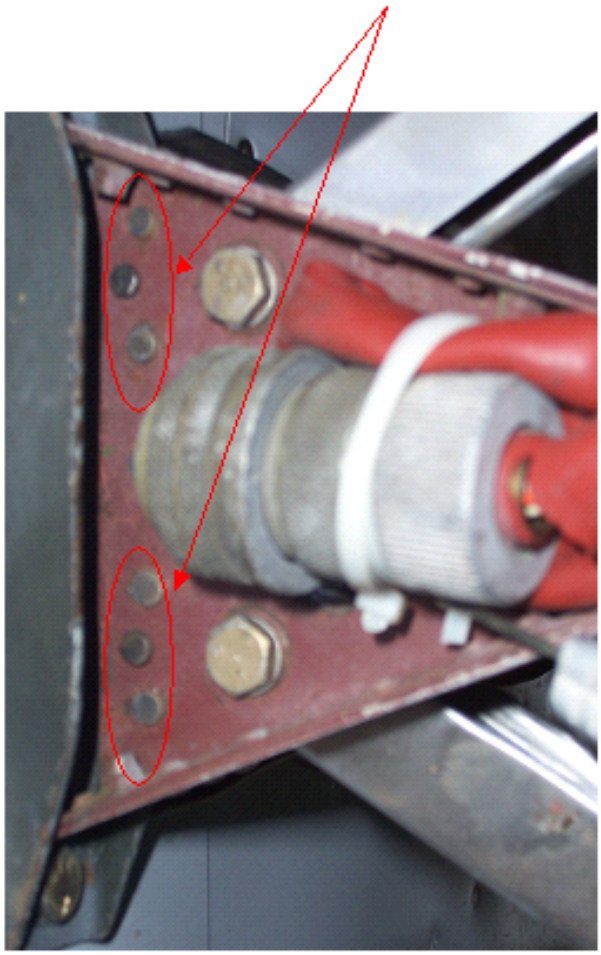

Figure A.41 Location of Replaced Rivets in Pylon Assembly

Figure A.42 Stiffeners Applied to Pylon Skin

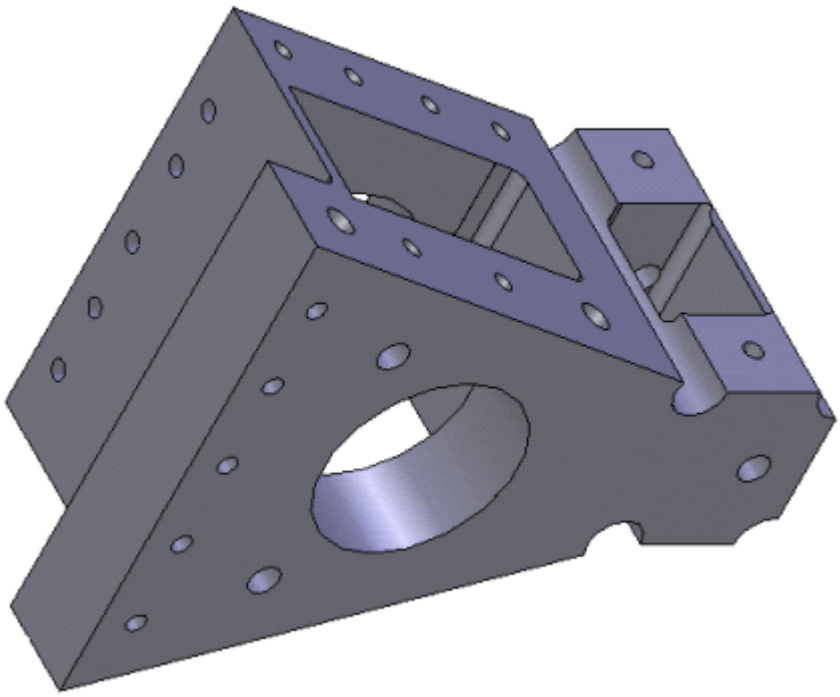

Figure A.43 Solid Bulkhead for Pylon Assembly

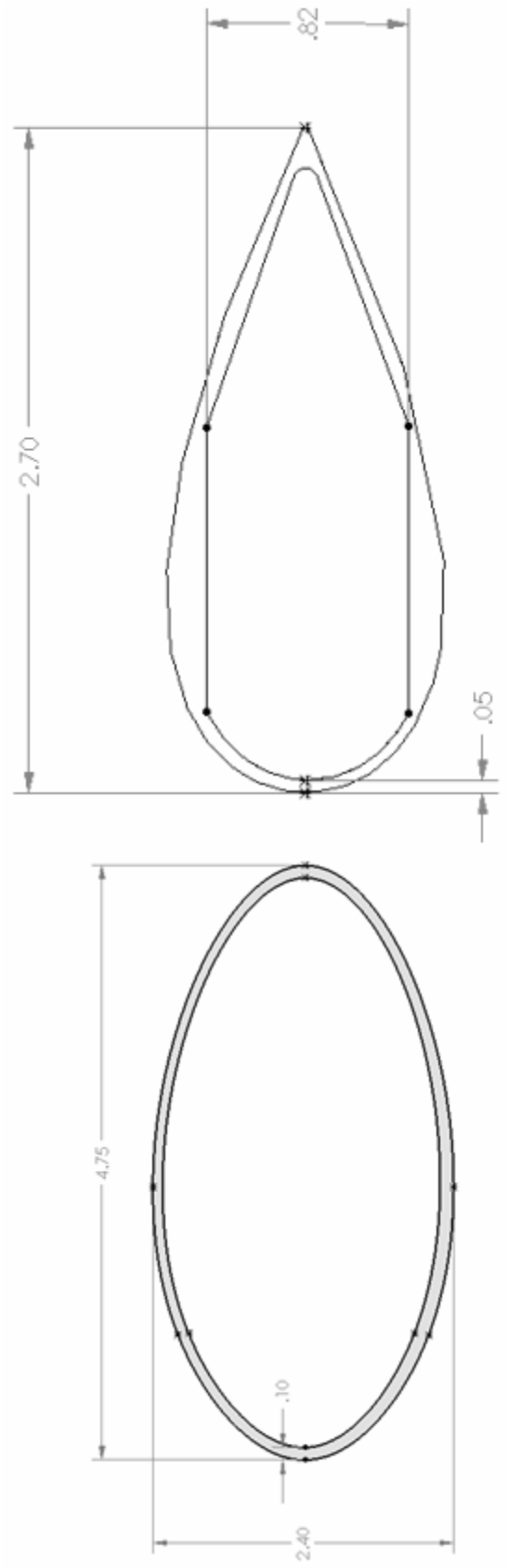

Figure A.44 Strut Profiles; Cessna 172 (Left), Fairing (Right)

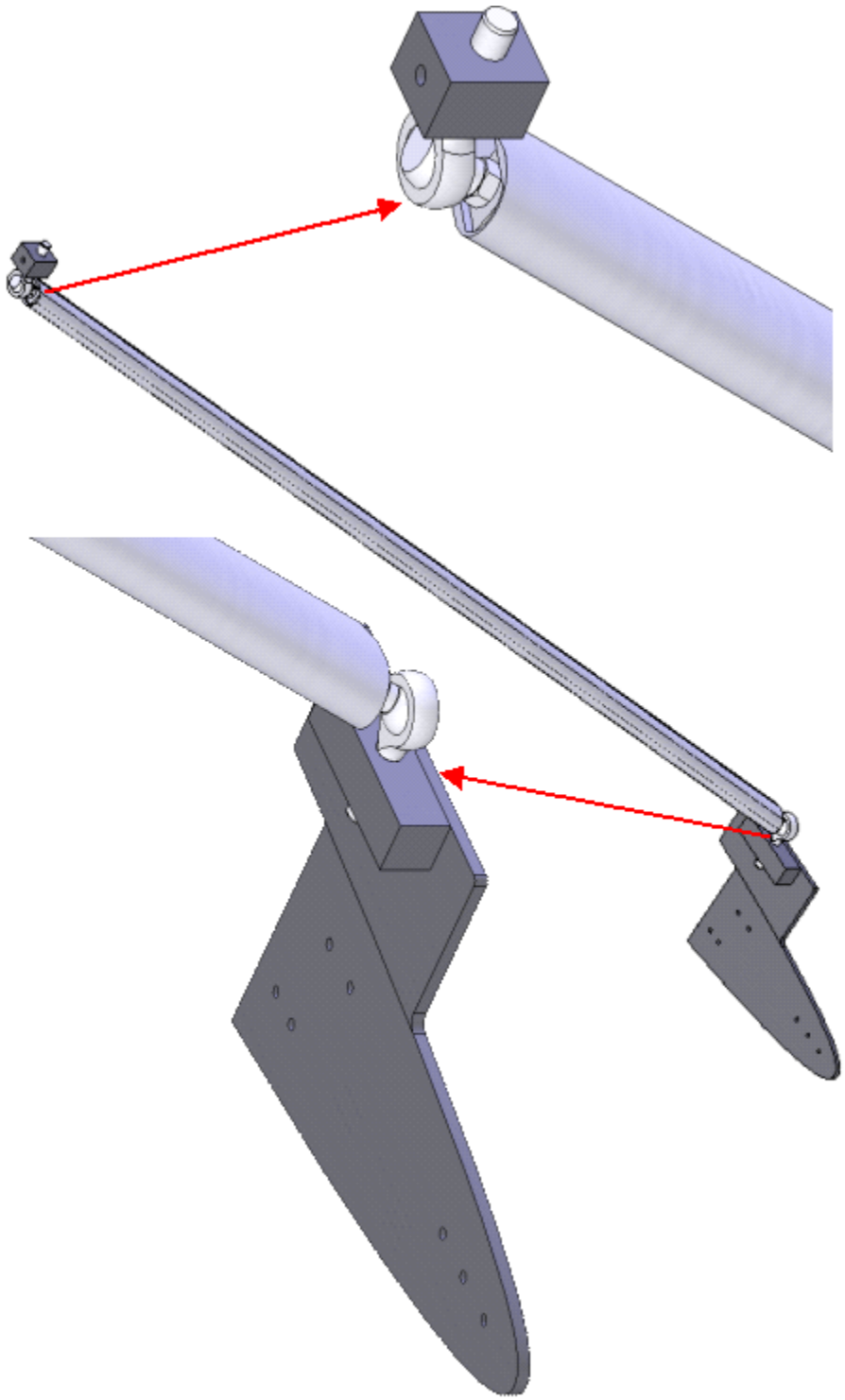

Figure A.45 Overview of Strut Featuring Dual Ball Joints

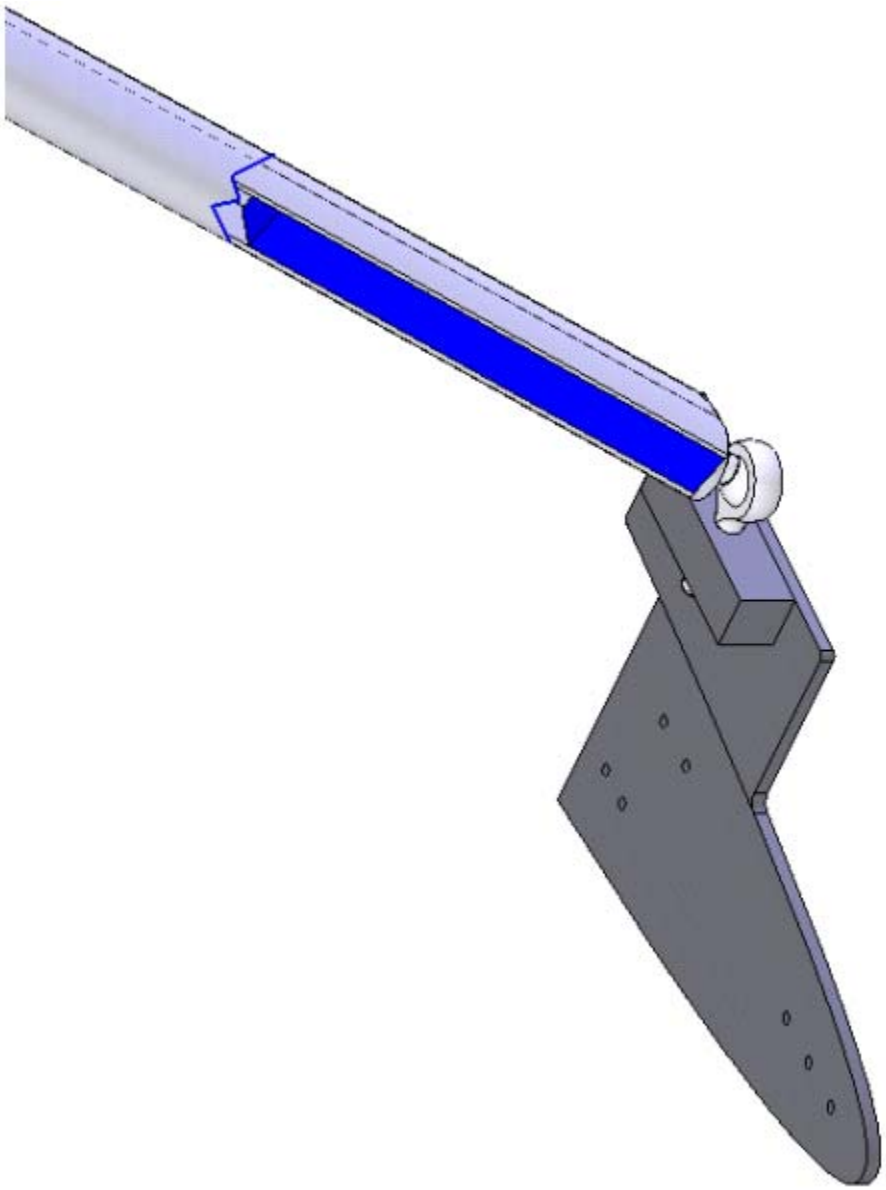

Figure A.46 Cut Away Revealing Strut Insert Inside Strut Profile

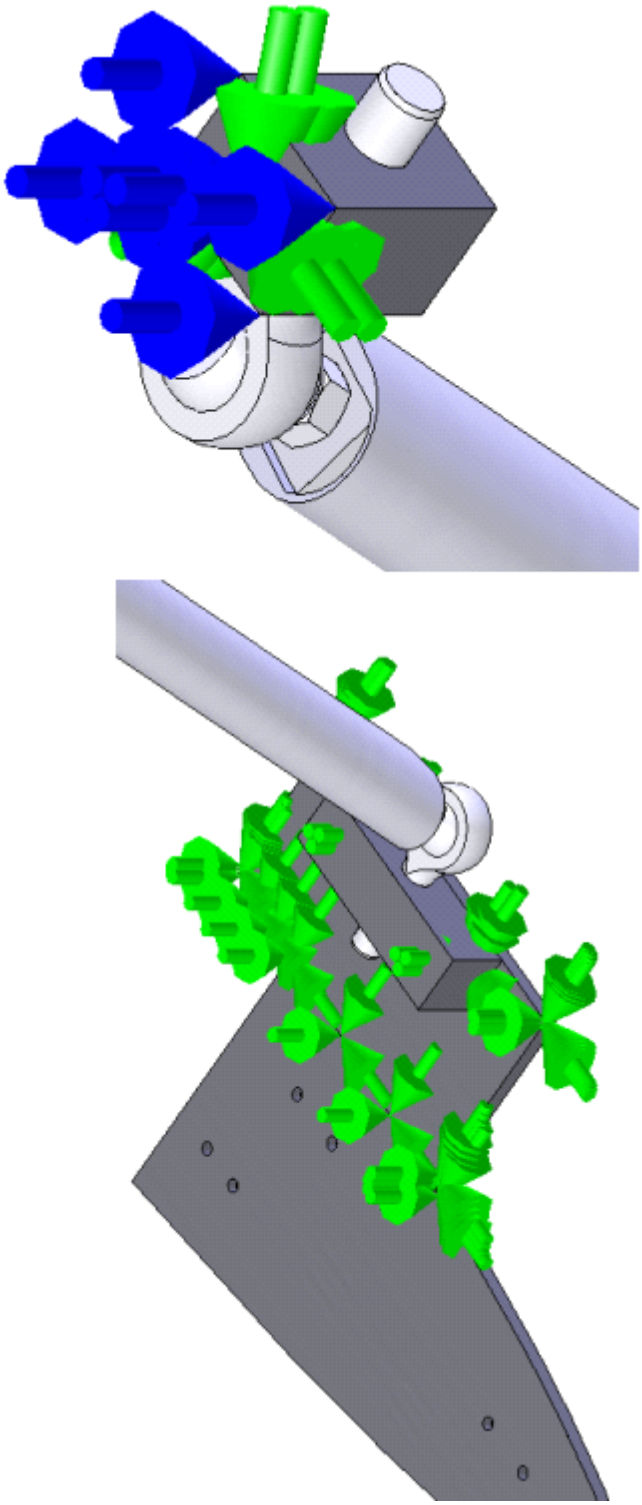

Figure A.47 Restraints Applied to Both Strut Attachment Points

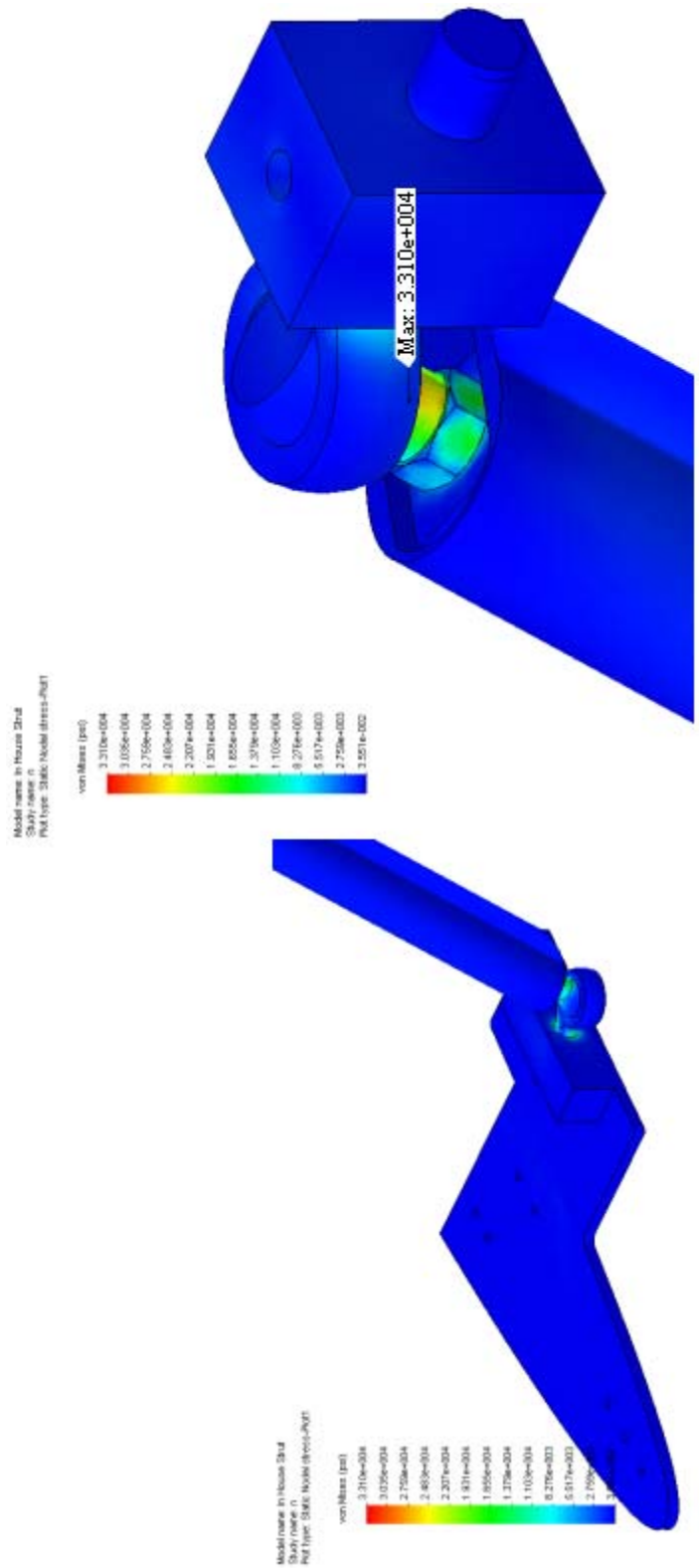

Figure A.48 Results Illustrating Concentrations of Stress in Both Ball Joints

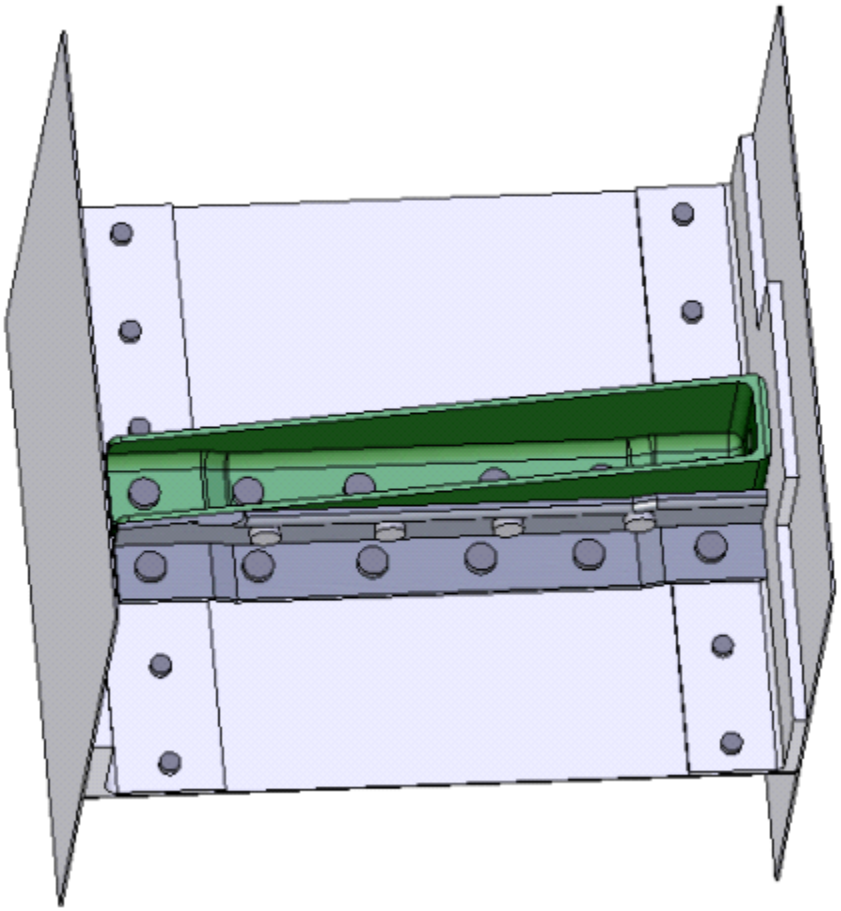

Figure A.49 Tie Down Assembly

Figure A.50 Setup of Preliminary Static Load Test

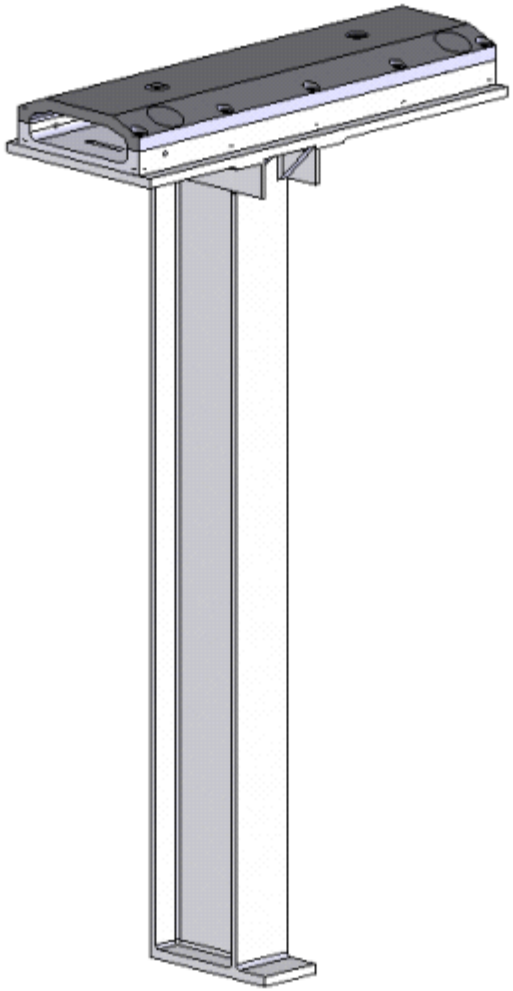

Figure A.51 Static Model Used to Simulate True Airfoil Model

Figure A.52 Location of Load Cells During Preliminary Static Load Test

Figure A.53 Setup for Second Static Load Test

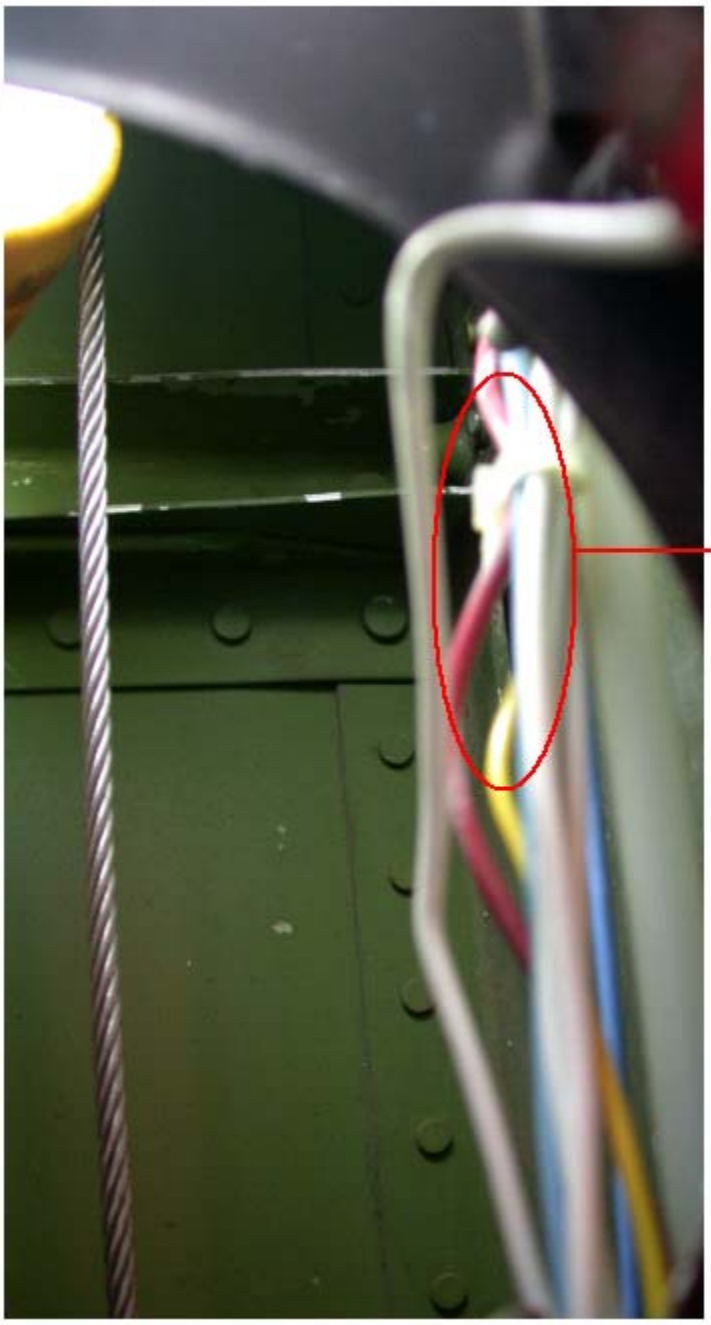

Figure A.54 Observed Separation in Tie-Down Location During Static Load Test with True Airfoil Model

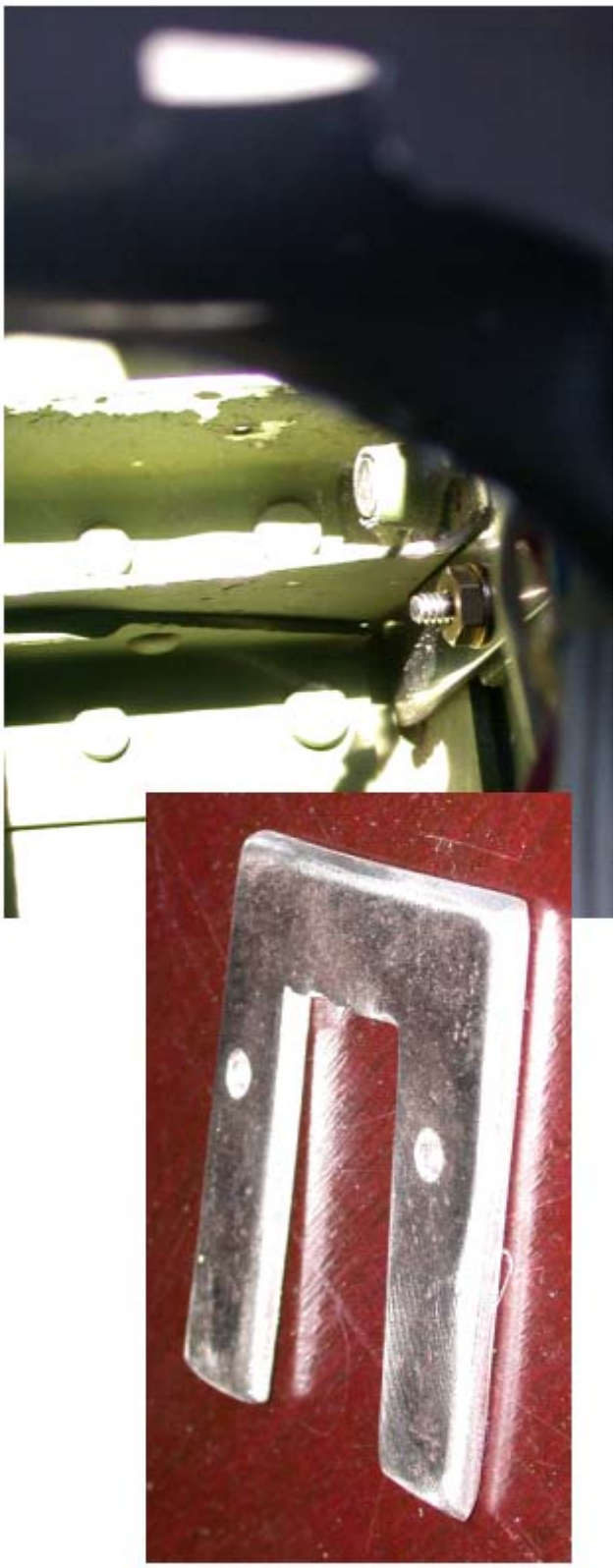

Figure A.55 Steel Clip Added to Tie Down Assembly

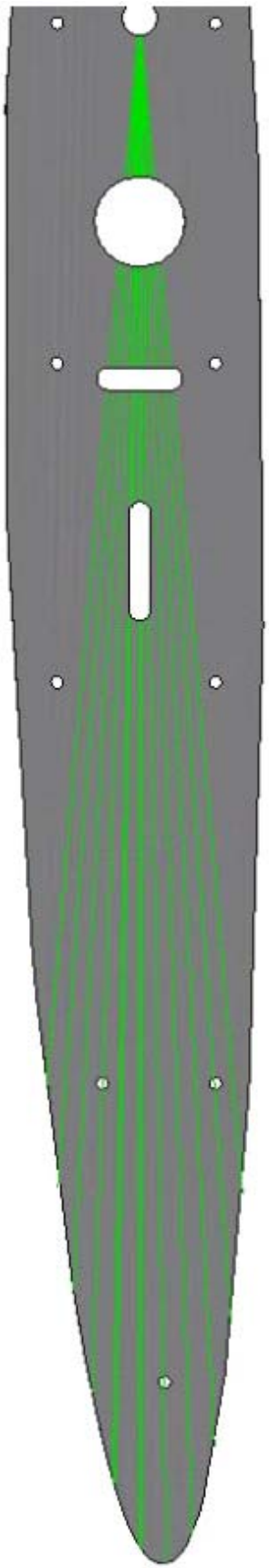

Figure A.56 Location of Etched Lines to Ensure Angle of Attack Alignment

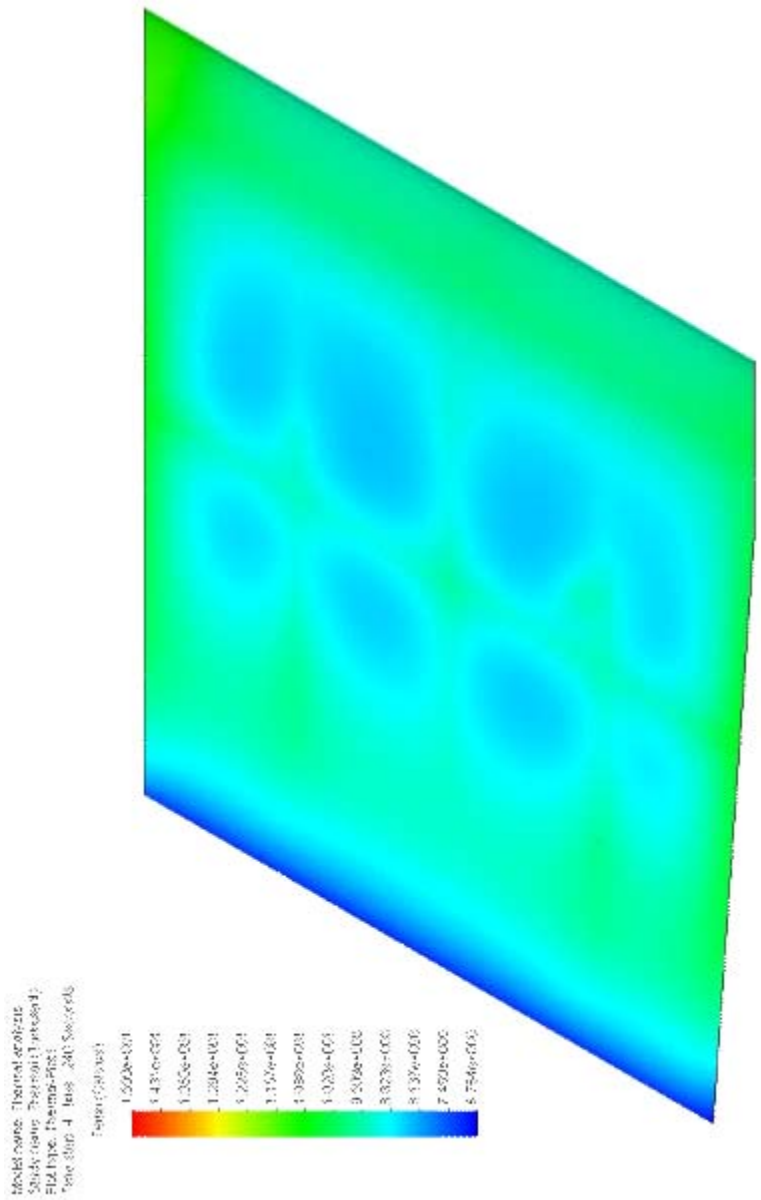

Figure A.57 Thermal Analysis Showing Uneven Cooling due to Internal Structure

APPENDIX B
AIRFOIL BLUEPRINTS

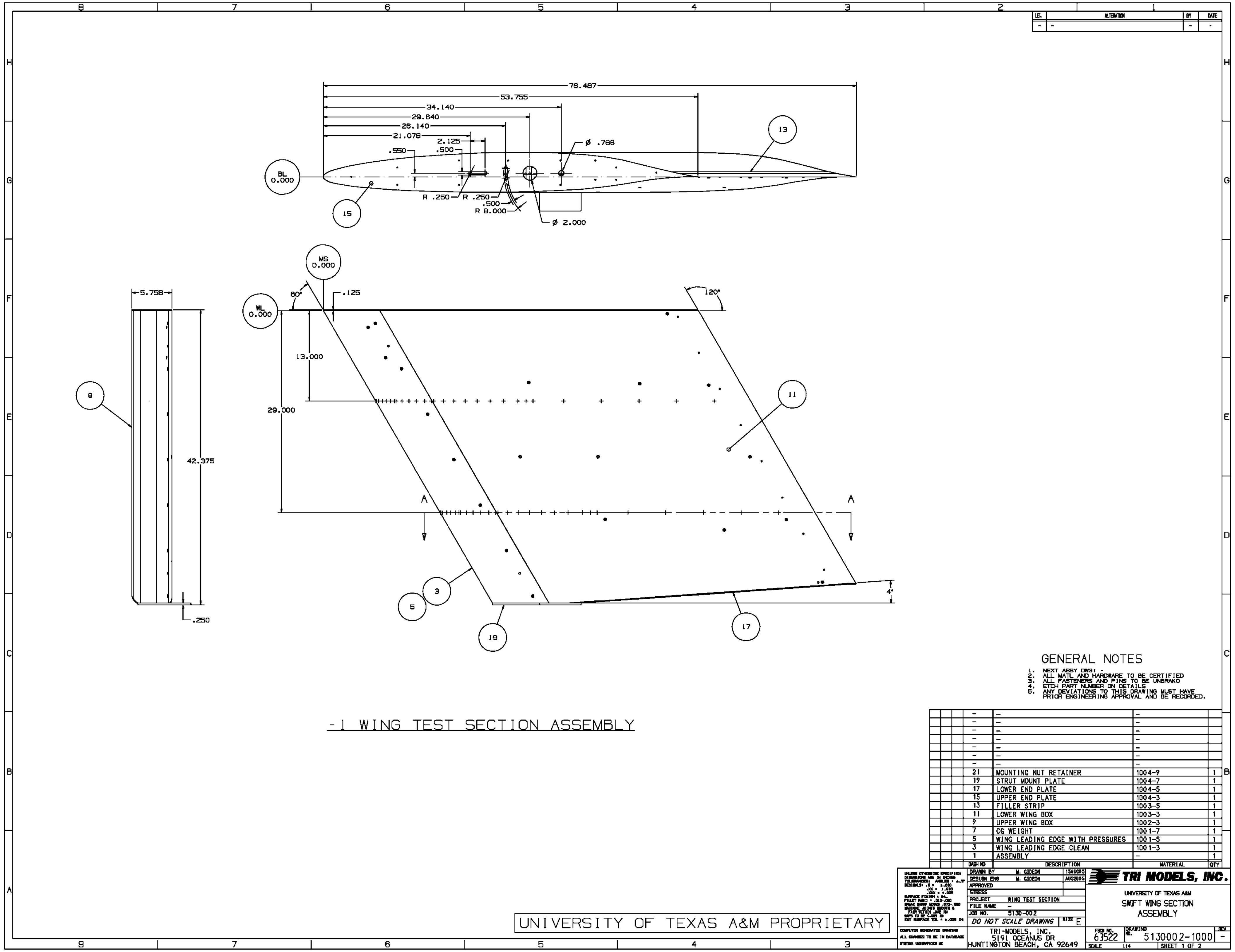
76.487
53.755
34.140
29.640
26.140
21.078
2.125
.550
.500
Ø .766
R .250
R .250
.500
R 8.000
Ø 2.000
BL 0.000
MS 0.000
WL 0.000
5.758
60°
.125
120°
13.000
29.000
42.375
.250
4°
A
A
-1 WING TEST SECTION ASSEMBLY
GENERAL NOTES
1. NEXT ASSY DWG: -
2. ALL MATL AND HARDWARE TO BE CERTIFIED
3. ALL FASTENERS AND PINS TO BE UNBRAKO
4. ETCH PART NUMBER ON DETAILS
5. ANY DEVIATIONS TO THIS DRAWING MUST HAVE PRIOR ENGINEERING APPROVAL AND BE RECORDED.
21 MOUNTING NUT RETAINER 1004-9 1
19 STRUT MOUNT PLATE 1004-7 1
17 LOWER END PLATE 1004-5 1
15 UPPER END PLATE 1004-3 1
13 FILLER STRIP 1003-5 1
11 LOWER WING BOX 1003-3 1
9 UPPER WING BOX 1002-3 1
7 CG WEIGHT 1001-7 1
5 WING LEADING EDGE WITH PRESSURES 1001-5 1
3 WING LEADING EDGE CLEAN 1001-3 1
1 ASSEMBLY - 1
DASH NO DESCRIPTION MATERIAL QTY
DRAWN BY M. GIDEON 15AUG05
DESIGN ENG M. GIDEON AUG2005
APPROVED
STRESS
PROJECT WING TEST SECTION
FILE NAME -
JOB NO. 5130-002
DO NOT SCALE DRAWING
SIZE E
TRI MODELS, INC.
UNIVERSITY OF TEXAS A&M
SWIFT WING SECTION ASSEMBLY
TRI-MODELS, INC.
5191 OCEANUS DR
HUNTINGTON BEACH, CA 92649
FSCM NO. 63522
DRAWING NO. 5130002-1000
REV -
SCALE 1:4
SHEET 1 OF 2
UNIVERSITY OF TEXAS A&M PROPRIETARY

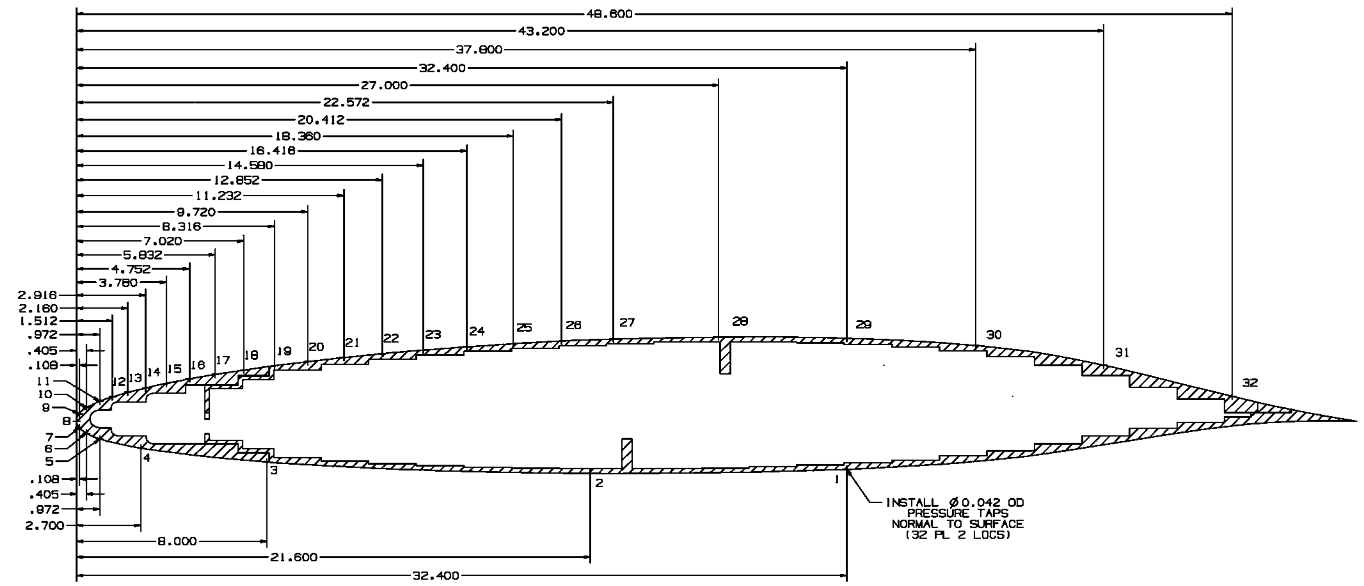

SECTION A-A
TYPICAL BOTH WL

NUMBER	CHORD	SPAN	MS	BL	WL
1-1	-32.400	13.000	39.905	-2.015	-13.000
1-2	-21.600	13.000	29.105	-2.188	-13.000
1-3	-8.000	13.000	15.505	-1.707	-13.000
1-4	-2.700	13.000	10.205	-1.117	-13.000
1-5	-0.972	13.000	8.477	-0.733	-13.000
1-6	-0.405	13.000	7.910	-0.492	-13.000
1-7	-0.108	13.000	7.613	-0.260	-13.000
1-8	0.000	13.000	7.505	0.022	-13.000
1-9	0.108	13.000	7.613	0.328	-13.000
1-10	.405	13.000	17.148	0.575	-13.000
1-11	0.972	13.000	8.477	0.855	-13.000
1-12	1.512	13.000	9.017	1.042	-13.000
1-13	2.160	13.000	9.665	1.228	-13.000
1-14	2.916	13.000	10.421	1.416	-13.000
1-15	3.780	13.000	11.285	1.608	-13.000
1-16	4.752	13.000	12.257	1.798	-13.000
1-17	5.832	13.000	13.337	1.985	-13.000
1-18	7.020	13.000	14.525	2.171	-13.000
1-19	8.316	13.000	15.821	2.353	-13.000
1-20	9.720	13.000	17.225	2.530	-13.000
1-21	11.232	13.000	18.737	2.700	-13.000
1-22	12.852	13.000	20.357	2.862	-13.000
1-23	14.580	13.000	22.085	3.013	-13.000
1-24	16.416	13.000	23.921	3.153	-13.000
1-25	18.360	13.000	25.865	3.277	-13.000
1-26	20.412	13.000	27.917	3.384	-13.000
1-27	22.572	13.000	30.077	3.471	-13.000
1-28	27.000	13.000	34.505	3.562	-13.000
1-29	32.400	13.000	39.905	3.507	-13.000
1-30	37.800	13.000	45.305	3.206	-13.000
1-31	43.200	13.000	50.705	2.375	-13.000
1-32	48.600	13.000	56.105	1.057	-13.000
-	-	-	-	-	-
-	-	-	-	-	-

NUMBER	CHORD	SPAN	MS	BL	WL
2-1	-32.400	29.000	39.905	-2.015	-29.000
2-2	-21.600	29.000	38.343	-2.188	-29.000
2-3	-8.000	29.000	24.743	-1.707	-29.000
2-4	-2.700	29.000	19.443	-1.117	-29.000
2-5	-0.972	29.000	17.715	-0.733	-29.000
2-6	-0.405	29.000	17.148	-0.492	-29.000
2-7	-0.108	29.000	16.851	-0.260	-29.000
2-8	0.000	29.000	16.743	0.022	-29.000
2-9	0.108	29.000	16.851	0.328	-29.000
2-10	0.405	29.000	17.148	0.575	-29.000
2-11	0.972	29.000	17.715	0.855	-29.000
2-12	1.512	29.000	18.255	1.042	-29.000
2-13	2.160	29.000	18.903	1.228	-29.000
2-14	2.916	29.000	19.659	1.416	-29.000
2-15	3.780	29.000	20.523	1.608	-29.000
2-16	4.752	29.000	21.495	1.798	-29.000
2-17	5.832	29.000	22.575	1.985	-29.000
2-18	7.020	29.000	23.763	2.171	-29.000
2-19	8.316	29.000	25.059	2.353	-29.000
2-20	9.720	29.000	26.463	2.530	-29.000
2-21	11.232	29.000	27.975	2.700	-29.000
2-22	12.852	29.000	29.595	2.862	-29.000
2-23	14.580	29.000	31.323	3.013	-29.000
2-24	16.416	29.000	33.159	3.153	-29.000
2-25	18.360	29.000	35.103	3.277	-29.000
2-26	20.412	29.000	37.155	3.384	-29.000
2-27	22.572	29.000	39.315	3.471	-29.000
2-28	27.000	29.000	43.743	3.562	-29.000
2-29	32.400	29.000	49.143	3.507	-29.000
2-30	37.800	29.000	54.543	3.206	-29.000
2-31	43.200	29.000	59.943	2.374	-29.000
2-32	48.600	29.000	65.343	1.057	-29.000
-	-	-	-	-	-
-	-	-	-	-	-

GENERAL NOTES

1. NEXT ASSY DWG: -
2. ALL MATL AND HARDWARE TO BE CERTIFIED
3. ALL FASTENERS AND PINS TO BE UNBRAKO
4. ETCH PART NUMBER ON DETAILS
5. ANY DEVIATIONS TO THIS DRAWING MUST HAVE PRIOR ENGINEERING APPROVAL AND BE RECORDED.

DASH NO	DESCRIPTION	MATERIAL	QTY
-	-	-	1

UNIVERSITY OF TEXAS A&M PROPRIETARY

DRAWN BY	M. GIDEON	15AUG05
DESIGN ENG	M. GIDEON	AUG2005
APPROVED		
STRESS		
PROJECT	WING TEST SECTION	
FILE NAME	-	
JOB NO.	5130-002	
DO NOT SCALE DRAWING	SIZE E	

TRI MODELS, INC.

UNIVERSITY OF TEXAS A&M
SWIFT WING SECTION
ASSEMBLY

COMPUTER GENERATED DRAWING
ALL CHANGES TO BE IN DATABASE

TRI-MODELS, INC.
5191 OCEANUS DR
HUNTINGTON BEACH, CA 92649

FSCM NO. 63522 | DRAWING NO. 5130002-1000 | REV -
SCALE 1:2 | SHEET 1 OF 1

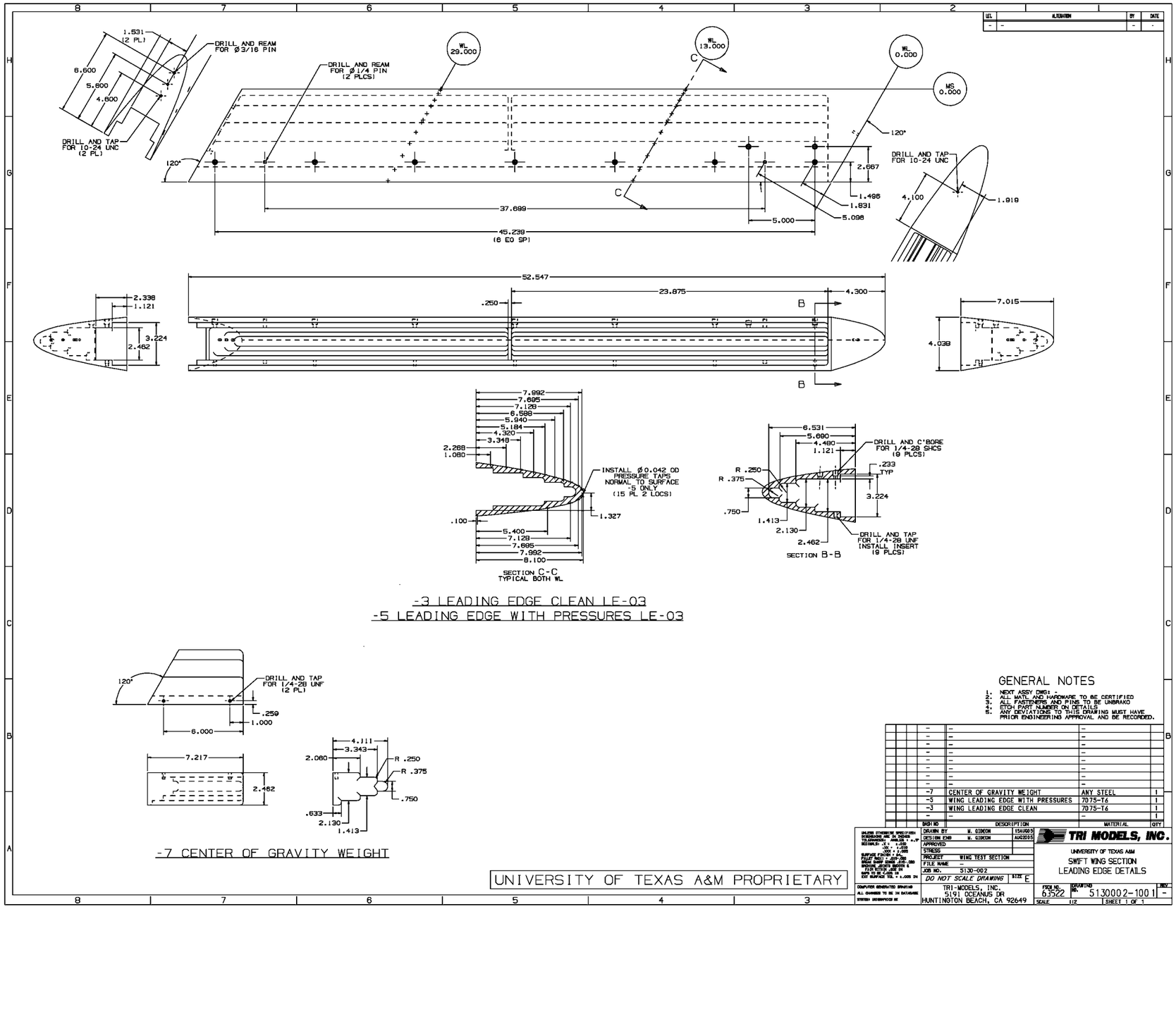
1.531 (2 PL)
DRILL AND REAM FOR Ø3/16 PIN
8.600
5.600
4.600
DRILL AND TAP FOR 10-24 UNC (2 PL)
DRILL AND REAM FOR Ø1/4 PIN (2 PLCS)
WL 29.000
WL 13.000
WL 0.000
MS 0.000
120°
2.667
1.498
1.831
5.098
37.699
5.000
45.239 (8 EQ SP)
DRILL AND TAP FOR 10-24 UNC
4.100
1.818
52.547
23.875
4.300
.250
B
2.338
1.121
3.224
2.462
7.015
4.038
7.992
7.695
7.128
6.588
5.940
5.184
4.320
3.348
2.288
1.080
INSTALL Ø0.042 OD PRESSURE TAPS NORMAL TO SURFACE -5 ONLY (15 PL 2 LOCS)
.100
1.327
5.400
7.128
7.695
7.992
8.100
SECTION C-C TYPICAL BOTH WL
6.531
5.690
4.490
1.121
DRILL AND C'BORE FOR 1/4-28 SHCS (8 PLCS)
R .250
R .375
.233 TYP
3.224
.750
1.413
2.130
2.462
DRILL AND TAP FOR 1/4-28 UNF INSTALL INSERT (8 PLCS)
SECTION B-B
-3 LEADING EDGE CLEAN LE-03
-5 LEADING EDGE WITH PRESSURES LE-03
120°
DRILL AND TAP FOR 1/4-28 UNF (2 PL)
.250
1.000
6.000
7.217
2.462
4.111
3.343
2.080
R .250
R .375
.750
.633
2.130
1.413
-7 CENTER OF GRAVITY WEIGHT
GENERAL NOTES
1. NEXT ASSY DWG: -
2. ALL MATL AND HARDWARE TO BE CERTIFIED
3. ALL FASTENERS AND PINS TO BE UNBRAKO
4. ETCH PART NUMBER ON DETAILS
5. ANY DEVIATIONS TO THIS DRAWING MUST HAVE PRIOR ENGINEERING APPROVAL AND BE RECORDED.
-7 CENTER OF GRAVITY WEIGHT ANY STEEL 1
-5 WING LEADING EDGE WITH PRESSURES 7075-T6 1
-3 WING LEADING EDGE CLEAN 7075-T6 1
DASH NO DESCRIPTION MATERIAL QTY
DRAWN BY M. GIDEON 15AUG03
DESIGN ENG M. GIDEON AUG2015
APPROVED
STRESS
PROJECT WING TEST SECTION
FILE NAME -
JOB NO. 5130-002
DO NOT SCALE DRAWING SIZE E
TRI-MODELS, INC. 5191 OCEANUS DR HUNTINGTON BEACH, CA 92649
TRI MODELS, INC.
UNIVERSITY OF TEXAS A&M
SWIFT WING SECTION
LEADING EDGE DETAILS
FSCM NO. 63522
DRAWING NO. 5130002-1001
REV -
SCALE 1/2
SHEET 1 OF 1
UNIVERSITY OF TEXAS A&M PROPRIETARY

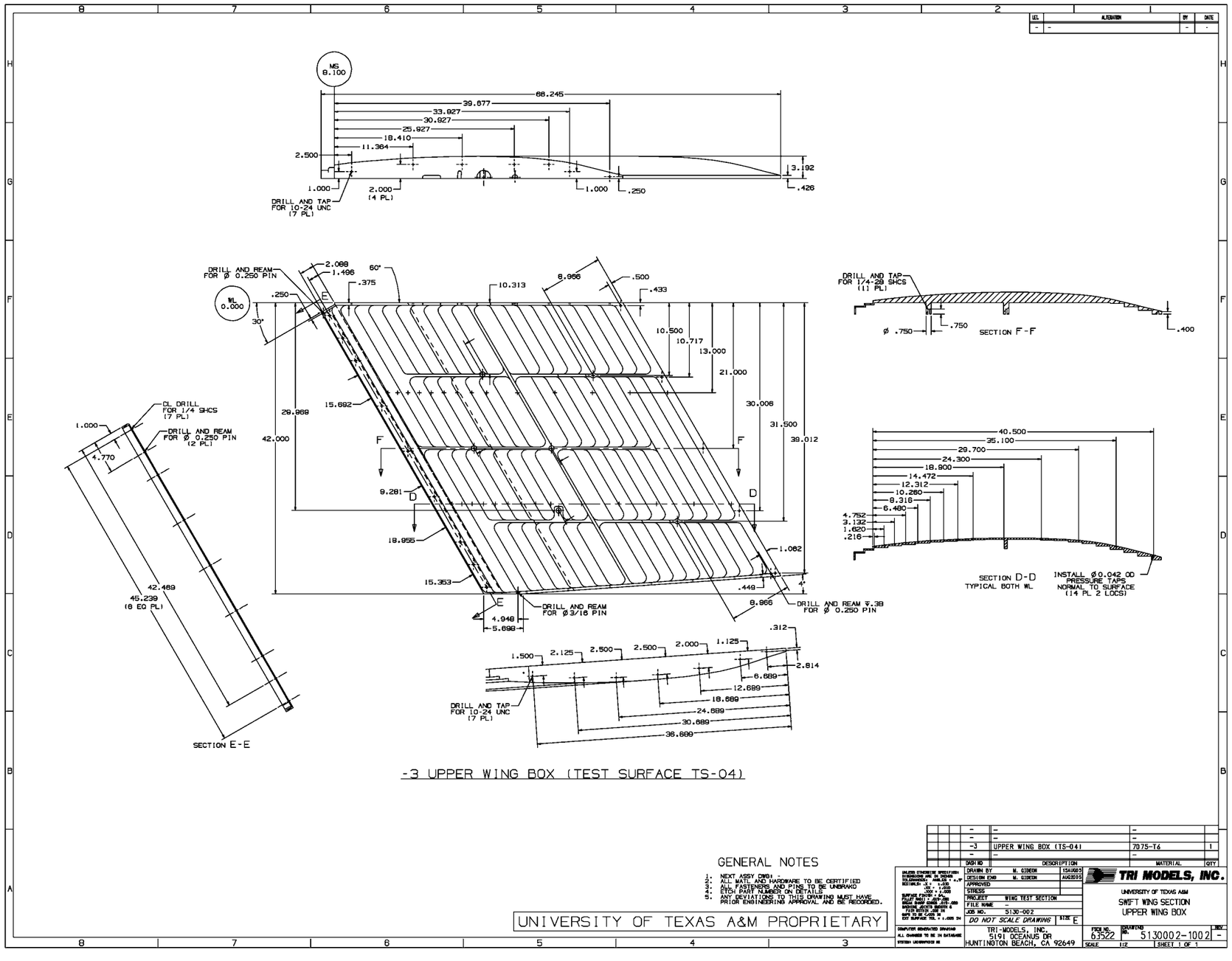

-3 UPPER WING BOX (TEST SURFACE TS-04)

DASH NO	DESCRIPTION	MATERIAL	QTY
-	-	-	
-	-	-	
-3	UPPER WING BOX (TS-04)	7075-T6	1
-	-	-	

DRAWN BY	M. GIDEON	15AUG03
DESIGN ENG	M. GIDEON	AUG2003
APPROVED		
STRESS		
PROJECT	WING TEST SECTION	
FILE NAME	-	
JOB NO.	5130-002	
DO NOT SCALE DRAWING	SIZE E	

TRI MODELS, INC.

UNIVERSITY OF TEXAS A&M
SWIFT WING SECTION
UPPER WING BOX

TRI-MODELS, INC.
5191 OCEANUS DR
HUNTINGTON BEACH, CA 92649

FSCM NO. 63522 | DRAWING NO. 5130002-1002 | REV -
SCALE 1/2 | SHEET 1 OF 1

GENERAL NOTES

1. NEXT ASSY OMIT -
2. ALL BOLTS AND HARDWARE TO BE CERTIFIED
3. ALL FASTENERS AND PINS TO BE UNBRAKO
4. ETCH PART NUMBER ON DETAILS
5. ANY DEVIATIONS TO THIS DRAWING MUST HAVE PRIOR ENGINEERING APPROVAL AND BE RECORDED.

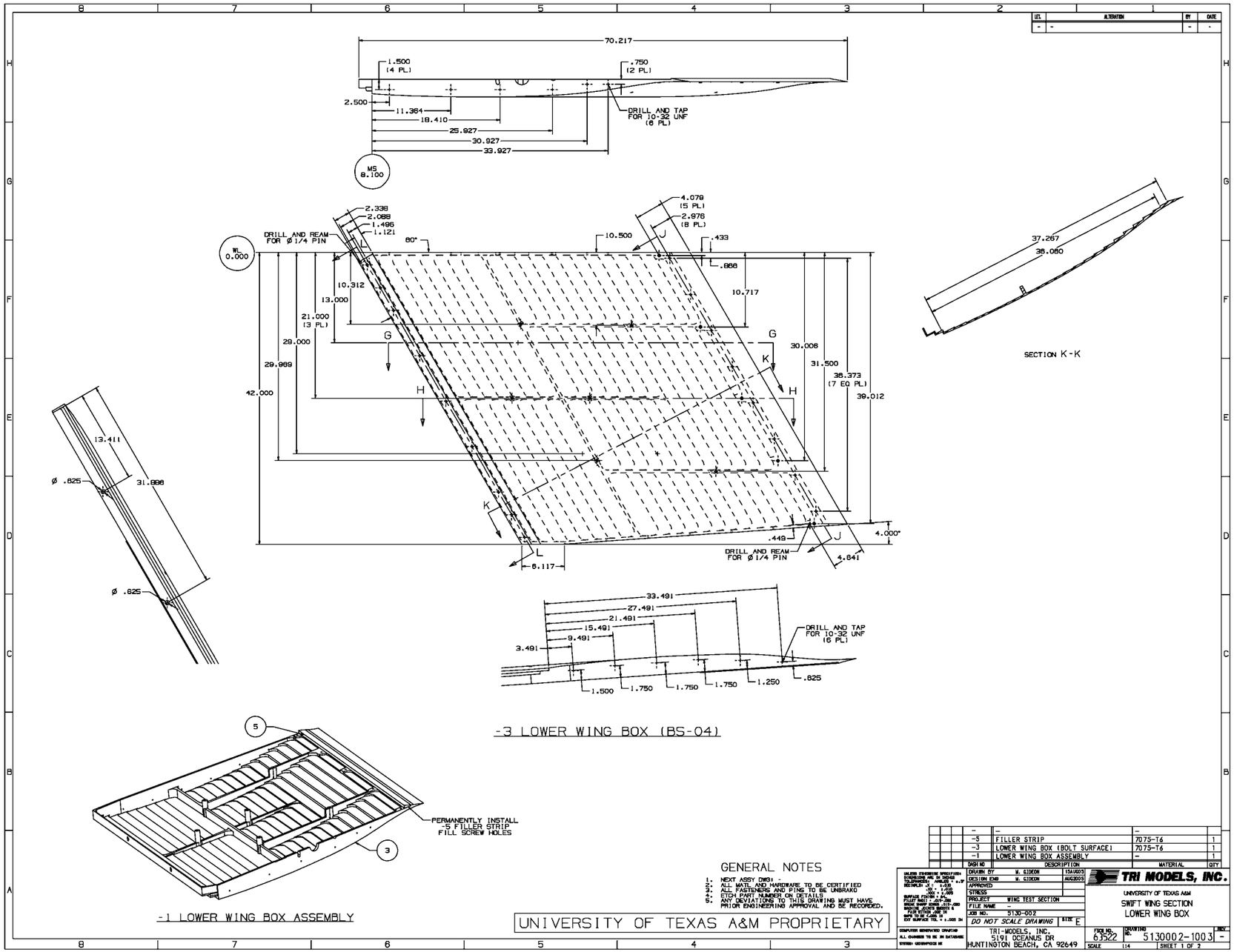

GENERAL NOTES

1. NEXT ASSY DWG: -
2. ALL MATL AND HARDWARE TO BE CERTIFIED
3. ALL FASTENERS AND PINS TO BE UNBRAKO
4. ETCH PART NUMBER ON DETAILS
5. ANY DEVIATIONS TO THIS DRAWING MUST HAVE PRIOR ENGINEERING APPROVAL AND BE RECORDED.

DASH NO	DESCRIPTION	MATERIAL	QTY
-	-	-	
-5	FILLER STRIP	7075-T6	1
-3	LOWER WING BOX (BOLT SURFACE)	7075-T6	1
-1	LOWER WING BOX ASSEMBLY	-	1

DRAWN BY	W. GIDEON 15AUG03
DESIGN ENG	W. GIDEON AUG2003
APPROVED	
STRESS	
PROJECT	WING TEST SECTION
FILE NAME	-
JOB NO.	5130-002
DO NOT SCALE DRAWING	SIZE E

TRI MODELS, INC.

UNIVERSITY OF TEXAS A&M
SWIFT WING SECTION
LOWER WING BOX

TRI-MODELS, INC.
5191 OCEANUS DR
HUNTINGTON BEACH, CA 92649

FSCM NO. 63522 | DRAWING NO. 5130002-1003 | REV -
SCALE 1:4 | SHEET 1 OF 2

UNIVERSITY OF TEXAS A&M PROPRIETARY

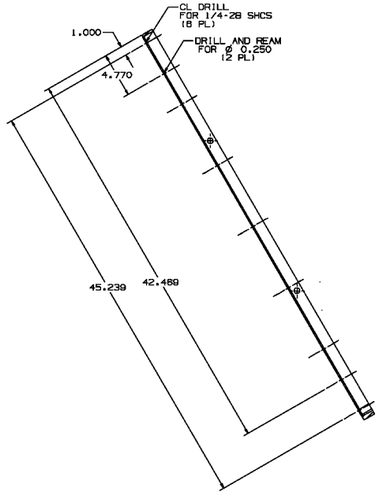

SECTION L-L

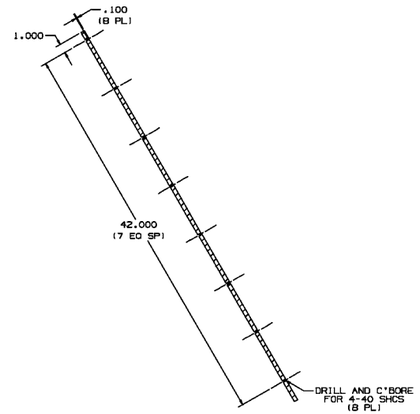

SECTION J-J

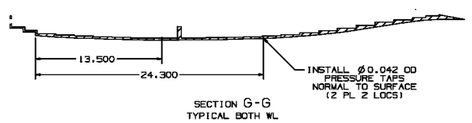

SECTION G-G
TYPICAL BOTH WL

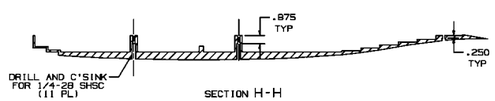

SECTION H-H

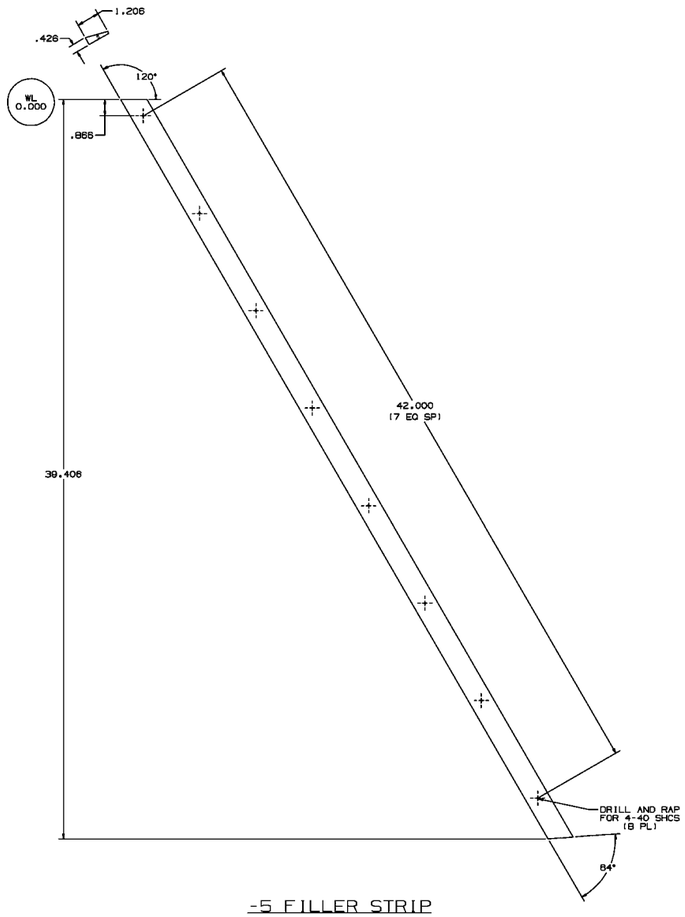

-5 FILLER STRIP
SCALE 1/2

GENERAL NOTES

1. NEXT ASSY DWG: -
2. ALL MAT'L AND HARDWARE TO BE CERTIFIED
3. ALL FASTENERS AND PINS TO BE UNBRAKD
4. ETCH PART NUMBER ON DETAILS
5. ANY DEVIATIONS TO THIS DRAWING MUST HAVE PRIOR ENGINEERING APPROVAL AND BE RECORDED.

DASH NO	DESCRIPTION	MATERIAL	QTY
-	-	-	1

DRAWN BY	M. GIXON	10AUG03
DESIGN ENG	M. GIXON	AUG2005
APPROVED		
STRESS		
PROJECT	WING TEST SECTION	
FILE NAME	-	
JOB NO.	5130-002	
DO NOT SCALE DRAWING	SIZE	E

TRI MODELS, INC.

UNIVERSITY OF TEXAS A&M
SWEPT WING SECTION
LOWER WING BOX

TRI-MODELS, INC.
5191 OCEANUS DR
HUNTINGTON BEACH, CA 92649

FSCM NO. 63522 | DRAWING NO. 5130002-1003 | REV -
SCALE 1:4 | SHEET 2 OF 2

UNIVERSITY OF TEXAS A&M PROPRIETARY

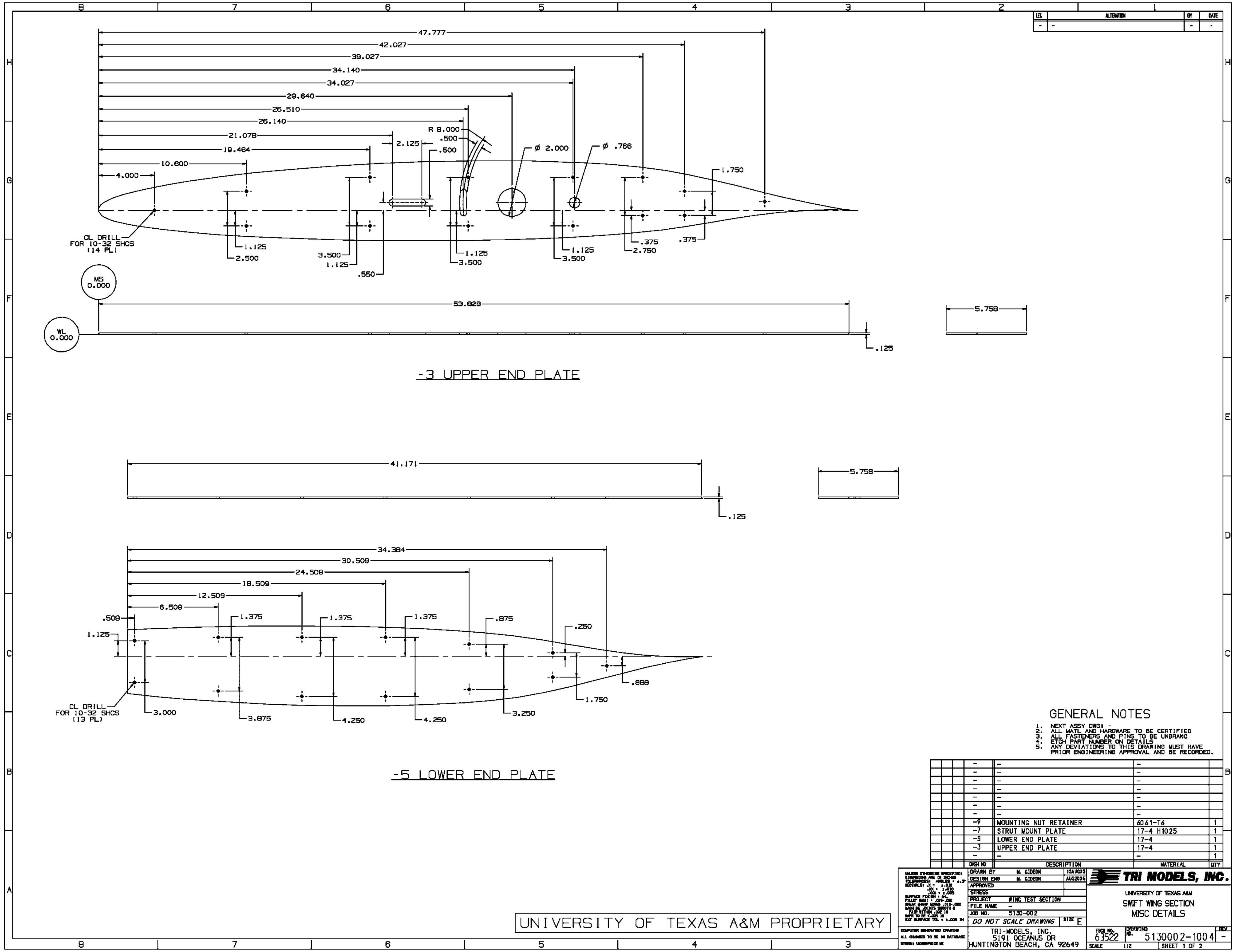
-3 UPPER END PLATE
47.777
42.027
39.027
34.140
34.027
29.640
26.510
26.140
21.078
19.464
10.600
4.000
R 8.000
.500
2.125
.500
Ø 2.000
Ø .766
1.750
CL DRILL FOR 10-32 SHCS (14 PL)
1.125
2.500
3.500
1.125
.550
1.125
3.500
1.125
3.500
.375
2.750
.375
MS 0.000
WL 0.000
53.828
.125
5.758
-5 LOWER END PLATE
41.171
.125
5.758
34.384
30.509
24.509
18.509
12.509
6.509
.509
1.125
1.375
1.375
1.375
.875
.250
.888
1.750
CL DRILL FOR 10-32 SHCS (13 PL)
3.000
3.875
4.250
4.250
3.250
GENERAL NOTES
1. NEXT ASSY DWG: -
2. ALL MATL AND HARDWARE TO BE CERTIFIED
3. ALL FASTENERS AND PINS TO BE UNBRAKO
4. ETCH PART NUMBER ON DETAILS
5. ANY DEVIATIONS TO THIS DRAWING MUST HAVE PRIOR ENGINEERING APPROVAL AND BE RECORDED.
-9 MOUNTING NUT RETAINER 6061-T6 1
-7 STRUT MOUNT PLATE 17-4 H1025 1
-5 LOWER END PLATE 17-4 1
-3 UPPER END PLATE 17-4 1
DASH NO DESCRIPTION MATERIAL QTY
DRAWN BY M. GIDEON 15AUG05
DESIGN ENG M. GIDEON AUG2005
APPROVED
STRESS
PROJECT WING TEST SECTION
FILE NAME -
JOB NO. 5130-002
DO NOT SCALE DRAWING
SIZE E
TRI MODELS, INC.
UNIVERSITY OF TEXAS A&M
SWIFT WING SECTION
MISC DETAILS
TRI-MODELS, INC.
5191 OCEANUS DR
HUNTINGTON BEACH, CA 92649
FSCM NO. 63522
DRAWING NO. 5130002-1004
REV -
SCALE 1:2
SHEET 1 OF 2
UNIVERSITY OF TEXAS A&M PROPRIETARY

LTR	ALTERATION	BY	DATE
-	-	-	-

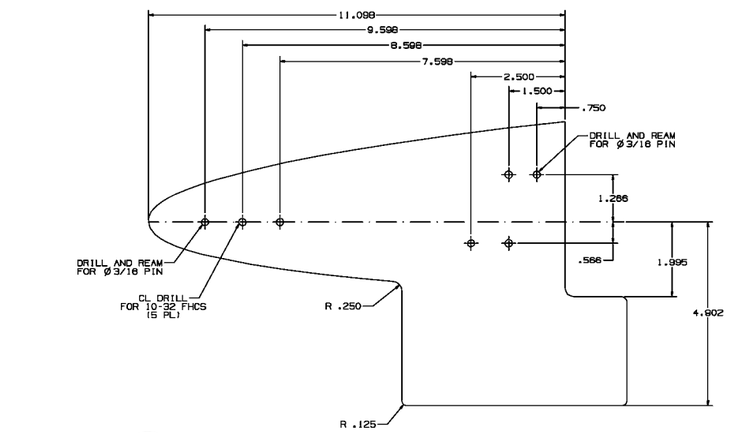

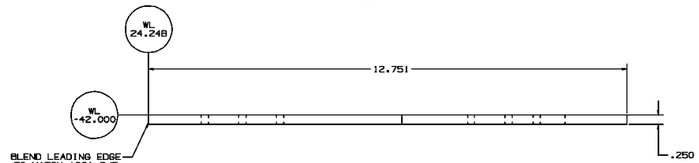

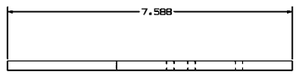

-7 STRUT MOUNT PLATE

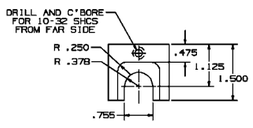

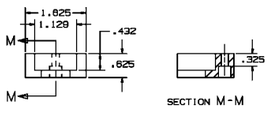

-9 MOUNT NUT RETAINER

GENERAL NOTES

1. NEXT ASSY DWG: -
2. ALL MATL AND HARDWARE TO BE CERTIFIED
3. ALL FASTENERS AND PINS TO BE UNBRAKO
4. ETCH PART NUMBER ON DETAILS
5. ANY DEVIATIONS TO THIS DRAWING MUST HAVE PRIOR ENGINEERING APPROVAL AND BE RECORDED.

DASH NO	DESCRIPTION	MATERIAL	QTY
-	-	-	-

UNIVERSITY OF TEXAS A&M PROPRIETARY

DRAWN BY	M. GIDEON 15AUG03
DESIGN ENG	M. GIDEON AUG2003
APPROVED	
STRESS	
PROJECT	WING TEST SECTION
FILE NAME	-
JOB NO.	5130-002
DO NOT SCALE DRAWING	SIZE E

TRI-MODELS, INC.
5191 ODEANUS DR
HUNTINGTON BEACH, CA 92649

TRI MODELS, INC.

UNIVERSITY OF TEXAS A&M
SWIFT WING SECTION
MISC DETAILS

FSCM NO.	DRAWING NO.	REV
03522	5130002-1004	-

SCALE 1:2 SHEET 2 OF 2

APPENDIX C
MOUNTING STRUCTURE BLUEPRINTS

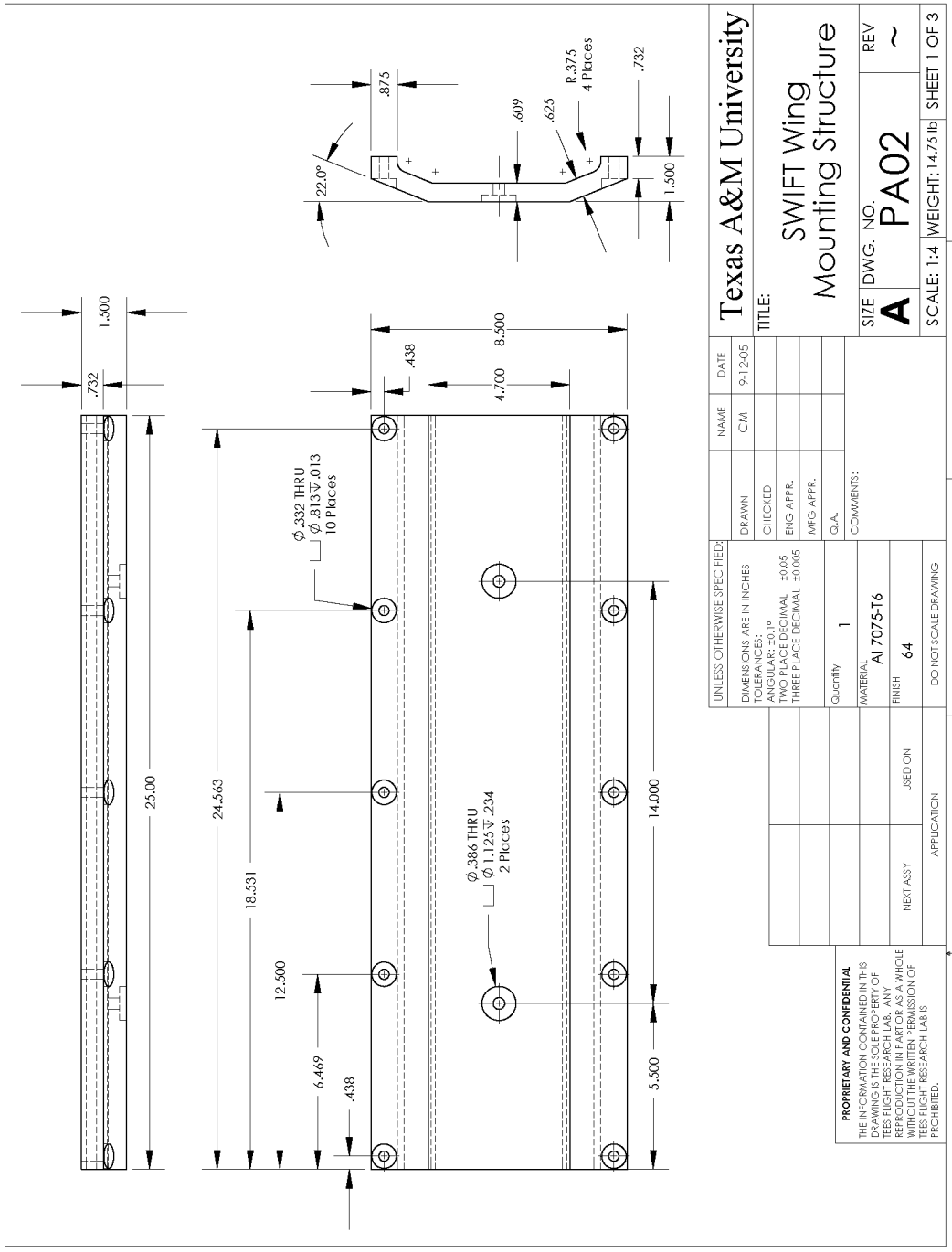
.732
1.500
25.00
24.563
18.531
12.500
6.469
.438
Ø.332 THRU
Ø.813 ▽.013
10 Places
Ø.386 THRU
Ø1.125 ▽.234
2 Places
.438
8.500
4.700
14.000
5.500
22.0°
.875
.609
.625
R.375
4 Places
.732
1.500
UNLESS OTHERWISE SPECIFIED:
DIMENSIONS ARE IN INCHES
TOLERANCES:
ANGULAR: ±0.1°
TWO PLACE DECIMAL ±0.05
THREE PLACE DECIMAL ±0.005
Quantity 1
MATERIAL
Al 7075-T6
FINISH 64
NEXT ASSY
USED ON
APPLICATION
DO NOT SCALE DRAWING
NAME
DATE
DRAWN CM 9-12-05
CHECKED
ENG APPR.
MFG APPR.
Q.A.
COMMENTS:
Texas A&M University
TITLE:
SWIFT Wing
Mounting Structure
SIZE A
DWG. NO. PA02
REV ~
SCALE: 1:4
WEIGHT: 14.75 lb
SHEET 1 OF 3
PROPRIETARY AND CONFIDENTIAL
THE INFORMATION CONTAINED IN THIS DRAWING IS THE SOLE PROPERTY OF TEES FLIGHT RESEARCH LAB. ANY REPRODUCTION IN PART OR AS A WHOLE WITHOUT THE WRITTEN PERMISSION OF TEES FLIGHT RESEARCH LAB IS PROHIBITED.

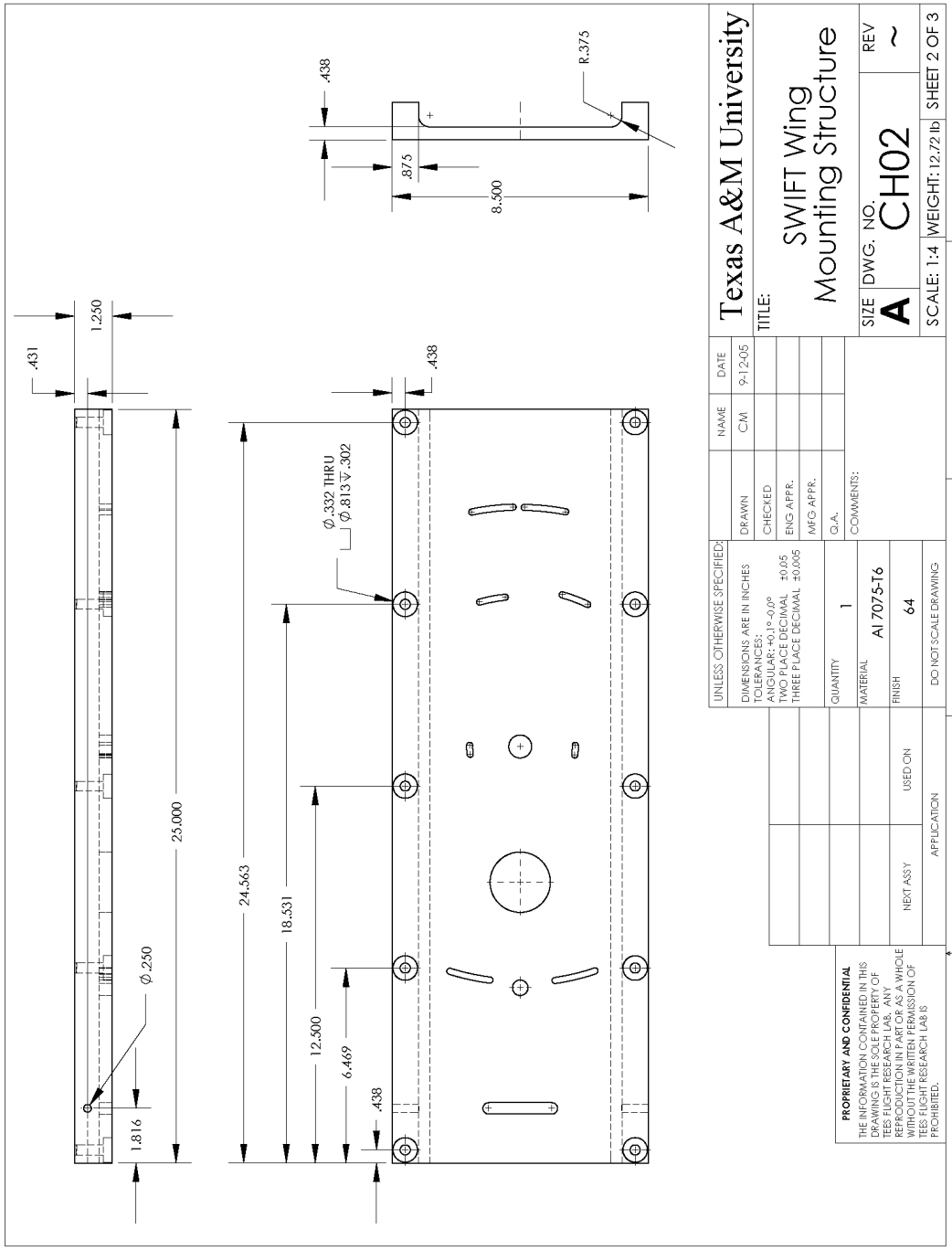
.431
1.250
.438
R.375
.438
.875
8.500
Ø.332 THRU
Ø.813 ▽ .302
Ø.250
1.816
25.000
24.563
18.531
12.500
6.469
.438
UNLESS OTHERWISE SPECIFIED:
DIMENSIONS ARE IN INCHES
TOLERANCES:
ANGULAR: +0.1° -0.0°
TWO PLACE DECIMAL ±0.05
THREE PLACE DECIMAL ±0.005
QUANTITY 1
MATERIAL Al 7075-T6
FINISH 64
DO NOT SCALE DRAWING
NEXT ASSY
USED ON
APPLICATION
DRAWN CM 9-12-05
CHECKED
ENG APPR.
MFG APPR.
Q.A.
COMMENTS:
Texas A&M University
TITLE:
SWIFT Wing
Mounting Structure
SIZE A
DWG. NO. CH02
REV ~
SCALE: 1:4
WEIGHT: 12.72 lb
SHEET 2 OF 3
PROPRIETARY AND CONFIDENTIAL
THE INFORMATION CONTAINED IN THIS DRAWING IS THE SOLE PROPERTY OF TEES FLIGHT RESEARCH LAB. ANY REPRODUCTION IN PART OR AS A WHOLE WITHOUT THE WRITTEN PERMISSION OF TEES FLIGHT RESEARCH LAB IS PROHIBITED.

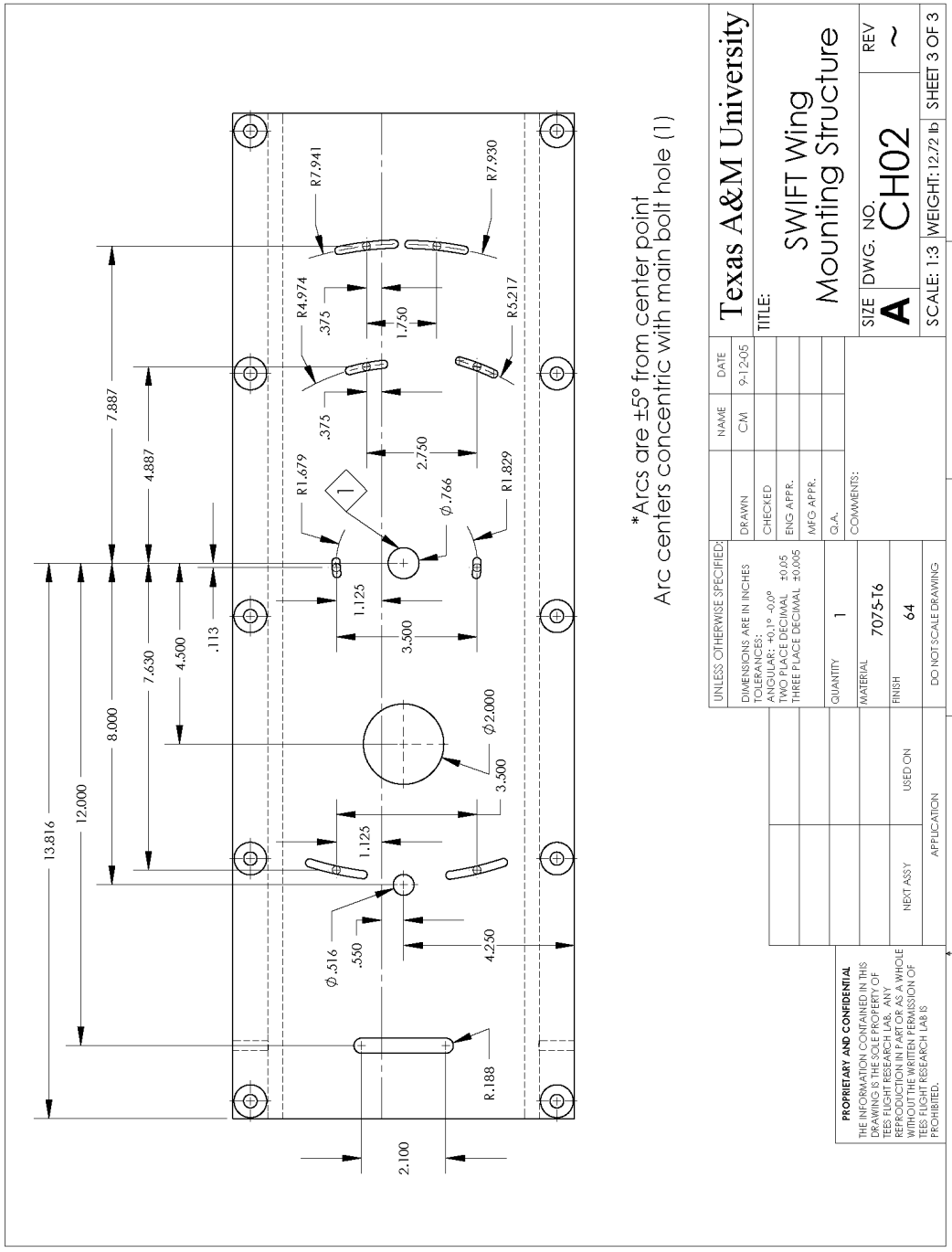
*Arcs are ±5° from center point
Arc centers concentric with main bolt hole (1)
13.816
12.000
8.000
7.630
4.500
.113
7.887
4.887
2.100
R.188
Ø.516
.550
4.250
1.125
1.125
3.500
Ø2.000
3.500
R1.679
1
Ø.766
R1.829
2.750
.375
.375
1.750
R4.974
R5.217
R7.941
R7.930
UNLESS OTHERWISE SPECIFIED:
DIMENSIONS ARE IN INCHES
TOLERANCES:
ANGULAR: ±0.1° -0.0°
TWO PLACE DECIMAL ±0.05
THREE PLACE DECIMAL ±0.005
QUANTITY 1
MATERIAL 7075-T6
FINISH 64
DO NOT SCALE DRAWING
NAME
DRAWN CM
CHECKED
ENG APPR.
MFG APPR.
Q.A.
COMMENTS:
DATE
9-12-05
Texas A&M University
TITLE:
SWIFT Wing
Mounting Structure
SIZE A
DWG. NO. CH02
REV ~
SCALE: 1:3
WEIGHT: 12.72 lb
SHEET 3 OF 3
NEXT ASSY
USED ON
APPLICATION
PROPRIETARY AND CONFIDENTIAL
THE INFORMATION CONTAINED IN THIS DRAWING IS THE SOLE PROPERTY OF TEES FLIGHT RESEARCH LAB. ANY REPRODUCTION IN PART OR AS A WHOLE WITHOUT THE WRITTEN PERMISSION OF TEES FLIGHT RESEARCH LAB IS PROHIBITED.

VITA

Name: Christopher William McKnight

Address: 6921 E. Laguna Azul Ave
Mesa, AZ 85209

Email Address: mcknight.chris@gmail.com

Education: M.S., Aerospace Engineering, Texas A&M University, 2006
B.S., Mechanical Engineering, The University of Dayton, 2004